Aus der medizinischen Klinik mit Schwerpunkt Rheumatologie und klinische Immunologie der Medizinischen Fakultät Charité – Universitätsmedizin Berlin

In Kooperation mit
The ANZAC Research Institute
The University of Sydney, Australia

DISSERTATION

Long-term effects of transgenic disruption of glucocorticoid signalling in mature osteoblasts and osteocytes in K/BxN mouse serum-induced arthritis

zur Erlangung des akademischen Grades
Doctor medicinae (Dr. med.)

vorgelegt der Medizinischen Fakultät
Charité – Universitätsmedizin Berlin

von
Tazio David Maleitzke
aus Karlsruhe

Datum der Promotion: 22.09.2017

Abstract

Aim: The role of endogenous glucocorticoids (GC) in bone metabolism in the inflammatory processes present in rheumatoid arthritis (RA) is yet not as well understood as the role of therapeutic GCs used widely in the treatment for RA. The aim of the present study was to investigate the impact of endogenous GCs on erosion and reparation processes in bone during the chronic phase of arthritis through a long-term murine experiment.

Methods: The effects of autoantibody mediated K/BxN serum transfer arthritis in Col2.3-11ß-HSD type 2 transgenic (tg) mice and their wildtype (WT) littermates were investigated over a time course of 42 days. Through the osteoblast specific collagen type 1 promoter Col 2.3, the enzyme 11ß-hydroxysteroid dehydrogenase type 2 (11ß-HSD type 2), which converts active cortisol into inactive cortisone, was overexpressed and disrupted the effects of active GCs on osteoblasts. Arthritis progression was evaluated daily through clinical assessment and ankle size measurements. Samples were harvested on day 42 and histology, immunohistochemistry, and radiological micro-computed tomography (micro-CT) studies were performed.

Results: Acute arthritis occurred in all experimental animals with a clinical peak around day 10. Afterwards, inflammation declined gradually until day 42. As in previous studies there were less pronounced signs of joint inflammation and cartilage damage in tg animals compared to WT littermates. Yet it appeared that bone erosions were either equally distributed or more pronounced in tg mice compared to WT littermates. This seemed to not only be due to arthritis driven bone resorption, but might have to do with the fact that bone turnover is bigger in tg animals, yet lower again in arthritic tg animals.

Conclusion: Through the disruption of GC signalling in osteoblasts over a 42-day experiment we were able to show an influence of endogenous GCs on the fulminant clinical course of arthritis and the following bone repair process. Most findings in this long-term study were non-significant, yet the observed differences between tg and WT animals go in accordance with previous studies. It is plausible that the reason for our results, which differ partly from previous publications, might lie in changes of the genomic status of the experimental animals used in this study compared to mice used in former experiments. Our results indicate an essential and vital role for endogenous GCs in the intact bone metabolism.

Keywords: Rheumatoid arthritis, glucocorticoids, 11ß-HSD type 2, K/BxN

Kurzdarstellung

Zielsetzung: Die Rolle endogener Glucocorticoide (GC) auf den Knochenstoffwechsel in inflammatorischen Prozessen wie der Rheumatoiden Arthritis (RA) ist bisher nicht so gut verstanden wie jene therapeutisch angewandter GC. Ziel der vorliegenden Arbeit war es, den Einfluss endogener GC auf die chronische Phase der Arthritis mit besonderem Blick auf Erosions- und Reparationsvorgängen im Knochen anhand eines Langzeitexperiments im Tiermodell zu erfassen.

Methoden: Über einen Zeitraum von 42 Tagen wurden die Effekte der durch Auto-Antikörper vermittelten K/BxN Serum Transfer Arthritis im Col2.3-11ß-Hydroxysteroid Dehydrogenase Typ 2 (Col2.3-11ß-HSD Typ 2) transgenen (tg) Mausmodell gegen den Wildtyp (WT) untersucht. Im Col2.3-11ß-HSD Typ 2 Mausmodell wird durch den Osteoblasten spezifischen Kollagen Typ 1 Promotor, Col 2.3, das Enzym 11ß-HSD Typ 2, welches biologisch aktives Cortisol in biologisch inaktives Cortison überführt, überexprimiert und verhindert somit die Wirkung aktiver GC an Osteoblasten. Das klinische Bild der Arthritis wurde durch tägliche klinische Untersuchungen und Messungen des Knöcheldurchmesser evaluiert. Die an Tag 42 gewonnen Proben wurden histologisch, immunhistochemisch, histomorphometrisch und durch radiologische Mikro-Computertomographie (Mikro-CT) Analysen untersucht.

Ergebnisse: Eine akute Arthritis stellte sich bei allen Tieren mit klinischem Höhepunkt der Entzündungsreaktion um Tag 10 ein, welche im Anschluss stetig bis Tag 42 abklang. Wie in vorausgegangenen Studien zeigten sich weniger Entzündungszeichen sowie geringere Knorpelschäden in tg Mäusen im Vergleich zu WT Tieren. Knöcherne Erosionen zeigten sich bei tg Tieren allerdings gleich oder sogar stärker ausgeprägt als bei WT Tieren. Dies scheint nicht nur an der durch Arthritis verstärkten Knochenresorption zu liegen, sondern auch daran dass der Knochenumsatz bei tg Tieren höher, jedoch bei arthritisch tg Tieren wiederum geringer ist.

Schlussfolgerung: Durch die Unterbrechung des GC Signalwegs in Osteoblasten über 42 Tage konnten wir eine, wenn auch nicht signifikante, Beeinflussung des klinischen Verlaufs der fulminanten Arthritis sowie der sich anschließenden Reparaturprozesses durch endogene GC feststellen. Die vorwiegend nicht-signifikanten Unterschiede zwischen tg und WT Tieren stimmen mit Aussagen aus Vorgänger Studien überein. Es ist plausible dass ein Hauptgrund für teils abweichende Ergebnisse eine Veränderung des genomischen Status der Tiere im Vergleich zu vorausgegangenen Studien ist. Die gezeigten Ergebnisse weisen darauf hin dass endogene GC eine essenzielle und unabdingbare Rolle im intakten Knochenstoffwechsel spielen.

Stichwörter: Rheumatoide Arthritis, Glucocorticoide, 11ß-HSD Typ 2, K/BxN

Table of Contents

List of abbreviations

11 β -HSD	11ß-hydroxysteroid dehydrogenase
ACPA	antibodies to citrullinated protein antigens
ACTH	adrenocorticotropic hormone
AES	aminopropyltriethoxysilane
AIA	antigen-induced arthritis
AME	apparent mineralocorticoid excess
ArKO	aromatase knock out
BLT1	leukotriene B4 receptor 1
BMD	bone mineral density
BV/TV	bone volume/total volume
CAIA	collagen antibody-induced arthritis
CBG	corticosteroid-binding globulin
cDNA	complementary deoxyribonucleic acid
cGR	cytosolic glucocorticoid receptor
CIA	collagen-induced arthritis
Col2.3	2.3 kb collagen type I
CRP	C reactive protein
CRH	corticotropin-releasing hormone
CTR	control
DKK	dickkopf-related protein
DNA	deoxyribonucleic acid
dNTP	deoxyribonucleoside triphosphates
EDTA	ethylene diamine tetraacetic acid
ESR	erythrocyte sedimentation rate
Fc	fragment crystallizable
FcγR	activating IgG receptor
G6PI	glucose-6-phosphate-isomerase
GC	glucocorticoid
GIO	glucocorticoid-induced osteoporosis
GR	glucocorticoid receptor
HSP	heat shock protein

H&E	hematoxylin and eosin
IgG	immune globulin G
IgM	immune globulin M
IL	interleukin
iκB	inhibitor of nuclear factor κB
KO	knock out
LPS	lipopolysaccharide
mAb	monoclonal antibody
MBL	mannose-binding lectin
MC	mineralocorticoid
mGR	membrane-bound glucocorticoid receptor
MHC	major histocompatibility complex
micro-CT	micro-computed tomography
MR	mineralocorticoid receptor
mRNA	messenger ribonucleic acid
N.Oc/BS	number of osteoclasts/bone surface
NAD	nicotinamide adenine dinucleotide
NADPH	nicotinamide adenine dinucleotide phosphate
NF-κB	nuclear factor κB
NKT	natural killer T cells
NOD	non-diabetic obesity
Ob.S/BS	osteoblasts/bone surface
Oc.S/BS	osteoclasts/bone surface
OCN	osteocalcin
OPG	osteoprotegerin
PBS	phosphate buffered saline
PCR	polymerase chain reaction
PFA	paraformaldehyde
pOBCol2.3-GFR	a green fluorescent protein marker of mature osteoblasts
RA	rheumatoid arthritis
RANKL	receptor activator of NF-κB ligand
RF	rheumatoid factor
RMA	repeated measures analysis
RNA	ribonucleic acid

ROI	region of interest
S-to-R	stressed-to-relaxed
SEGRA	selective glucocorticoid receptor agonists
SSWAHS	Sydney South West Area Health Services
Tb.N	trabecular number
Tb.Sp	trabecular separation
Tb.Th	trabecular thickness
TBE	TRIS-Borate-EDTA-Buffer
TBS	trabecular bone score
TCR	T cell receptor
Tfh	follicular helper T cells
tg	transgenic
TNFα	tumor necrosis factor α
TRAP	tartrate-resistant acid phosphatase
Wnt	wingless Int-1
WT	wildtype

1 INTRODUCTION

1.1 Glucocorticoids

1.1.1 Discovery of glucocorticoids

First discovered for its anti-inflammatory potential by Philip Showalter Hench and colleagues in 1948, 17-hydroxy-11-dehydrocorticosterone (named 'compound E' at the time and cortisone today) was administered to 14 rheumatoid arthritis (RA) patients, which resulted in remarkable clinical improvements in all subjects (1). 2 years later, Philip Showalter Hench, Tadeus Reichstein and Edward Calvin Kendal together received the Nobel Prize in Medicine or Physiology "for their discoveries relating to the hormones of the adrenal cortex, their structure and biological effects" (2).

The remarkable discovery of the potential use of this adrenal hormone in the treatment of RA and the ability to synthetically produce sufficient amounts of it were the starting point for a wide-range use of 'glucocorticoids' (GCs), a term often used in clinical context today and which tells of its various unique characteristics. GCs are metabolic hormones provided by our body to prepare for and react to stressful situations, where more resources are needed than normally. This can be shown by the strong involvement of GCs in glucose metabolism. Described already by West et al. in 1959, GCs stimulate gluconeogenesis to provide glucose in states of stress or early fasting (3). Yet excessively elevated GC levels, e.g. in Cushing's disease, lead to additional hepatic glucose production (4), glucose intolerance (5) and eventually peripheral insulin resistance (6, 7) in which case insulin is no longer able to sufficiently stimulate glucose uptake by muscle and fat cells (8, 9). The close connection between glucose and GCs also appears vice versa, as glucose intake causes GC levels to rise (10, 11), which in summary explains the term 'gluco' in 'glucocorticoid'.

GCs are produced in the zona fasciculata of the adrenal cortex, a layer of cells named after its fascicle-like arrangement in the middle of the adrenal cortex. Hence, the site of glucocorticoid production gave rise to the middle part of its name, 'cortic'. The adrenal cortex is part of the hypothalamic-pituitary-adrenal axis and GC production is regulated through a feedback loop in a circadian rhythm with higher GC levels in the morning (12). The adrenal gland's production of GCs is stimulated by the adrenocorticotropic hormone (ACTH) produced by the anterior pituitary. In turn, ACTH production is stimulated by corticotropin-releasing hormone (CRH) from the hypothalamus in response to physical and emotional stress (13).

The suffix 'oid' can be equated with "resembling". As all GCs are 21-carbon steran derivatives that interact with the glucocorticoid receptor (GR) (14), their unique chemical structure explains the ending 'oid' in 'ster<u>oids</u>' or 'glucocortic<u>oids</u>'.

GCs can be divided into naturally occurring GCs and synthetic GCs. Naturally occurring GCs, or endogenous GCs, exist in both active and inactive forms. In humans, the active form is called cortisol, whilst the inactive form is called cortisone. In rodents, the active form is called corticosterone and the inactive form 11-dehydrocorticosterone. They all have both glucocorticoid and mineralocorticoid effects. Induction of gluconeogenesis, proteolysis, lipolysis (15, 16) and a negative nitrogen balance (17) can be attributed to GCs. Mineralocorticoids (MC) on the other hand affect water and electrolyte balances and cause increased sodium retention as well as potassium excretion (18). Moreover, GCs have strong anti-inflammatory and immunosuppressive effects (19, 20).

The chemical structure of synthetic GCs is similar to that of cortisol. The commercial production of GCs commonly aims to nearly eliminate the often unwanted mineralocorticoid effects and amplify the desired glucocorticoid effects. Different synthetic GCs like prednisolone (equivalent to a GC dose of 5 mg) or hydrocortisone (equivalent to a GC dose of 20 mg) vary in potency as well as in duration of action (21, 22). GCs are one of the most commonly prescribed drugs in medicine and especially in rheumatology they have been an indispensable therapeutic agent for many decades. This becomes evident when looking at RA patients in rheumatological care in Germany. In 2014, the prescription rate for GCs was as high as 48% for patients receiving prednisolone at a dose of 5 mg. 8.5% of patients received less than 5 mg of prednisolone, 37.7% received dosages between 5 and 7.5 mg and 2.1% were administered higher dosages than 7.5 mg (23). Statistics from 2005 in Germany show even higher prescription rates for GCs when looking at the times GCs were prescribed in combination with other rheumatological drugs, such as tumor necrosis factor inhibitors (81%), cyclosporin A (80%), or leflunomide (77%) (24).

1.1.2 Genomic actions of glucocorticoids

The mechanisms of action of GCs are fairly well understood and basically divided into 2 pathways: a genomic and a non-genomic pathway. In the past it was believed that mainly the genomic pathway could explain the key effects of GCs. In the genomic pathway, GCs bind to the cystolic glucocorticoid receptor (cGR), a homodimer serving as a carrier, which, once activated by GCs, undergoes a conformational change and translocates from the cytoplasm to the nucleus as a ligand-receptor complex. Inside the cellular nucleus, the complex recruits co-regulators and

interacts with the glucocorticoid response element found in the promoter or the intragenic region of genes targeted by GCs.

Without stimulation, GRs reside in the cytoplasm bound to chaperone proteins such as heat shock protein (HSP) 90 and HSP70 awaiting binding of GCs (25). Through alternative splicing and alternative translation initiation, different GR isoforms occur. GRα is known to be primarily responsible for the GR actions described above, GRβ on the other hand, is a dominant negative inhibitor and antagonist to GRα (26). Additional post-translational mechanisms expand the variety of GRs through phosphorylation and acetylation causing a lower affinity of GRs to GCs (27).

The binding of the ligand-receptor complex to the glucocorticoid response element leads to an increased transcription of anti-proliferative and anti-inflammatory target genes through up-regulated gene expression or transactivation. Transactivation leads to an increase in secretory leukocyte proteinase inhibitor (28), mitogen-activated kinase phosphatase 1 (29) as well as annexin 1, interleukin-10 (IL-10) and inhibitor of nuclear factor κB (iκB) (30, 31). Anti-inflammatory actions are also caused by transrepression, a mechanism whereby the ligand-receptor complex inhibits promoting effects of pro-inflammatory transcription factors such as activation protein-1 and nuclear factor κB (NF-κB) by binding to the transcription factors itself or necessary coactivators and thus 'blocking' the translational process. NF-κB and activation protein-1, both crucial orchestrators of the inflammatory responses, induce a wide range of genes encoding cytokines, cytokine receptors and adhesion molecules such as IL-1β, IL-2, IL-6, IL-8, tumor necrosis factor α (TNFα), granulocyte/macrophage colony-stimulating factor, IL-2-receptor and intercellular adhesion molecule-1 as reviewed here (32-35). The development of selective glucocorticoid receptor agonists (SEGRAs) as highly specific anti-inflammatory drugs, which transrepress but do not or barely transactivate, is a result of these insights. These drugs promise fewer side effects than conventional GC therapy (36, 37), but their use is also discussed controversially as clinical evidence of their effects is still limited. The model of transrepression versus transactivation is often criticized for an oversimplification of the underlying genetic mechanisms of GR activity (38). Yet, a review from 2015 about Compound A, a unique non-steroidal SEGRA which was used in *in vitro* and *in vivo* studies, shows promising anti-inflammatory and anti-cancer effects with less side effects and less patient resistance than conventional GCs (39).

1.1.3 Non-genomic actions of glucocorticoids

In 2008, as the understanding of the non-genomic pathways of GCs increased, Stahn and Buttgereit provided a classification for categorizing the rapid effects of GCs which could not be contributed to genomic actions. As an alternative to the Mannheim classification (40) and the classification used by Haller and colleagues (41), the rapid GC actions were divided into 1) non-specific interactions of GC with cellular membranes, 2) non-genomic effects mediated by the cGR, and 3) specific interactions with membrane-bound glucocorticoid receptors (mGR). The interactions of GCs with cellular membranes are believed to lead to a reduced ATP production through an increase in mitochondrial proton leak and an inhibition of oxidative phosphorylation of several immune cells as well as reduced calcium and sodium cycling across membranes. Altogether this decelerates the cell metabolism of immune cells and eventually leads to immunosuppression and anti-inflammatory effects (42-44).

In addition to the classic genomic function of the cGR, it has also been found to have additional rapid anti-inflammatory functions. These comprise for example the inhibited production of arachidonic acid and consequently its inflammatory prostaglandins, thus inducing a shift toward the synthesis of anti-inflammatory arachidonic acid-based endocannabioids (45). Finally, GCs can act through the mGR, a receptor expressed in small numbers on human monocytes and B cells. It is upregulated when immune cells are stimulated by lipopolysachharide (LPS), and the number of mGRs correlates positively with disease activity in RA and negatively with GC treatment in patients suffering from systemic lupus erythematosus. Altogether this underlines the crucial and indispensable involvement of mGRs in the process of immune modulation (46, 47).

1.1.4 Corticosteroid-binding globulin

The tissue availability of GCs is regulated in several ways with the purpose of adjusting the amount of active GCs to current needs at different sites in the body. The binding of GCs to their main transport protein corticosteroid-binding globulin (CBG) is one of these ways. While 80-90% of GCs are bound to CBG, only 4-5% are circulating in free fraction. The rest is bound to albumin (48). CBG, which is found predominantly in liver tissue, but also in lung, testis and kidney tissue, was discovered to be part of the serine protease inhibitor family with a structure similar to α1-antitrypsins'. Typical for members of the serine protease inhibitor family, CBG undergoes an irreversible stressed-to-relaxed (S-to-R) conformational change through cleavage when exposed to proteolytic stress (49). In the event of inflammation mimicked by human

neutrophil elastase, CBG is cleaved to its reactive loop causing a 10-fold decrease in its binding affinity toward cortisol (50, 51). This leads to a release of cortisol directly on the site of inflammation enabling cortisol to modify the inflammatory response. In accordance with this, it has been shown that CBG's plasma concentration decreases in patients with inflammation, septic shock and burn injuries (52, 53).

1.2   The role of 11β-HSD

1.2.1   11β-HSD and its protective function

Regulating the available amounts of free fraction GCs is a crucial construct regulated by the intracellular and bidirectional enzyme 11ß-hydroxysteroid dehydrogenase (11β-HSD). 2 isoforms have been found in mammalian tissue determining biological activity on a pre-receptor level. *In vivo*, 11β-HSD type 1 mainly converts the inactive form cortisone (11-hydrocorticosterone in rodents) to its C11-hydroxylated and active metabolite cortisol (corticosterone in rodents) in a reaction driven by oxo-reductase activity when provided with the cofactor nicotinamide adenine dinucleotide phosphate (NADPH). In turn, 11β-HSD type 2, which is nicotinamide adenine dinucleotide (NAD)-dependent, converts cortisol (11-hydrocorticosterone in rodents) to cortisone (corticosterone in rodents) through a dehydrogenase reaction leaving C11 with a keto group and therefore inactive.
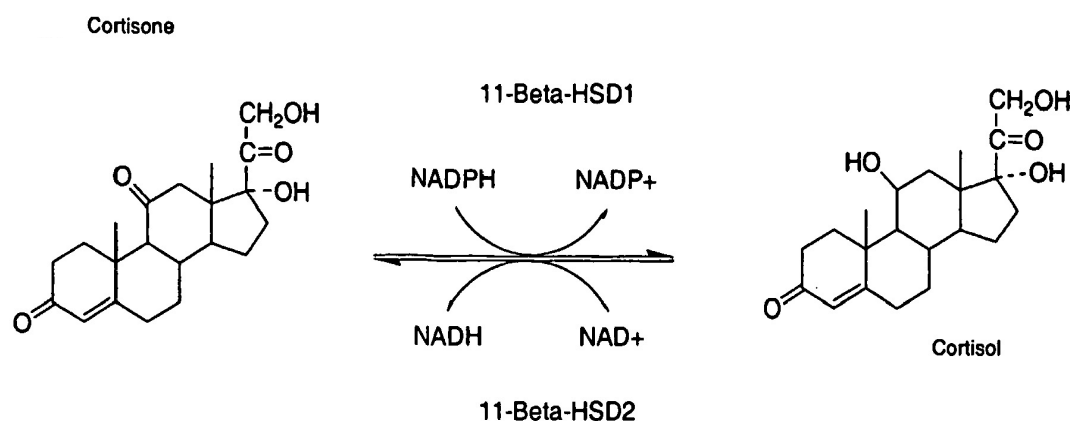

Figure 1.2.1.1: Enzymatic conversion of cortisone to cortisol and respectively cortisol to cortisone. Adapted from Balkovec et al. 2007 (54).

Although 11β-HSD type 1 also shows a predominant dehydrogenase activity when extracted, intact cell models show that oxo-reductase activity is dominating in both hepatic and adipose tissues in which the enzyme is highly expressed (55-58). When 11β-HSD type 1 is overexpressed in these insulin sensitive tissues, equilibrium lies in favour of biologically active GCs which results in central obesity and insulin resistance as shown in a monozygotic twin study in 2004 by Kannisto et al. (59). The metabolic effects of hyperglycaemia and hyperinsulinemia in mice could, however, be markedly reversed when medically inhibiting 11β-HSD type 1 (60). Other studies have shown a significantly improved insulin sensitivity, decreased blood fats (61) and, interestingly, even resistance to cognitive impairment in men and mice when inhibiting 11β-HSD type 1 (62, 63).

11β-HSD type 2 has been found to be the key factor which allows certain tissues to be specifically sensitive to aldosterone but not to GCs. The importance of this function becomes evident when bearing in mind that GCs have the same affinity to the mineralocorticoid receptor (MR) as aldosterone itself, and that GC circulation levels are 100- to 1000-fold higher than those of aldosterone. Yet, the tissues of the kidneys, colon and salivary glands are in fact somewhat protected from overwhelming activation by GCs despite their expression of MR, which does not distinguish between MCs and GCs as ligands (64-67). Placental and fetal tissues, which are associated with GRs rather than MRs, also show a high activity of 11β-HSD type 2, indicating a protective function of the enzyme towards embryonic development from growth inhibiting effects and subsequent hypertension in the new-born (68-70). The effects caused by a lack of 11β-HSD type 2 can be observed in individuals with apparent mineralocorticoid excess (AME), a condition with just more than 100 reported cases to date. AME is a rare yet debilitating autosomal recessive disease with a mutation in the HSD11B2 gene that leads to a lack of 11β-HSD type 2 causing severe metabolic impairment. In this condition, overstimulation of MRs by GCs occurs in aldosterone-sensitive tissues leading to hypertension, hypokalemia, hypernatremia and often growth retardation, thus demonstrating the striking importance of a pre-receptoral regulation of GCs (71, 72). This effect can be mimicked by excessive liquorice intake where the active ingredient glycyrrhizic acid inhibits 11β-HSD type 2 activity (73) and leads to a condition referred to as pseudohyperaldosteronism.

1.2.2   11β-HSD in bone

In addition to its various expressions in hepatic and adipose tissue with mainly reductive (cortisol activating) actions, and foremost dehydrogenase (cortisol inactivating) actions in

kidney, colon, salivary glands, placental and fetal tissues, 11β-HSD type 1 is also detectable in primary cultures of human osteoblast cells (74) and fresh human bone (75). Although 11β-HSD type 2 is not found in murine primary osteoblast cultures or bone tissues, the enzyme was shown to be present in human (74) and rat osteosarcoma cell lines (76) as well as in human fetal bone tissue (70). These findings, which are consistent with the presence of GRα on osteoblasts (77), underline the importance of 11β-HSD as a pre-receptor regulator of GCs especially in bone metabolism.

The striking side effects of endogenous GCs, first described by Harvey Cushing, are a clinical phenomenon physicians and patients are well aware of and fear (78). Bone loss and poor bone quality are some of the most characteristic symptoms of excessive GC levels in Cushing's Syndrome and GC-induced osteoporosis (GIO). The complex role of GCs in bone metabolism becomes evident when looking at their catabolic effect and inhibition of osteoblast proliferation on one hand and their crucial role in promoting osteoblast differentiation on the other.

1.2.3   Bone loss due to endogenous and exogenous glucocorticoids

Bone loss due to excess GCs in humans and rodents basically occurs in 2 phases. A rapid phase, during which overwhelming bone resorption leads to a decrease in bone mass and therefore poor bone structure, followed by an extended later phase, in which insufficient bone formation leads to an additional decrease in bone mass and loss of stability. As a reason for these effects, Weinstein described reduced cell numbers of osteoblasts and osteoclast-progenitors as well as an increase in osteoblast apoptosis in mice treated with GCs for 27 days. Bone mineral density (BMD) was significantly lower in mice receiving high doses of prednisolone compared to a placebo-treated control (CTR) group. These results were consistent with findings showing that the vertebral cancellous areas as well as the trabecular width were both markedly decreased in GC-treated mice. The decreased trabecular width and the consecutively decreased trabecular number imply a total resorption of trabecular profiles. Osteocalcin (OCN), a marker of osteoblast activity, was decreased, with over 50% in the prednisolone group, indicating a notable reduction in bone formation. This is also supported by a dose-dependent decrease in mineral apposition rate in the intervention group (79). GCs seem to extend the lifespan of osteoclasts and therefore allow a higher number of these cells to be in involved in bone resorbing processes. Furthermore, bisphosphonates, known to protect bone from resorption due to a complete resistance to enzymatic hydrolysis, were not able to fulfil their pro-apoptotic potential towards osteoclasts in

GC-treated mice. Yet they were able to protect osteoblasts from the pro-apoptotic effects of GCs (80).

A lack of sex steroids, such as testosterone, has a similar catabolic effect on bone tissue similar to a state of excessive GC exposure during prednisolone treatment. Interestingly, GC treatment itself can lead to a suppression of sex hormones (81, 82). It has therefore been discussed whether the effect of GCs on bone is due to decreased concentrations of sex steroids (and therefore an increase in osteoblastogenesis and osteoclastogenesis with a higher remodelling rate and poor bone quality) or through a direct effect of GCs on bone (with a down-regulation of osteoblastogenesis as well as osteoclastogenesis and subsequently poor bone quality due to a lower remodelling rate). In addition to well known negative effects of excessive GCs on bone, such as GIO and Cushing's disease, through direct impact on osteoblasts and osteocytes (83), studies have also revealed sex hormone-related bone changes. Aromatase-deficient ArKO mice, which are depleted of estrogen and androgen effects due to an androgen receptor knock out (KO), present with an osteopenic phenotype and decreased cancellous bone volume compared to their wildtype (WT) littermates (84). Oz et al. showed no phenotype changes in the bone of newborn ArKO mice, yet adult ArKO mice presented with a decreased femur length and lower BMD (85). To shed light on the question of which mechanism holds the main responsibility for bone loss and poor bone quality, Weinstein et al. conducted further experiments and came to the conclusion that the direct effects of GCs on bone override the catabolic effect of steroidal sex hormones. While there was no additional loss of vertebral bone, mineral density or loss of compression strength in orchiectomized mice treated with prednisolone, bone resorption and activation frequencies were significantly decreased in the GC-treated orchiectomized group compared to orchiectomized mice receiving placebo. Upregulation in osteoblast and osteoclast progenitor cells was also prevented by GCs when administered to orchiectomized mice, which was not the case in the placebo group. Furthermore, an increase in the number of osteoblasts and osteoclasts in bone marrow was prevented by GCs, but occurred in non-GC receiving orchiectomized mice. This allows the conclusion that skeletal effects of GCs override the effects mediated through sex hormones. In addition, it could be shown that the prednisolone-treated group did not show any significant changes in serum testosterone or seminal vesicle weight compared to the placebo-receiving group, opposing the suggested negative effect of GCs on sex hormones further above (86).

Clinical studies have shown that the risk of fracture is as high as 75% in the first 3 months of GC therapy initiation. A substantial decline in BMD only occurs at a later time point of disease progression though. Various dosages, ranging from 2.5 to 10 mg of prednisone per day and even

the use of inhaled GCs were all associated with an increased risk of fractures due to GIO. Patients suffering from GIO show fewer osteoblasts and more osteocyte apoptosis in histomorphometric studies. Interestingly osteocyte apoptosis comes with a reduction in vascular endothelial growth factor, skeletal angiogenesis, bone interstitial fluid and bone strength. The increased risk of fractures in GIO patients might therefore be attributed to osteocyte apoptosis and a loss of bone strength before a substantial loss of BMD can even take place. Yet if patients show a low BMD, vertebral fractures or undergo long-term GC treatment, which cannot be discontinued, fracture risk-reducing drugs are recommended (87). In 2007, Saag et al. showed that patients suffering from established GIO received significantly more skeletal benefits from the anabolic agent teriparatide compared to patients treated with the bisphosphonate alendronate. Skeletal benefits included increased BMD at the lumbar spine and the total hip as well as fewer new vertebral fractures (88). In 2016 teriparatide also proved to be superior to alendronate in regard to trabecular bone score (TBS) in patients with GIO (89). TBS represents the trabecular structure, the number of trabeculae and their connectivity. A high TBS therefore represents fracture-resistant bone architecture and a strong and healthy bone. The difference between alendronate and teriparatide lies in the fact that alendronate acts as an anti-resorptive agent, whereas the latter serves as an anabolic agent for skeletal tissue.

In order to further investigate the direct impact of GCs on the skeleton as well as the specific effect of 11β-HSD isoenzymes on bone, the mouse model of an overexpressed 11β-HSD type 2 in osteoblasts has proven to be very helpful. Through an overexpression of the 11β-HSD type 2 gene linked to a 2.3 kb collagen type I (Col2.3) promoter, its dehydrogenase activity shifts the equilibrium in favour of inactive 11-dehydrocorticosterone in mature osteoblasts and osteocytes on a pre-receptor level. The Col2.3-11β-HSD2 mouse model was first described by Sher et al. in 2004 (90) and is further described in *Animals and Methods*.
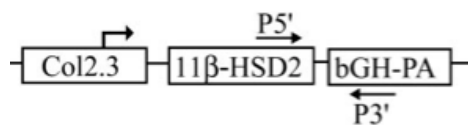

Figure 1.2.3.1: 11β-HSD type 2 complementary deoxyribonucleic acid (cDNA) with p5' forward and p3' reverse primers. CDNA was cloned downstream of a 2.3 kb fragment of a rat Col1a1 promoter. Borrowed from Sher et al., 2004 (90).

Compared to their WT littermates, Col2.3-11β-HSD2 transgenic (tg) mice were found to have a 10-15% decrease in femoral cortical bone area and thickness. These *in vivo* findings were

accompanied by *ex vivo* results from primary calvarial osteogenic cultures showing that osteoblast differentiation and function were also impaired in tg mice (shown by pOBCol2.3-green fluorescent protein, OCN messenger ribonucleic acid (mRNA) and nodule mineralization as late-stage markers of osteogenic differentiation). These results support the hypothesis that endogenous GCs play a crucial and supportive role in forming and maintaining healthy bone structures (91). However, as crucial as endogenous GCs may be for the development of bone structure and function, as vulnerable are bone structure and composition when exposed to high levels of exogenous GCs. This was shown in a similar model in which exogenous GCs were administered to the experimental mice. Expression of 11β-HSD type 2 specifically in osteoblasts and osteocytes was achieved by inserting the enzyme's cDNA downstream from the osteoblast-specific OCN promoter. When exposed to excessive GC levels, the increased osteoblast and osteocyte apoptosis rate that was seen in WT mice was markedly decreased in tg mice. Bone formation rate was higher in tg mice, and their vertebral compression strength was also preserved as opposed to their WT littermates. Hence, it could be concluded that GCs have a direct impact on bone formation cells, and that a loss of skeletal strength is due to a decreased number of osteocytes caused by GCs (92).

1.2.4   11β-HSD and inflammation in bone

Human MG-63 sarcoma cells were the first cells to be discovered expressing both isoforms of 11β-HSD reciprocally within the same cell. In these cells, inflammation, mimicked by IL1β and TNFα, led to an increase in cortisone-to-cortisol conversion rate as well as a strong induction of 11β-HSD type 1 mRNA. At the same time, there was a decrease in cortisol-to-cortisone conversion rate as well as a decrease in 11β-HSD type 2 mRNA. It could also be shown that these effects were reversible and reproducible by means of removal and reintroduction of cytokine exposure, respectively (93). A rise in 11β-HSD type 1 was also detectable in human osteoblasts with age and when exposed to GCs indicated again by increased cortisone-to-cortisol conversion rate and 11β-HSD type 1 mRNA levels (94). In addition to these findings, it could be shown that not only each factor in isolation leads to an increase in 11β-HSD type 1 activity, but that the combination of pro-inflammatory cytokines and GCs leads to a dramatic increase in 11β-HSD type 1 activity. These findings in primary human osteoblasts, synovial fibroblasts and MG63 cells call into question the pure suppressive role of GCs in an inflammatory process and show a possibility of sensitization and agonist function of GCs and pro-inflammatory cytokines in bone (95). Pointing far beyond its sole role in protecting MR affiliated tissues from GC

excess, 11β-HSD seems to have a very crucial role in regulating GC distribution on a cellular level in bone and inflammation.

1.2.5   11β-HSD and bone resorption

Cooper et al. found a significant decrease in bone resorption markers in the osteoporotic process when inhibiting 11β-HSD. Pyridinoline and doxypyridinoline, both collagen crosslinks, were notably decreased when inhibiting 11β-HSD through a liquorice derivate known as carbenoxolone. This suggests a supportive role of 11β-HSD enzymes in osteoclast-driven processes, noting that carbenoxolone inhibits both 11β-HSD type 1 and type 2. Understandably it was therefore difficult to specify which isoform was responsible for the changes observed (75). In accordance with clinical findings, Roldan et al. have shown that GCs have an isolated effect on bone loss in systemic inflammatory diseases such as RA (96). It comes as no surprise that GCs, when administered to healthy individuals, decrease bone formation markers such as OCN and N-terminal propeptide of type I collagen. Yet, the activity of 11β-HSD type 1 was also a positive predictor of the decrease of bone formation markers in prednisolone-treated individuals. All this suggests that 11β-HSD type 1 bears the main responsibility for bone resorbing changes amongst the 2 11β-HSD isoforms. The likelihood of developing GIO might therefore also be due to inter-individual differences in 11β-HSD type 1 activity (97) and could explain why some people are more prone to develop of the disease than others.

1.2.6   Anabolic effects of glucocorticoids and 11β-HSD in bone development

In spite of the roles of 11β-HSD type 1 and administered GCs in bone resorption processes, GCs remain a crucial contributor to healthy bone development. They play a vital part in the differentiation process of osteoblasts, which becomes evident through the dose-dependent increase of alkaline phosphatase, mineralization rate and an increased overall cell number of osteoblasts in the human fetal osteoblastic cell line SV-HFO. Not only were GCs needed for osteoblast differentiation, but the time point of GC exposure also seemed to be important. Mineralization failed when cells were exposed to GCs too late in their development. Therefore, mineralization was still taking place when stimulated with GCs on day 7 or 9, but not when stimulated on day 12 or later. Furthermore, it was shown that developing osteoblasts which had not been treated with GCs expressed high levels of 11β-HSD type 1. GC-treated osteoblasts

undergoing differentiation, however, exhibited less than 20% of the 11β-HSD type 1 expression of the former non-treated osteoblasts. This suggests a pivotal role of 11β-HSD type 1 in compensating for a potential lack of local cortisol in the differentiation process (98, 99).

According to these findings, *in vitro* and *in vivo* studies using the Col2.3-11β-HSD2 mouse model have shown that an interruption of the GC pathway in mature osteoblasts and osteocytes leads to impaired bone development (90, 100-102). Results show that bone morphology parameters like bone volume over total volume (BV/TV), trabecular number (Tb.N) and trabecular thickness (Tb.Th) of the tibia were significantly decreased in Col2.3-11β-HSD2 tg mice compared to WT mice. Similar results were obtained from vertebra samples. Periosteal and endosteal perimeters were significantly decreased, while cortical thickness seemed to be similar in both groups. Although the tibial length was only marginally decreased in Col2.3-11β-HSD2 tg mice, maximum load and bending modulus were again significantly reduced in this group. Due to the fact that Col2.3-11β-HSD2 tg mice were significantly lighter in body weight, it should be noted that when adjusted to body weight, most of the differences between the groups became non-significant. Yet, differences in cortical and trabecular bone as well as bone strength and stiffness assessed by maximum load and bending modulus remained significant. These results emphasize the importance of endogenous GCs to the development of tibial and vertebral bone. Accordingly, Col2.3-11β-HSD2 tg mice had lower bone volume, poorer bone structure and reduced strength and stiffness independently of gender (100). It has also been shown that HSD1$^{-/-}$ mice, deficient in 11β-HSD type 1, show normal bone development with similar formation and resorption parameters compared to their WT littermates. The age-related bone loss of HSD1$^{-/-}$ mice is similar to that of WT mice, leaving bone marrow composition the only difference between the 2 groups: In contrast to the bone marrow of WT mice, the bone marrow of HSD1$^{-/-}$ mice showed total absence of adipocytes. The function of bone marrow adipocytes is unknown, but it has been speculated that they function as energy reservoirs for urgent haematopoiesis in case of blood loss, for ossification in case of fractures, or simply as passive space-filling matter (103).

1.3   The K/BxN arthritis model

1.3.1   K/BxN arthritis as a model for human rheumatoid arthritis

The characteristics of RA range from chronic synovitis with cartilage degradation and damage to underlying bone erosions in joints and systemic manifestation such as vasculitis. The disease's

symptom complex is characterized by an inflammatory component driven by TNFα and pro-inflammatory cytokines such as IL-1 and IL-6 affecting synovial and cartilage cells as well as osteoclasts. Inhibiting osteoclast activity through denosumab, a human monoclonal antibody, has proven to limit bone erosion and structural damage (104, 105).

Mimicking various aspects of human RA in an *in vivo* mouse model has seen many different approaches: from T-cell dependent collagen-induced arthritis (CIA) and antigen-induced arthritis (AIA) to T-cell independent K/BxN arthritis and IL-1 tg arthritis (106).

The starting point for experiments with the spontaneous arthritis model of K/BxN arthritis in mice was a rather coincidental finding. C57BL/6 mice, a strain tg for a T cell receptor (TCR) that together with the I-A^k major histocompatibility complex (MHC) class II molecule recognizes peptides of bovine pancreas ribonuclease (RNase), were crossed with I-A^{g7} MHC class II molecule expressing non-diabetic obesity (NOD) mice. NOD mice are mice with a likelihood to develop autoimmune diseases such as diabetes mellitus type I (107). With crossing the mice came the unexpected discovery of a phenotype which spontaneously developed severe destructive polyarthritis within 4 to 5 weeks. Arthritis developed spontaneously with pronounced inflammation with red and swollen joints of the paws. Clinical features of RA continued to progress as mice grew older; hyperextension of the ankle, valgus deviation of the knee and hyperpronation of the toes became visible and seemed to also result in compromised mobility and reduced reproductive behaviour (108, 109). Histologically, arthritis became manifest in pannus formation and erosion of cartilage and bone of mainly the distal joints.

The underlying principle and pathogenesis of the model is the activation of B cells by tg T cells and the crucial secretion of autoantibodies by B cells. Specificity is gained by MHC class II molecules through which the K/BxN TCR not only recognises the bovine RNase peptide but also glucose-6-phosphate isomerase (G6PI). G6PI is normally responsible for catalysing the enzymatic interconversion of D-glucose-6-phosphate and D-fructose-6-phosphate. Recognition of G6PI in the K/BxN mouse model, however, results in secretion of autoantibodies against G6PI by B cells through TCR and MHC class II molecule recognition and cluster of differentiation (CD) 40 signalling. CD40 signalling triggers activated B cells to secrete antibodies, and CD40 deficient K/BxN mice are therefore not able to develop arthritis (110). Furthermore, K/BxN mice treated with CD40 ligand antibodies before arthritis onset presented with a delayed or no initiation of the disease. When the mice were treated with CD40 ligand antibodies only after the onset of RA, no difference in arthritis development was observed when comparing to the CTR group (111). IL-33, a member of the IL-1 family and high in endothelial cells and fibroblasts of the synovium in RA, however, seems to play no or only a minor role in

K/BxN arthritis. According to the study by Martin et al., IL-33 is not required to develop arthritis in the K/BxN model. Confirming this, IL-33 KO mice did not develop less arthritis than their WT littermates when both received K/BxN serum injections (112). This shows that the K/BxN arthritis model certainly has a lot of similarities, but also some differences from human RA, which is important to note. Similarities include symmetrical arthritis with a destructive component as well as a chronically progressive course of the disease. Whereas RA in man spares the distal interphalangeal joints and does not affect the spine, K/BxN arthritis spares the hip (but not the distal interphalangeal) joints and does in fact involve the spine. In addition, rheumatoid factor (RF), an autoantibody against the Fc (fragment crystallizable)-part of immune globulin G (IgG), is not present in K/BxN mice, while RA patients test positive for it in 70% of the cases. RF, however, can also occur in healthy individuals and individuals with neoplasms or chronic infections which reduces its diagnostic specificity (113). In clinical practice, an additional test for detecting antibodies to citrullinated protein antigens (ACPAs) is therefore included when diagnosing RA. ACPA testing is part of the 2010 ACR/EULAR Rheumatoid Arthritis Classification Criteria which are composed of 4 clusters: serology (RF and ACPA), acute phase reactants (C-reactive protein and erythrocyte sedimentation rate (CRP and ESR)), joint symptoms and duration of symptoms. Each cluster is given numerical scores which are then added up to a final score. This scoring method aims at achieving early diagnosis and treatment of RA (114).

1.3.2   K/BxN serum-induced arthritis through serum transfer

The clinical similarities to RA in humans and the 100% incidence of arthritis made the K/BxN model quite valuable for studying the pathogenesis of RA. The added advantage of this model is that it is transferable. As described by Korganow et al., either cells or serum of K/BxN arthritic mice can be transferred into a different strain of mice. Intravenously injected K/BxN splenocytes into healthy mice led to severe arthritis within 8 days that was neither clinically nor histologically distinguishable from the one K/BxN mice developed. Splenocytes depleted of either T or B cells were, however, unable to cause arthritis in the cell-receiving mice. The group of Korganow then transferred serum of K/BxN mice to B cell- and lymphocyte-deficient mice which led yet again to severe joint swelling and a 100% incidence of arthritis. This indicated an independent role of soluble IgG antibodies in the serum, and fractioning the serum into an IgG and non-IgG fraction proved that only IgG molecules were in fact able to cause the disease. The main difference between K/BxN mice and the serum transfer model is that the latter is transient

with a more heterogeneous disease manifestation. This was shown by a great difference in severity of joint lesions of neighbouring joints in histology. Repeated injections were, however, able to maintain the disease's activity over time, whereas mice injected only once began to show remission of the arthritis after 15 days. As this occurred in lymphocyte deficient RAG$^{0/0}$ mice, Korganow et al. suggested that rather than missing T or B cell input, the known instability of IG molecules might be the reason for the transience of the transfer model (110).

1.3.3 Fc receptors in K/BxN arthritis

Two anti-GPI autoantibody subtypes were found in the K/BxN serum: IgG1 and IgG2 (115). Both bind to activating IgG receptor (FcγR) FcγRIIIA, one of three targeted receptors by IgG antibodies. The other two receptors, FcγRI and FcγRIV, can solely be targeted by IgG2 (116). FcγRII acts as an inhibiting receptor for cellular activation upon ligation (117). Fc receptors can be understood as a link between immune complexes and the immune system. Mice lacking FcγRI develop the full clinical picture of K/BxN serum transfer arthritis (118). The inhibiting receptor FcγRII seems to have an immunosuppressing role, as FcγRII KO mice show a more pronounced arthritis progression than WT mice (119, 120). FcγRIIIA KO mice also develop arthritis but in a less severe form than WT animals. The contribution of FcγRIV was further demonstrated in a FcγRI/IIB/IIIA$^{0/0}$ FcεRI/II$^{0/0}$ 5 KO model by Mancardi et al., where mice only expressing FcγRIV as an activating IgG FcR developed arthritis. The clinical appearance was, however, described as milder compared to the one of the WT group. If FcγRIV was blocked additionally, no arthritis developed. Interestingly, FcγRIV has affinity for IgG2 but not for IgG1, which suggests an independent role of this isotype in the development of serum transfer K/BxN arthritis (116). This finding challenges the assumption that K/BxN arthritis is mainly caused by IgG1 (115).

1.3.4 Effector cells in K/BxN arthritis

IgG2 activating receptor FcγRIV is found alongside FcγRIIIA on monocytes, macrophages and neutrophils with an additional expression of FcγRIIIA on mast cells. Interestingly, the importance of mast cells in autoimmunity (121, 122) has been challenged in recent studies. Thus, it was possible to induce the full development of K/BxN arthritis in mast cell-deficient mice. Yet, macrophages and monocytes alongside neutrophils were crucial for inducing the disease (116, 123, 124). The pivotal role of neutrophils and their numerous receptors associated with an

immune response such as complement component 5a receptor, FcγR and leukotriene B4 receptor (BLT1) has become evident in several studies (124). Activation of neutrophils has been shown to be dependent on leukotriene B4, a lipid chemoattractant and inflammatory mediator. Leukotrienes, especially leukotriene B4, are crucial to the initiation and progression of K/BxN arthritis (125), and BLT1, located on neutrophils, is responsible for endothelial adhesion, chemotaxis and recruitment or retention of leukocytes (126, 127). This self-orchestrated autocrine recruitment of neutrophils is characterized by production of neutrophil active chemokines and neutrophil chemokine receptors such as CCR1 and CXCR2 attracting more neutrophils into the affected joint. Furthermore, it has been shown that neutrophils expressing IL-1, a cytokine which plays a vital role in initiating arthritis, also need BLT1 to deliver the cytokine to the site of inflammation (128).

As mice depleted of macrophages (through clodronate liposome treatment) do not show any signs of arthritis, macrophages seem to be equally important for the development of K/BxN arthritis, and arthritis can be induced when reconstituting mice with naïve macrophages (129). Macrophages develop from monocytes when entering a specific tissue site, and monocytes can be subdivided into classical, intermediate and non-classical based, on their function and cell-surface molecules (130). Ly6C– is a type of non-classical monocyte found in mice. Ly6C– cells travel to the inflamed joint where they develop into, and increase the number of, M1 macrophages. The 2 subclasses of macrophages, M1 and M2, have mainly opposite yet sometimes complementary roles in the course of arthritis. M1 phenotype macrophages are classically activated and responsible for the inflammatory phase, whilst alternatively activated M2 phenotype macrophages are responsible for the resolution phase of the inflammation. Macrophages initially have a set of both M1 and M2 genes, and in the resolution phase, a shift from the M1 to the M2 phenotype seems to appear. This, alongside the action of tissue-resident macrophages, which maintain joint integrity, terminates the inflammation (131).

Kim et al. have found that the binding of IgG to FcγRIII on natural killer T cells (NKT) leads to their activation in K/BxN arthritis. Further, activated NKT enhance the production of IL-4, IL-10, IL-13 and IFN-γ. Mice deficient in NKT did not develop arthritis, and transferring NKT was only able to initiate arthritis when NKT were of WT descent with functioning FcγRIII (132).

1.3.5   Cytokines, T cell subsets and gut microbiota in K/BxN arthritis

Cytokines are proteins that regulate growth and differentiation of cells as well as cell signalling in the state of inflammation. As part of the pro-inflammatory cascade in RA, multiple cytokines

and inflammatory mediators play an important role in murine K/BxN arthritis. IL-1 was described by Ji et al. as central in the disease progression of arthritis as IL-1-deficient mice did not develop any clinical or histological signs of arthritis. Experiments on TNFα did, however, not result in clear conclusions. KO mice for TNFα showed either no or delayed onset of arthritis, and the degree of inflammation remained under the maximum of what was observed in WT animals. More interestingly, it was found that mice deficient in TNFR1 and TNFR2, the 2 only known receptors for TNFα, showed a clear development of arthritis as seen in WT mice. Ji et al. therefore concluded that TNFα has a distinct role in K/BxN arthritis, but is not absolutely essential. The group further showed that IL-6 is not involved in the development of K/BxN serum transfer arthritis, as IL-6 deficient mice developed a full clinical picture of arthritis (133). These findings are also interesting in regard to human RA and other inflammatory rheumatic diseases in which monoclonal antibodies against both TNFα (Infliximab) and IL-6 (Tocilizumab) are successfully used in treatment (134, 135). Studies investigating the role of IL-17 cytokines have come to contradicting results. The conclusion that IL-17 indeed plays an important role in K/BxN serum transfer arthritis was proposed by Katayama et al., who showed that neutrophils act as an essential source of IL-17 and that IL-17A KO mice developed a much less severe form of arthritis. (136). Jacobs et al. showed that neutralizing IL-17 through an anti-IL-17 monoclonal antibody (mAb) strongly suppressed the enhancement of arthritis. This underlined the pro-inflammatory role of IL-17 in K/BxN serum transfer arthritis (137). However, Block et al. challenged these findings and concluded that IL-17 was not essential for the development of arthritis because IL-17 KO mice developed full-blown arthritis like their IL-17-sufficient littermates (138). Human mAb targeting IL-17 showed promising results in safety and efficacy with clinically relevant response rates in RA and psoriasis arthritis patients. Secukinumab was approved for the treatment of psoriasis in 2015 by the United States Food and Drug Administration (FDA) and is currently under investigation for the treatment of RA (139). In summary, the pro-inflammatory range of cytokines in K/BxN arthritis indicates that the disease cannot be attributed to one single subset of helper T cells. Subsets of helper T cells are formally defined by their individual cytokine profiles. In K/BxN arthritic mice, different subsets all differentiating from naïve T cells seem to be required. A study showing the crucial involvement of IL-4 in K/BxN arthritis stated that elements of both the Th1 and Th2 response are present in the K/BxN murine model. Supportive of this, the group found that K/BxN T cells expressed high amounts of both IFN-γ, typical for a Th1 response, and IL-4, a hallmark of a Th2 response (140). Another important subset of helper T cells are follicular helper T cells (Tfh). The presentation of antigens by B cells to Tfh drives B cells to differentiate into germinal centre B cells which hyper

mutate and undergo a class switch, resulting in further differentiation into plasma cells and memory B cells. T cell-produced IL-4 and Il-2 play a vital role in the differentiation and activation of Tfh and plasma cells. *In vivo* findings have shown that eliminating segmented filamentous bacteria from the gut (by starting antibiotic treatment at birth) reduced the Tfh and germinal centre B cell population in secondary lymphoid organs throughout the body, and no K/BxN arthritis developed. Furthermore, Tfh were absolutely essential for disease induction, as mice insufficient in T cell specific Bcl6, a transcription factor for Tfh differentiation and function, did not develop the disease either. These very interesting findings shed light on the link between intestinal microbial colonization, differentiation of T cell subsets and development of arthritis (138).

1.3.6 The complement system's alternative pathway in the K/BxN serum transfer mouse model

After autoantibodies start inducing arthritis, different key effectors come into play. One of the fast and important response systems is the complement pathway, a rapid immune-modulating pathway striking in the wake of inflammation. More precisely, there are three additional pathways leading to cell lysis through various sophisticated steps. The complement system consists of more than 20 serum proteins of which the majority are regulatory proteins and receptors which upon activation essentially lead to immune cytolysis, anaphylaxis and hemolysis. The classical pathway depends on antibodies (IgG and IgM) binding to pathogens. Once bound, the antibody undergoes a conformational change within its Fc-component that enables C1q to bind to it, which in turn activates C1r and cleavage of C1s. Downstream of the cascade, anaphylatoxins (i.e. C4a and C4b) are cleaved, and pathogen-opsonizing phagocytosis (C3b) takes place. The final phase, which is identical in all three pathways, is initiated by C3 and C5. Interestingly, CRP, bacterial LPS, deoxyribonucleic acid (DNA) and ribonucleic acid (RNA), among other danger signals, are also able to activate the classical pathway. However, these danger signals are historically attributed to the alternative pathway in which C3 is activated through binding of, for example, bacteria-infected cells, proteins, polysaccharides and damaged tissue. To prevent constant activation of C3, control mechanisms like the binding of properdin to C3 exist. Through several intermediate steps, C3 activation leads to C5 implementation and initiation of the terminal enzymatic cascade. The lectin pathway is a mannose-binding lectin (MBL) dependent pathway. MBL binds to pathogenic surface proteins and by binding of MBL-associated serine proteases-1 and -2, it forms a multi-enzyme complex which eventually leads to

the described C3 and C5 pathway described above. In this common pathway, the lytic membrane attack complex forms a stable transmembrane pore which causes an osmotic imbalance and lysis of the target cell. Apart from the complement system's lytic abilities and the capability to protect the body from infection and inflammation, its cleavage products can opsonize antigens, leading to phagocytosis, specific antibody production and differentiation of B memory cells. The initiation of an anaphylactic reaction allows several components of the complement system to support migration of mast cells and basophile granulocytes which are then able to fight pathogens through the release of vasoactive substances like histamine and prostaglandins (141). The importance of the complement system and especially the alternative pathway to the skeletal system is accentuated by findings showing that C3 is absolutely crucial for osteoclast differentiation. The alternative pathway leads to C3 activation which is essential for bone marrow cells differentiating into osteoclasts after $1,25(OH)_2$ vitamin D_3 stimulation. Furthermore bone marrow cells are able to locally produce all necessary complement factors such as factor B and factor D to initiate the alternative pathway during osteoclast differentiation (142). Mice lacking factor B do not develop arthritis, and the same applies to mice lacking C5 (118) and C3 (143). As C3 is a key player in the complement cascade, it comes as no surprise that C3 is present in the synovium of RA patients (144) and arthritic mice. WT mice developing K/BxN arthritis after serum transfer showed C3 deposits in the synovium of the arthritic joints. The local deposit of C3 was, however, not needed to initiate arthritis, but circulating C3 produced by parenchymal cells distant from the joint was sufficient to do so (143). In the K/BxN serum transfer model, G6PI autoantibodies lead to C3 cleavage and C5 generation. In turn, C5 convertase cleaves C5 into C5a and C5b which remain bound to the target cell and initiate the membrane attack complex and cell lysis. Although it has been shown that the alternative pathway is the main pathway in K/BxN serum transfer arthritis, it is striking that antibodies usually activate the classical pathway. Anti-G6PI antibodies are mainly composed of the IgG1 subclass which is only a weak activator of the classical pathway, and therefore the alternative pathway remains the prevalent cascade in K/BxN arthritis (145). In summary, the key effectors of K/BxN arthritis are the FcγRIV and FcγRIIIA receptors, neutrophils, macrophages, NKT, cytokines such as IL-1, Tfh and the alternative complement pathway.

1.4 Aim of this study

In 2009 Buttgereit et al. were able to show for the first time that attenuating GC signalling specifically in osteoblasts abates the subacute phase of arthritis in mice. The experiment covered

a 14-day span, and changes became evident on day 7 and remained significant until the end of the experiment. The study compared WT mice and unique tg mice with interrupted GC signalling in mature osteoblasts and osteocytes through enzymatic GC inactivation in the course of K/BxN serum transfer arthritis. The study unveiled that functional endogenous GC signalling in osteoblasts is crucial for the continuous course of inflammatory arthritis and that a disruption leads to a less severe course of the disease. The degree of arthritis was evaluated through clinical examination of the animals, histopathological assessment, histomorphometry and micro-computed tomography (micro-CT) radiography. Interestingly, inflammatory joint infiltration and cartilage damage were more pronounced in arthritic WT K/BxN mice, yet, the results for bone erosions could only show a tendency toward less bone defects in arthritic tg K/BxN mice. Buttgereit et al. discussed if this observation was perhaps due to a relatively short duration of the experiment which would potentially not leave enough time for bone destruction to take place. It therefore remained unclear what role endogenous GCs would play in the longer lasting regenerative phase that follows the imminent inflammatory phase in the K/BxN serum transfer mouse model (146).

In 2012, Matzelle et al. conducted a study using arthritogenic K/BxN serum injections to induce arthritis in C57BL/6J mice in order to study the resolution process of arthritis. As expected, clinical signs of inflammation occurred and peaked at day 10. They were accompanied by upregulated inflammatory cytokines and histological signs of inflammation in the synovium. Furthermore, receptor activator of NF-κB ligand (RANKL) mRNA was upregulated in the arthritic synovium, whereas osteoprotegerin (OPG), also known as osteoclastogenesis inhibiting factor, was downregulated in the presence of inflammation. These findings were accompanied by a significantly increased number of tartrate-resistant acid phosphatase (TRAP)-positive osteoclasts in the arthritic group. RANKL is a soluble protein, enhancing bone resorption and an antagonist to OPG. OPG, on the other hand, is a cytokine receptor known to induce bone formation.

The study showed that clinical inflammation, RANKL mRNA, and osteoclast numbers all decreased as arthritis regressed by day 15 and disappeared from day 28 onwards.

The group therefore defined 3 arthritic phases: An inflammatory phase (day 0-10), a resolution phase (day 10-28), and a remodelling and repair phase (from day 28 onwards).

As inflammation declined, osteoblasts synthesizing bone were seen on the surface. This was accompanied by an increased expression of anabolic Wnt (wingless Int-1) mediators such as Wnt10b that promotes osteoblastogenesis, and DKK2 (dickkopf-related protein 2), a matrix mineralization-promoting Wnt antagonist (147). These results, which stress the importance of

the Wnt signalling pathway in osteoblastogenesis, are consistent with the findings of our group that described suppressed Wnt signalling in Col2.3-11β-HSD2 mice, with disrupted GC signalling in mature osteoblasts and osteocytes. Tg mice showed a hypoplastic and delayed cranial bone development with poor mineralization compared to the normal bone development and constitution observed in the WT group (148).

Our aim was to look at arthritis development over the course of 42 days using the well-established K/BxN serum transfer arthritis model. In order to investigate, in particular, the regeneration process of antibody-mediated serum transfer arthritis, we compared WT mice with tg Col2.3-11β-HSD2 mice with disrupted GC signalling in mature osteoblasts and osteocytes through locally upregulated 11β-HSD type 2 in a long-term study.

2 ANIMALS AND METHODS

2.1 Experimental animals and study design

Col2.3-11β-HSD2 tg mice were generated as originally described by Sher, Woitge et al. 2004 (90) and were kindly provided as a gift by Dr. Barbara Kream (Department of Medicine, University of Connecticut Health Center, Farmington, CT, USA). In accordance with the Institutional Animal Welfare Guidelines and an approved protocol (protocol number 2012/006) by Sydney South West Area Health Services (SSWAHS) Animal Welfare Committee, animals were housed in the animal facility of the ANZAC Research Institute (Sydney, Australia). Mice had access to food and water without restrictions and were exposed to a 12-hour light/dark cycle. Mice were taken out of their cages once every day at midday for the duration of the experiment to perform weighing, ankle size measurements and clinical assessments.
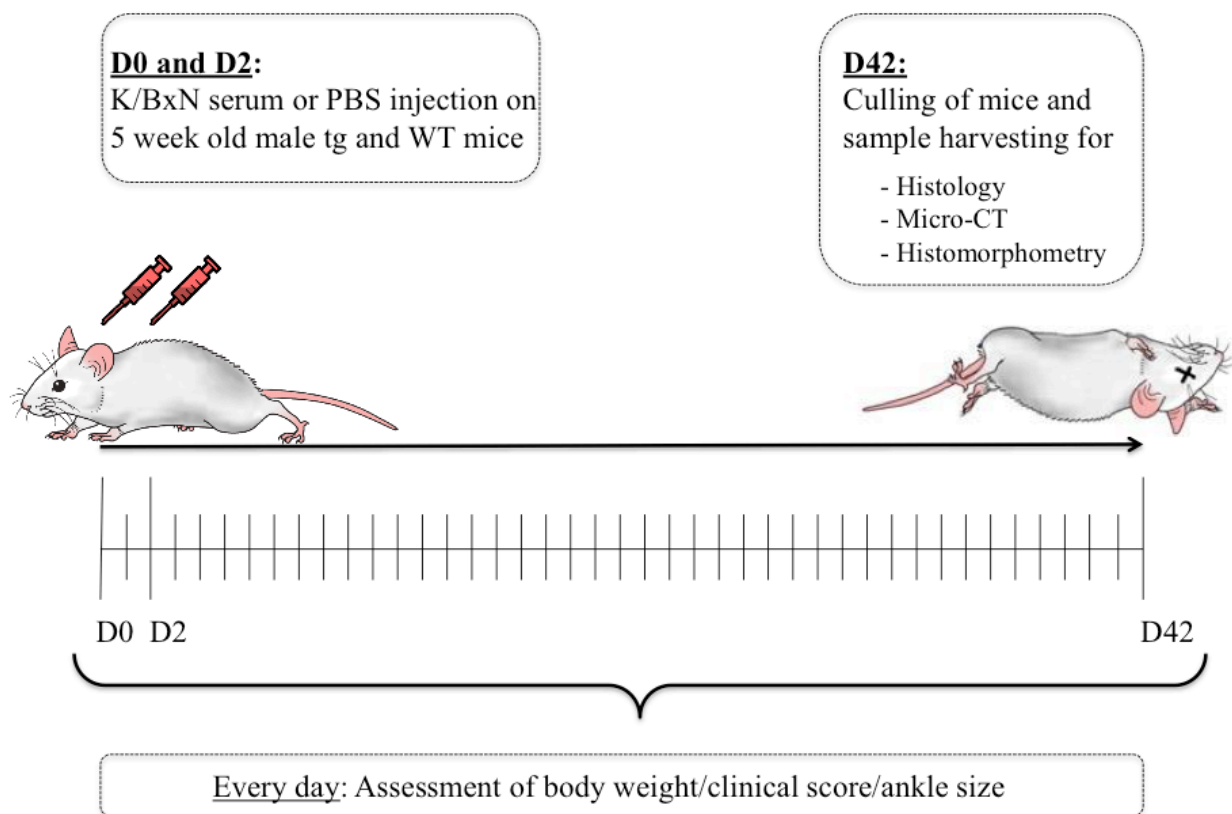
Figure 2.1.1: Experimental design of long-term 42-day K/BxN serum-induced arthritis study with injections on day 0 (D0) and day 2 (D2). Samples were harvested on day 42 (D42).

After disinfection with 80% ethanol, intraperitoneal injections of 150 µL K/BxN mouse serum or 150µl phosphate buffered saline (PBS) were performed on days 0 and 2 on 5-week-old Col2.3-11β-HSD2 tg mice (mean body weight 25.90 g ± 1.01 g) and their WT littermates (mean body weight 23.37 g ± 1.12 g) to observe the course and effects of a T cell-independent immune response to arthritic development as shown in figure 2.1.1. On day 42 of the experiment, euthanasia was performed, and samples were harvested. The inclusion criterion for mice was a body weight of 25 g ± 15% at 5 weeks of age. A total of 26 mice, 13 mice from both the tg group and 13 from the WT group, were randomly assigned to 4 experimental clusters (figure 2.1.2).
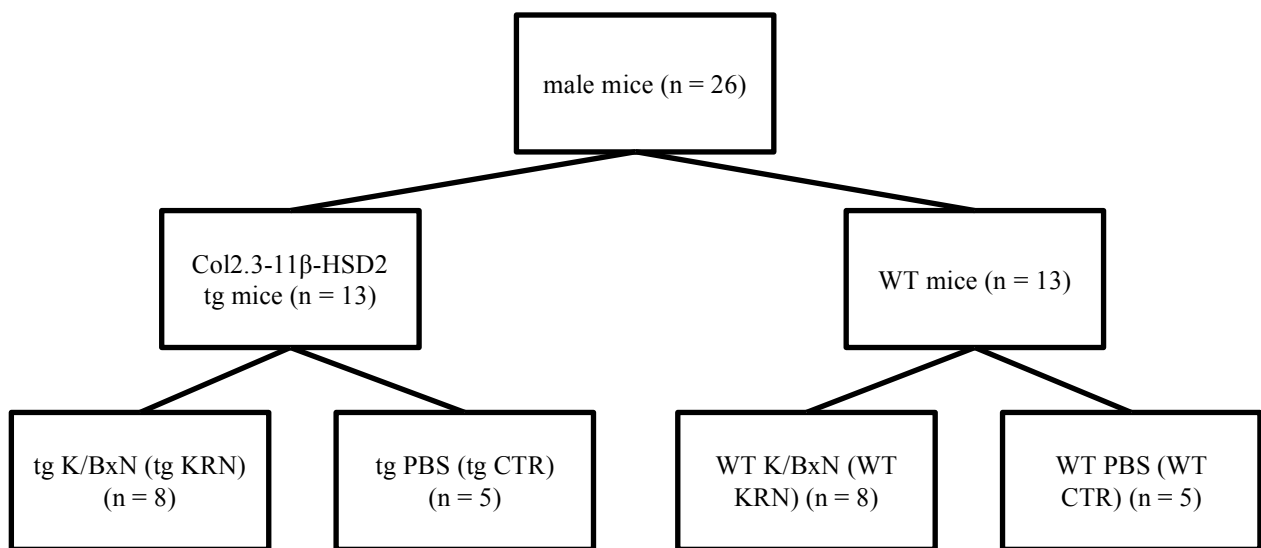
Figure 2.1.2: Distribution of different genetic mice types in the long-term 42-day K/BxN serum-induced arthritis study.

2.2   Genotype analysis

For DNA isolation toes were used. A toe sample was attained from each mouse between 7 and 12 days of age and incubated in a lysis mixture containing 98.3 µL Milli-Q water, 25 µL $MgCl_2$ (20 mM; Ajax Finechem Pty. Ltd., Taren Point, Australia), 25 µL DNA Polymerase 10x Reaction Buffer (Fisher Biotec Australia, Wembley, Australia) and 17 µL proteinase K (Roche Applied Sciences, Castle Hill, Australia). Every sample was incubated twice to deactivate proteinase K: 2 hours at 55°C and 15 minutes at 98°C. A polymerase chain reaction (PCR) (Eppendorf Mastercycler ep, Eppendorf AG, Hamburg, Germany) was used to amplify 5 µL of lysed DNA sample in 20 µL PCR reaction mixture containing 0.75 µL Mango Taq DNA

polymerase enzyme (1000 units; Bioline Pty Ltd., Randolph, MA, USA), 13.75 µL Milli-Q water (autoclaved), 2.5 µL 10x reaction buffer (Bioline Pty Ltd., Alexandria, Australia), 1 µL $MgCl_2$ (50 mM; Bioline Pty Ltd., Alexandria, Australia), 1 µL dNTPs (deoxyribonucleoside triphosphates 1 mM; Invitrogen Corp., Carlsbad, CA, USA), 1 µL HSD2 primers (10 mM). The first PCR cycle was performed at 94°C for 5 minutes followed by 30 cycles at 94°C for 30 seconds, 60°C for 30 seconds, 72°C for 45 seconds and terminated by 1 circle at 72°C for 5 minutes.

As part of the HSD2 gene, the forward oligonucleotide primer sequence 5'-ACC TTA GCC CCG TTG TAG-3' was used along with the reverse primer sequence 5'-G AGG GGC AAA GAA GAA CAG ATG-3', both found within the bovine GH polyadenylation region.

A 1.5% agarose gel was used as PCR matrix. For that purpose, 0.375 g agarose powder was dissolved in 25 mL 1 X TRIS-Borate-EDTA-Buffer (TBE) and 7µl SYBR safe (Invitrogen, Carlsbad, CA, USA) was added. The mixture was poured into a mini-sub cell (Bio-Rad Laboratories Inc., Hercules, CA, USA) with small format combs and left to settle for 40 minutes. Wells were loaded with PCR products and run at 100 volt for 30 minutes.

2.3   K/BxN mouse serum

To generate K/BxN mice which develop arthritis spontaneously, KRN-C57BL/6 mice tg for a TCR recognising a bovine ribonuclease peptide presented by a MHC class II were crossed with NOD mice that are prone to autoimmunity as described in chapter 1.3.1. Serum from 60-day old K/BxN mice was collected through intracardiac puncture, pooled and stored at -80°C. Eppendorf tubes with K/BxN serum were left to defrost at room temperature before administration.

2.4   Clinical assessment and score

Animals were taken out of their cages individually every day at room temperature to reduce potential internal stress responses. Mice were weighed to monitor general well-being and potential systemic effects of arthritis. Each of the 4 paws was rated by 2 independent observers who were blinded to the assigned groups of the animals. As described by Buttgereit et al. 2009, all 4 limbs were assessed with regard to swelling. Summing up the scores from each limb, a total score was calculated for each mouse with a possible maximum of 12 (146).

0	no swelling
1	mild-to-moderate swelling and erythematic ankle and/or 1 swollen digit
2	moderate swelling and erythematic ankle or swelling in 2 or more digits
3	marked swelling along all aspects of the paw or all 5 digits swollen

Swelling of the animals' rear paws was quantified by measuring each rear paw using a Vernier caliper (Vernier Software & Technology, Beaverton, OR, USA) to determine the maximum medial to lateral diameter of the ankle. Results from both ankles of the rear legs were averaged.

2.5   Anaesthesia

Before blood and tissue collection general anaesthesia and analgesia were attained by injecting a mix of 75 mg/kg body weight ketamine (Cenvet Pty. Ltd., Kings Park, Australia) and 10 mg/kg body weight xylazine (Cenvet Pty. Ltd., Kings Park, Australia) into the peritoneum.

2.6   Blood collection and serum preparation

When anaesthesia and analgesia were in full effect, blood was collected by intracardiac puncture with at 27-gauge needle attached to a 1 mL syringe. Promptly after blood collection, mice were sacrificed by cervical dislocation.

1 hour after collection, blood was spun down at 8,000 rounds per minute for 15 minutes. Supernatant was cautiously pipetted off the solid cellular pallet, placed in fresh tubes and stored at -80°C.

2.7   Spleen collection

Mice were placed in supine position and a medial skin incision was performed from just under the xiphoid to the pelvis. The peritoneum was carefully opened, and the spleen was identified in the upper left quadrant of the abdomen. It was gently detached from the gastrosplenic ligament and remaining connective tissue and dissected in full. Spleens were weighed immediately after collection.

2.8 Ankle joints

Left ankle joints including the tibia and fibula were dissected by incising along the anterior aspect of the femur and tibia, followed by disarticulation of the femurotibial joint. Skin was removed from the limb, and muscle tissue around the bones was thoroughly removed. Samples were stored in PBS for micro-CT analysis. Correspondingly, right ankle joints were harvested and prepared for histological and histomorphometric analysis.
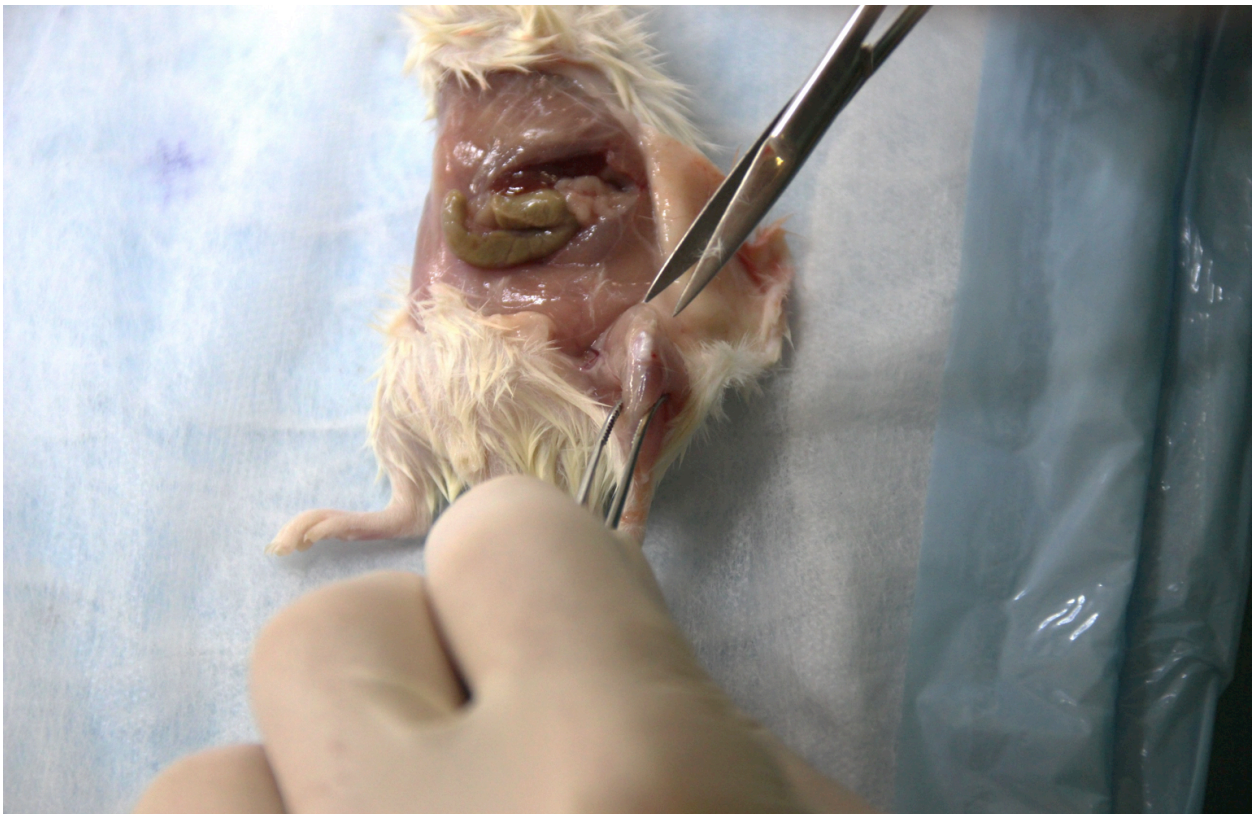

Figure 2.8.1: Dissection of the left hindlimb. Skin and spleen were removed by an anterior incision and the femurotibial joint is visible.

2.9 Histology

2.9.1 Sample preparation

Samples were fixed in paraformaldehyde 4% (PFA extra pure, Merck KGaA, Darmstadt, Germany) buffered with 0.1 mol/L phosphate buffer (AMRESCO Inc., Solon, OH, USA; pH 7.4) for 48 hours at 4°C. Samples were then decalcified in 10% ethylene diamine tetraacetic acid (EDTA, Fronine Laboratory Supplies, Taren Point, Australia; pH 7.0) for 21 days at 4°C. EDTA

was changed twice weekly. After the decalcification process, EDTA was removed with tap water and samples were transferred to an automated tissue processing machine (Leica TP 1020, Leica Microsystems GmbH, Wetzlar, Germany) for paraffin embedding. Samples were dehydrated in increasing concentrations of ethanol (50 v/v% 4 hours, 70 v/v% 4 hours, 95 v/v% 4 hours, 95 v/v% 4 hours, 100% 2 hours x 2, vacuum 2 hours) and cleared in xylene (vacuum 2 hours, 2 hours, vacuum 2 hours). Ankle joints were then embedded in double filtered paraffin wax (Paraplast Tissue Embedding Medium, Tyco Healthcare Group, Mansfield, MA, USA) before being cooled down on ice until they hardened.

Serial sections of 5 μm thickness were obtained in order to get a central lateral view of the ankle joint using a Leica microtome (Leica Microsystems GmbH, Wetzlar, Germany). Sections were mounted onto microscope slides coated with 3-aminopropyltriethoxysilane (AES, Sigma-Aldrich Inc., St. Louis, MO, USA).

2.9.2   Staining

2.9.2.1   Coating microscope slides with AES

Microscope slides were soaked in 60°C warm water and detergent 7x for 2 hours. Slides were then rinsed with cold water for 5 minutes and washed with distilled water twice for 5 minutes. Then the microscope slides were soaked in 80 v/v% ethanol for 2 hours before being dried in the warm room overnight. The next morning, the slides were dipped into AES solution (2%) for 30 seconds and then briefly dipped in acetone and distilled water. Slides were let to dry at room temperature overnight.

2.9.2.2   Staining preparation

Paraffin wax of mounted slides was melted on a hot plate (60°C) for 10 minutes. To dewax and rehydrate the slides, they were then dipped in 3 changes of xylene (each for 5 minutes) and 3 changes of 100% ethanol followed by 2 changes of 80% ethanol (each for 3 minutes). The microscope slides were rinsed with tap water and were then ready for staining.

2.9.2.3   H&E

The hematoxylin and eosin (H&E) stain is a crucial stain for any anatomical pathological diagnosis and gives a good overview of changes in affected bone material (149). Basophilic

structures such as cell nuclei and ribosomes appear violet-blue in the H&E stain, whereas eosinophilic structures such as cytoplasm present in a pink tone.

For the H&E staining process, hematoxylin (Lillie-Mayer's hemalum solution, Fronine Laboratory Supplies, Taren Point, Australia) and eosin (Eosin Y, Fronine Laboratory Supplies, Taren Point, Australia) were applied according to the following protocol. Slides were stained in hematoxylin for 7 minutes, carefully washed with tap water and stained with eosin for 10 minutes. This was followed by 3 changes of 100% ethanol (each for 3 minutes) and 2 changes of xylene (each for 2 minutes). Slides were then dried overnight at 37°C and mounted in DEPEX (BDH Ltd., Poole, UK) with a coverslip. Finished slides were rated by two individual investigators. Investigators were blinded to the sample being rated. Following an established scoring system (150), a score from 1 to 5 was given determining inflammatory cell infiltration, edema and hyperplasia of synovial lining.
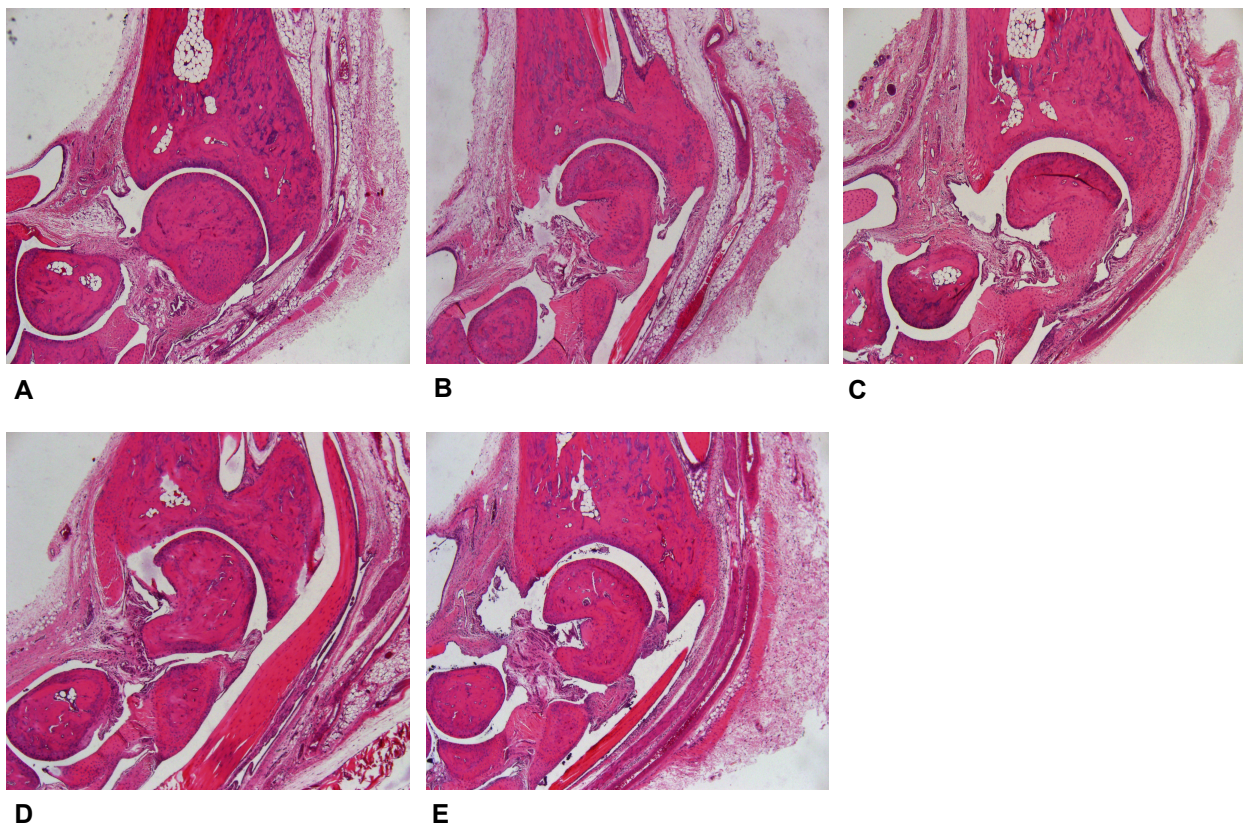
Figure 2.9.2.3.1: Joint inflammation in hematoxylin and eosin stain, 4x magnification. **A**: 0 = normal **B**: 1 = minimal infiltration of inflammatory cells in periarticular tissue **C**: 2 = mild infiltration **D**: 3 = moderate infiltration with moderate edema **E**: 4 = marked infiltration with marked edema **not depicted:** 5 = severe infiltration with severe edema. No picture of 5 shown, as none of the samples was rated 5. Scoring system adapted from Bendele et al., 1999 (150).

2.9.2.4   Toluidine blue

Toluidine blue is used histologically to interpret cartilage changes. Cartilage matrix is stained dark-blue, whereas structures such as cell nuclei and cytoplasm appear light blue. Therefore, proteoglycan contents and viability of cartilage tissue can be assessed (151, 152).

Slides were placed in toluidine blue solution (0.1%) for 15 minutes. Slides were then carefully rinsed with tap water and dried at 37°C overnight. Microscope slides were mounted with a coverslip in DEPEX (BDH Ltd., Poole, UK). Finished slides were again rated by two individual investigators, blinded to the sample being rated. Using an established scoring system (150), a score from 1 to 5 was given grading the loss of cartilage, chondrocytes and collagen disruption.
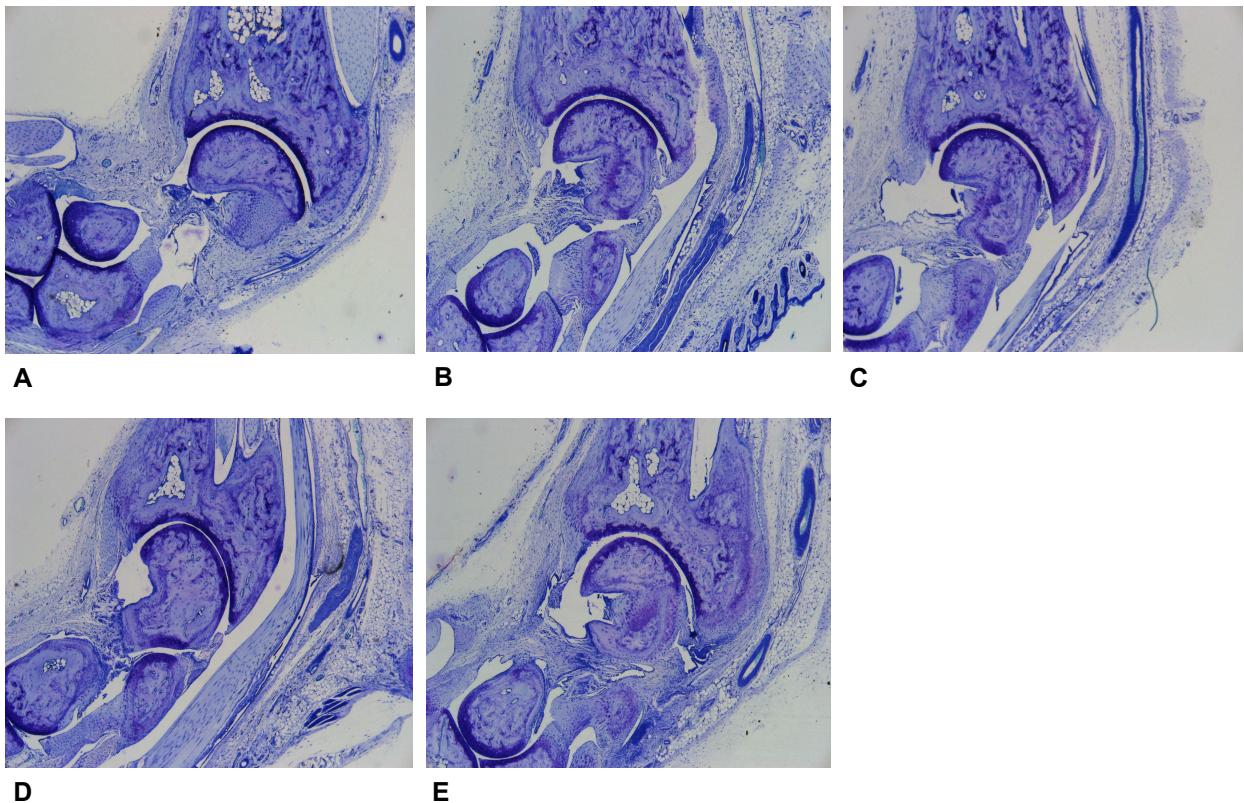
Figure 2.9.2.4.1: Cartilage damage and pannus scores in toluidine blue stain, 4x magnification. **A**: 0 = normal **B**: 1 = minimal-to-mild loss of cartilage evident with toluidine blue staining, with no obvious chondrocyte loss or collagen disruption **C**: 2 = mild loss of cartilage with toluidine blue staining, with mild focal (superficial) chondrocyte loss and/or collagen disruption **D**: 3 = moderate loss of cartilage with toluidine blue staining, with moderate multifocal (depth to middle zone) chondrocyte loss and/or collagen disruption **E**: 4 = marked loss of cartilage with toluidine blue staining, with marked multifocal (depth to deep zone) chondrocyte loss and/or collagen disruption **not depicted**: 5 = severe diffuse loss of cartilage with toluidine blue staining,

with severe multifocal (depth to tidemark) chondrocyte loss and/or collagen disruption. No picture of 5, shown as none of the samples was rated 5. Scoring system adapted from Bendele et al., 1999 (150).

2.9.2.5 TRAP

TRAP stain is a very sensitive marker for identifying and quantifying osteoclast activity and thus the process of bone resorption (153).

TRAP buffer consisting of sodium acetate anhydrous (50 mM, Fluka Chemie AG, Basel, Switzerland), potassium sodium tartrate (40 mM, pH 5.0, Sigma-Aldrich Inc., St. Louis, MO, USA) mixed with Milli-Q water and titrated to a pH of 5.0 with glacial acetic acid was created. The buffer was added to naphthol AS-MX phosphate (Sigma-Aldrich Inc., St. Louis, MO, USA), N,N-Dimethylformamide (Sigma-Aldrich Inc., St. Louis, MO, USA) and Fast Red Violet Luria Bertani salt (Sigma-Aldrich Inc., St. Louis, MO, USA) to create the TRAP stain which was then stored at 4°C for 7 days.

Dewaxed microscope slides were covered in TRAP stain for 0.5-2 hours depending on the speed of colour development. If colour had developed correctly, microscope slides were carefully rinsed with tap water to stop the reaction. Microscope slides were then counterstained with a 1:10 v/v solution of Harry's No. 3 haematoxylin (Fronine Laboratory Supplies, Taren Point, Australia) in Milli-Q water for 30 seconds. Again, microscope slides were carefully washed with tap water and dried overnight at 37°C. The following day, microscope slides were mounted with a coverslip using DEPEX (BDH Ltd., Poole, UK). Mounted and dried slides were rated by two individual investigators, blinded to the sample being rated, rated . An established scoring system with a ranking from 1 to 5 (150) was used to rate determined areas of bone resorption and to determine number of osteoclasts.
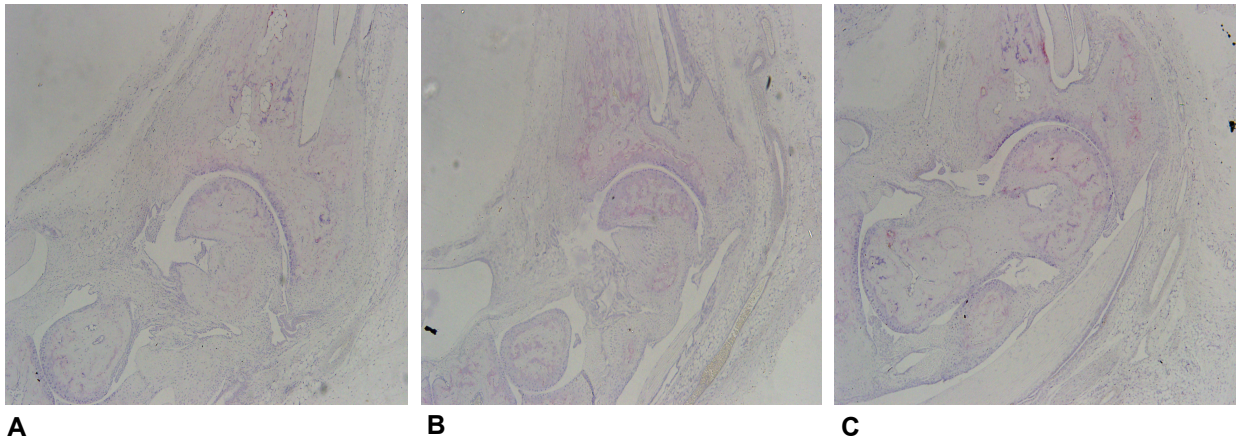
Figure 2.9.2.5.1: Bone resorption in TRAP stain, 4x magnification. **A**: 0 = normal **B**: 1 = minimal (small areas of resorption, not readily apparent on low magnification in the trabecular or cortical bone; few osteoclasts) **C**: 2 = mild (numerous areas of resorption, not readily apparent on low magnification in the trabecular or cortical bone, numerous osteoclasts) **not depicted**: 3 = moderate (obvious resorption of the medullary trabecular and cortical bone without full-thickness defects in the cortex; loss of some medullary trabeculae, lesion apparent on low magnification, numerous osteoclasts) **not depicted**: 4 = marked (full-thickness defects in the cortical bone, often with distortion of the profile of the remaining cortical surface, marked loss of the medullary bone, numerous osteoclasts, no resorption in the smaller tarsal bones) **not depicted**: 5 = severe (full-thickness defects in the cortical bone, often with distortion of the profile of the remaining cortical surface, marked loss of the medullary bone, numerous osteoclasts, resorption also present in the smaller tarsal bones). No pictures of 3, 4 or 5 shown, as none of the samples was rated 3, 4 or 5. Scoring system adapted from Bendele et al., 1999 (150).

2.10 Micro-CT

Micro-CT analysis has shown to be a reliable method for the assessment of 3-dimensional bone morphology to determine skeletal changes in rodents (154). CT images are computer-generated transverse images rendered from multiple (circular) X-ray images and obtained through the detection of X-rays absorbed by an object or sample. X-rays are created by a vacuum tube which serves as a radiation source. The term micro-CT is used to describe the pixel size of the images which is in the μm scale.

A Skyscan 1172 X-ray microtomograph (Bruker microCT, Kontich, Belgium) was used in combination with a Microsoft computer and CT analysing software (Bruker microCT, Kontich, Belgium) for image reconstruction. For the *in vitro* scanning, tibiotalar joints (including tibia)

were placed in the standard specimen holder. A piece of aluminium foil (1 mm) was attached as a correction filter to minimize the effect of beam hardening and artefacts in the processed images. Scans were done at 100 kV, 100 µA and a shutter speed of 590 milliseconds. With a resolution of 6.93 µm/pixel, 1,800 X-rays were collected for each scan. A modified Feldkamp cone-beam algorithm with beam hardening of 50% correction was used.
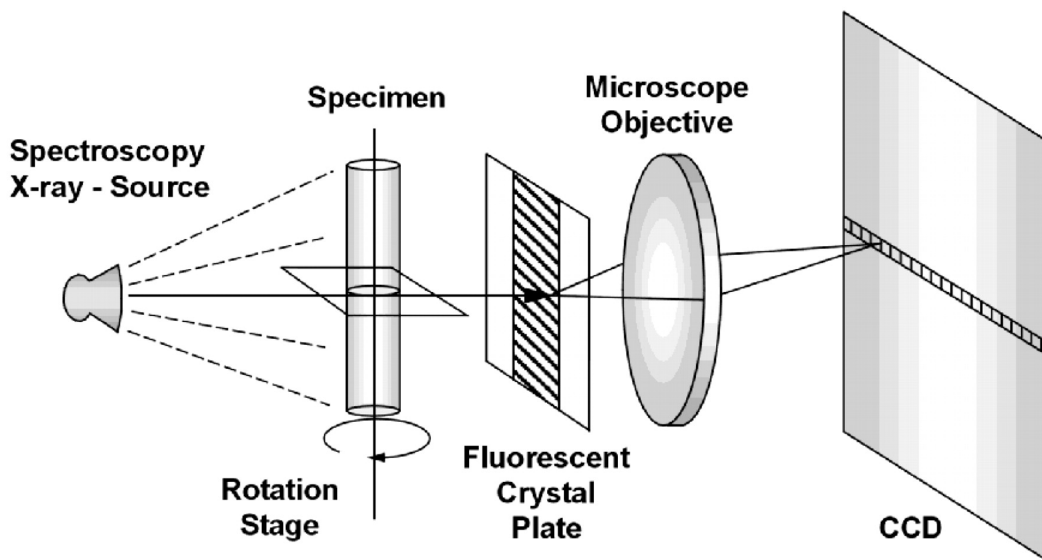

Figure 2.10.1: Schematic micro-CT set-up. Adapted by Bentley et al. 2002 (155) from Ritman et al. (156). CCD: Charged-couple device.

For analysis of the trabecular bone, CT analysing software (version 1.02, Bruker microCT, Kontich, Belgium) was used to define an area in the tibia that could be measured equally in all mice. The final 2-dimensional cross-section still showing the tibial growth plate with a joined medial and lateral aspect was therefore determined as a fixed point. A starting point for the trabecular measurements was defined as 66 slides (= 0.5 mm) distally to the fixed point. 132 slides (= 1 mm) distal to the fixed point were analysed and included in the region of interest (ROI).

The ROI was free hand-drawn around the bone in every cross-section in a circular manner using a computer mouse. Therefore, analysing all surfaces of the skeletal tibia above the length of 1 mm was possible. Every cross-section was checked for its ROI to only include parts of the tibia and to exclude all fibular elements. The binary images viewing mode was used to control the selected ROIs. The ROIs appear in a binary black-and-white mode while the unselected rest of the image appears in green. A selection of the grey scale index from 70 to 250 was applied to separate bone tissue (appearing white) from other tissues (appearing black) such as bone

marrow, muscle and other soft tissue. ROIs were used to measure the following morphological parameters in order to determine the bone's structure, density and volume:

- **BV/TV**: bone volume/total volume (%)

- **Tb.Sp:** trabecular separation (μm)

- **Tb.Th:** trabecular thickness (μm)

- **Tb.N:** trabecular number (/mm)

Based on the micro-CT images of the ankle joints, a semi-quantitative score was used to assess bone erosion of the cortical bone. Similar to the trabecular measurements, a fixed point was determined by using the last 2-dimensional cross-section that showed parts of the tibia, the fibula, the calcaneus and the last proximal segment of the talus.
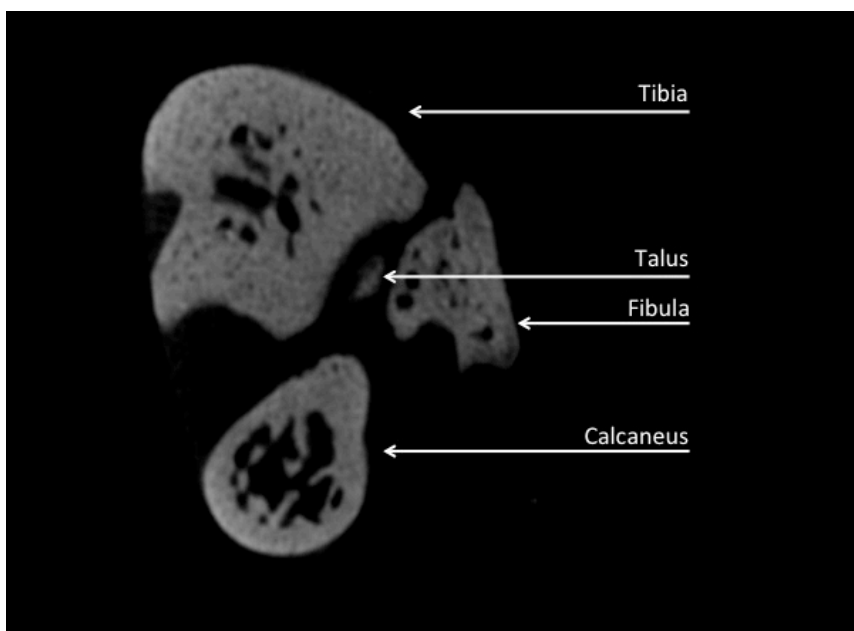
Figure 2.10.2: Coronal micro-CT cross-section of the ankle displaying the fixed point that shows the tibia, fibula, calcaneus and talus.

30 slides (= 0.2 mm) proximal of the fixed point the starting point was determined, and 132 slides (= 1 mm) proximally of the starting point were defined as the ROI. Every ROI was rated with a value ranging from 0 to 3.
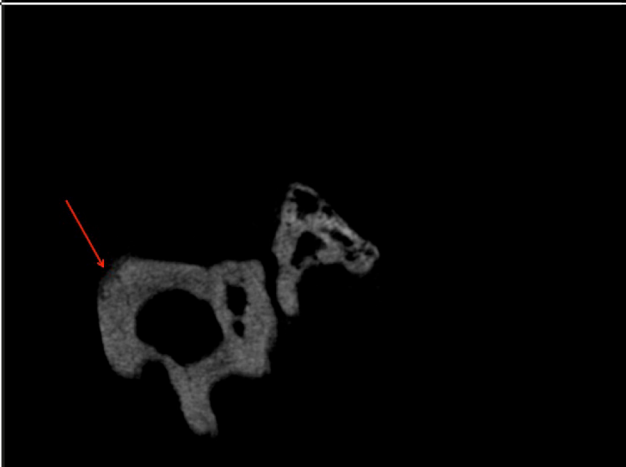
0 = no changes	
1 = mild bone transformation	
2 = moderate changes with erosions and vacuoles	
3 = severe changes with a partial or complete breakthrough of the corticalis	

Figure 2.10.3: Semi-quantitative bone erosion score to assess cortical bone changes. 0 = no changes, 1 = mild bone transformation, 2 = moderate changes with erosions and vacuoles, 3 = severe changes with partial or complete breakthrough of the corticalis. No picture of 3 shown as none of the samples were rated 3.

2.11 Histomorphometric analysis

TRAP stained tibia sections were used to morphologically identify different types of bone cells (osteoblasts, osteocytes and osteoclasts) and therefore the processes of bone resorption and formation. A light microscope (Leica Microsystems GmbH, Wetzlar, Germany) with a magnification of 100 was used to identify the growth plate of the tibiae. Photos were taken for documentation using QCapture Software (Quantitative Imaging Corp., Surrey, Canada). At a magnification of 200, the centre of the growth plate was identified as a fixed point. 300 μm distally, a total of 6 squares (400 μm x 400 μm) in 3 rows were analysed and defined as ROI using Bioquant Osteo II System (version 8; Bioquant Image Analysis Corp., Nashville, TN, USA). Analyses were performed by 2 independent and blinded investigators and averaged. Manual measurements were performed by free hand using a computer mouse to define cell types and surfaces in order to acquire results for the following histomorphometric parameters:

- **BV/TV**: bone volume/total volume (%). Percentage of newly formed bone volume of total tissue volume at defect site

- **Ob.S/BS**: osteoblast surface/bone surface (%). Percentage of bone surface covered with osteoblasts

- **N.Oc/BS**: number of osteoclasts/bone surface (per mm). Mean number of osteoclasts per mm bone surface

- **Oc.S/BS**: osteoclast surface/bone surface (%). Percentage of bone surface covered with osteoclasts

2.12 Statistical analysis

Normally distributed data between 2 groups were compared using the t-test. Comparing non-normally distributed data of 2 groups was done using the Mann-Whitney test. Values are mean values unless stated otherwise, and the standard deviation was calculated for all means. Results for body weight, ankle size and clinical score were measured using repeated-measures-analysis (RMA), a generalised linear model used for longitudinal studies. To control the overlay of arthritis and growth processes in our experiments, RMA were conducted uncorrected, corrected for growth rate and with testing for potential confounders, i.e. ankle size, on day 0 and body weight on day 0 as an adjusting covariate.

The growth rate was calculated from the linear correlation of a time-dependent growing ankle size over the body weight of the CTR animals. The calculated growth effect was then subtracted from the ankle size (arthritis effect = measured ankle size – growth effect). If the Mauchly-test was significant sphericity was disregarded, and the Greenhouse-Geisser correction was used. If the Mauchly-test wasn't significant sphericity was assumed, and the assumed sphericity value was used. If the Mauchly-test could not be calculated (due to extreme distribution), the Greenhouse-Geisser correction was used.

As body weight on day 0 in 5-week-old mice was significantly different between WT KRN and tg KRN groups and had an influence on body weight over the course of time, RMA for ankle size was corrected for growth rate using day 0 as the adjusting covariate. Taken from the RMA, the P_{KRN} values represent interaction day x group of within-subjects effects. The P_{KRN} values are the significance of difference in the time course of tg KRN and WT KRN mice. For statistical analysis, IBM SPSS version 19.0 software (IBM, Armonk, NY, USA) was used, and p values less than 0.05 were considered significant.

3 RESULTS

3.1 5-week-old arthritic Col2.3-11β-HSD2 tg mice versus arthritic WT mice

3.1.1 Body weight

To compare our findings with those of previous studies, we chose 5-week-old mice. Mice at 5 weeks of age still grow but show the full phenotype of arthritis after administration of K/BxN serum.

There was a significant difference in mean body weight between K/BxN arthritic Col2.3-11β-HSD2 tg (tg KRN) mice and their K/BxN arthritic WT (WT KRN) littermates on day 0 (p = 0.001). The body weight on day 0 had an influence on the increase in body weight over the course of time (p = 0.044). Furthermore, there was a significant difference between all 4 experimental groups over the course of the whole experiment (p = 0.001). A gain in body weight was equally seen in tg (tg KRN and tg CTR) and WT (WT KRN and WT KRN) mice with a tendency of tg mice to catch up with the initial weight difference present on day 0.
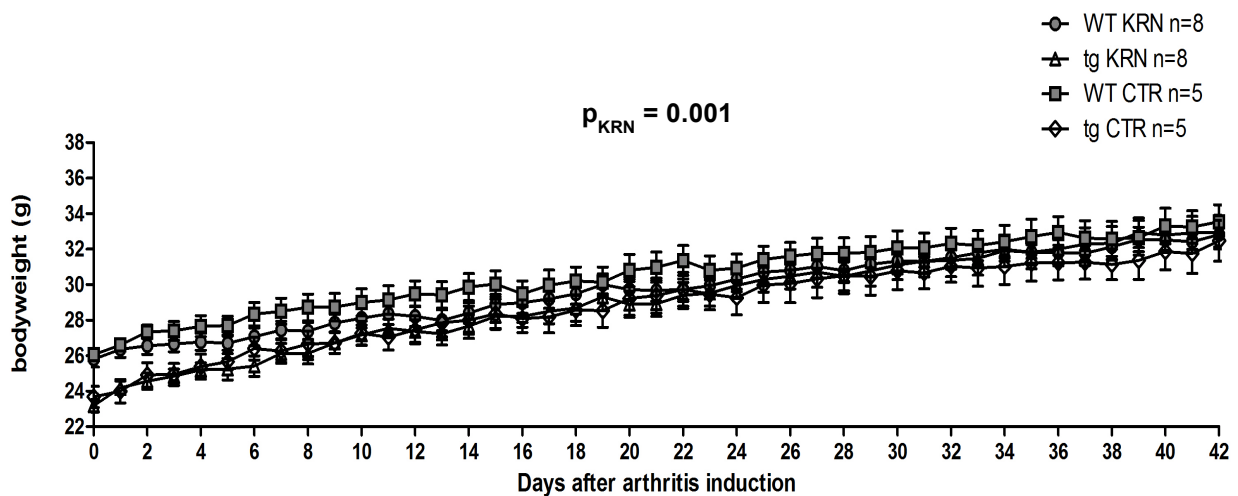

Figure 3.1.1.1: Development in body weight over 42 days of arthritic WT KRN and tg KRN mice after injection of K/BxN serum and of non-arthritic WT CTR and tg CTR mice after PBS injection. Through RMA the p_{KRN} value represents the defined significance of difference between all 4 groups.

3.1.2   Average ankle size

As body weight on day 0 had an influence on the increase in body weight over time, we aimed to minimize the influence of an overlay-effect of growth processes and arthritis itself. We therefore applied RMA to the average ankle size with correction for growth rate.

All mice in the tg and WT group treated with K/BxN serum developed acute arthritis. Arthritis peaked approximately on day 10, was followed by a plateau phase and gradually decreased from day 24 onwards. Ankle size measured daily on both rear paws showed no significant difference between tg KRN mice and their WT KRN littermates on day 0 (p = 0.247). The initial ankle size as well as body weight on day 0 had no influence on the ankle size over time.

We found no statistically significant difference in mean ankle size over time. However there was a tendency of bigger ankle sizes in WT KRN mice compared to the animals of the tg KRN group over the course of 42 days after injection of K/BxN serum on day 0 and day 2.
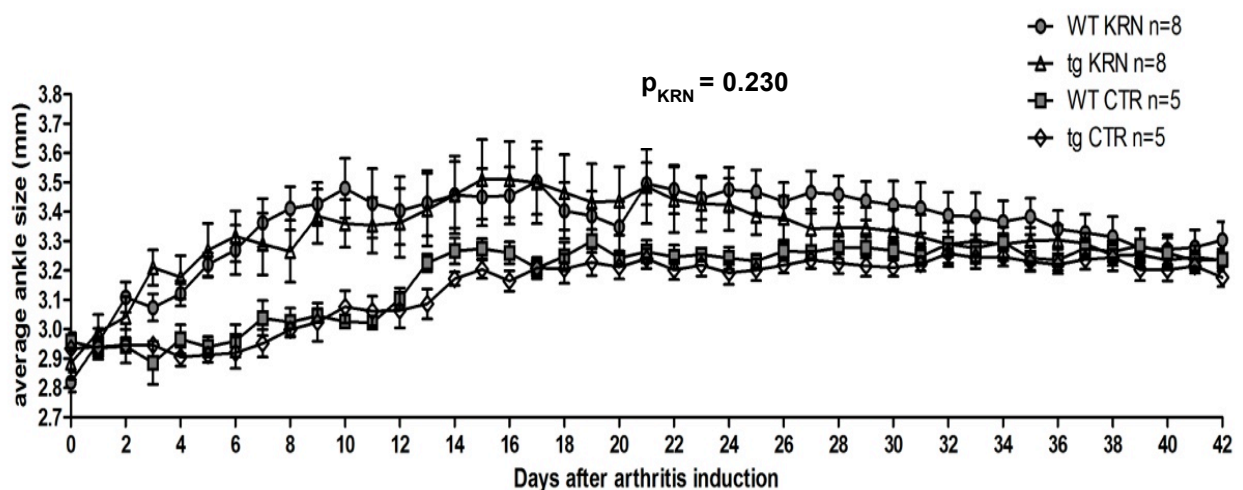

Figure 3.1.2.1: Development in average ankle size over 42 days of arthritic WT KRN and tg KRN mice after injection of K/BxN serum and non-arthritic WT CTR and tg CTR mice after PBS injection. Through RMA the p_{KRN} value represents the defined significance of difference in tg KRN and WT KRN mice after correction for growth rate.

3.1.3   Clinical score

There was no significant difference in the clinical score between the tg KRN and the WT KRN group. The score was assessed every day for a total of 42 days. The clinical score needed no

correction for growth rate, as a score of 0 was given to all animals on day 0 and the growth rate had no influence on the time course of the clinical score.
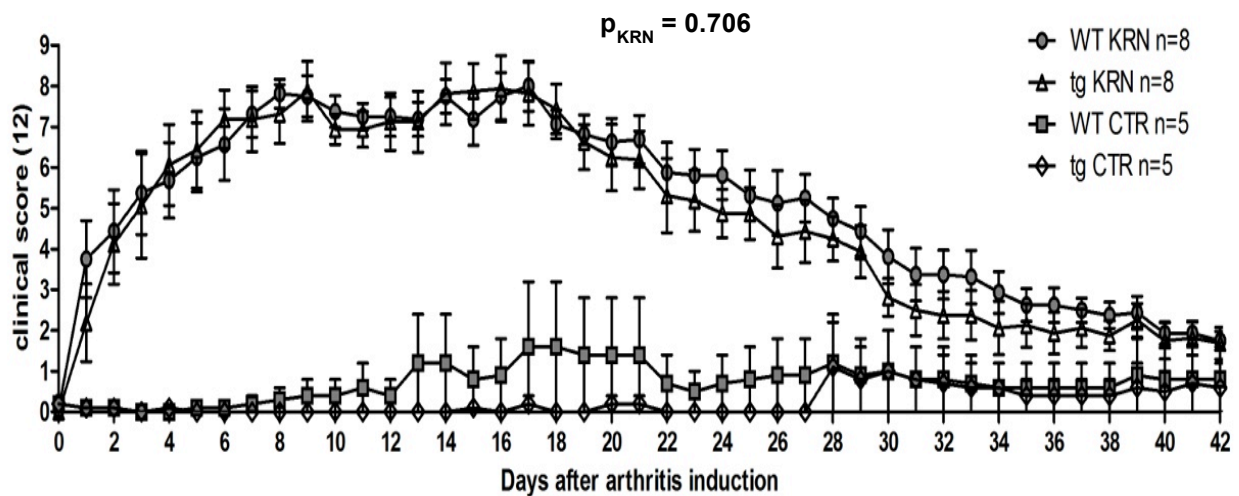

Figure 3.1.3.1: Course of clinical score over 42 days of arthritic WT KRN and tg KRN mice after injection of K/BxN serum and non-arthritic WT CTR and tg CTR mice after PBS injection. Through RMA the p_{KRN} value represents the defined significance of difference in tg KRN and WT KRN mice.

3.1.4   Histology

The histological assessment of harvested ankles on day 42 showed a significant difference in inflammation score (H&E stain) (p = 0.04) between the WT CTR and the WT KRN group. We were also able to show a significant difference (p = 0.03) between the WT CTR and tg CTR group in inflammation. Furthermore, a significant difference (p = 0.03) was observed in cartilage degradation (toluidine blue stain) between the WT CTR and the WT KRN mice. A tendency, but no significant difference could be shown for tg CTR mice versus tg KRN mice in inflammation and cartilage degradation. The difference between WT KRN mice and tg KRN mice was not significant, but tg KRN mice tended to score lower than WT KRN littermates in inflammation and cartilage degradation. WT KRN and tg KRN groups showed no significant difference concerning bone erosion (TRAP stain), however, a similar trend as in inflammation and cartilage degradation was observed, showing more bone erosion in the K/BxN serum injected WT KRN and tg KRN mice compared to the CTR groups. Further, there was no significant difference between tg KRN mice and WT KRN mice regarding bone erosion, yet the bone erosion score was higher for tg KRN mice.
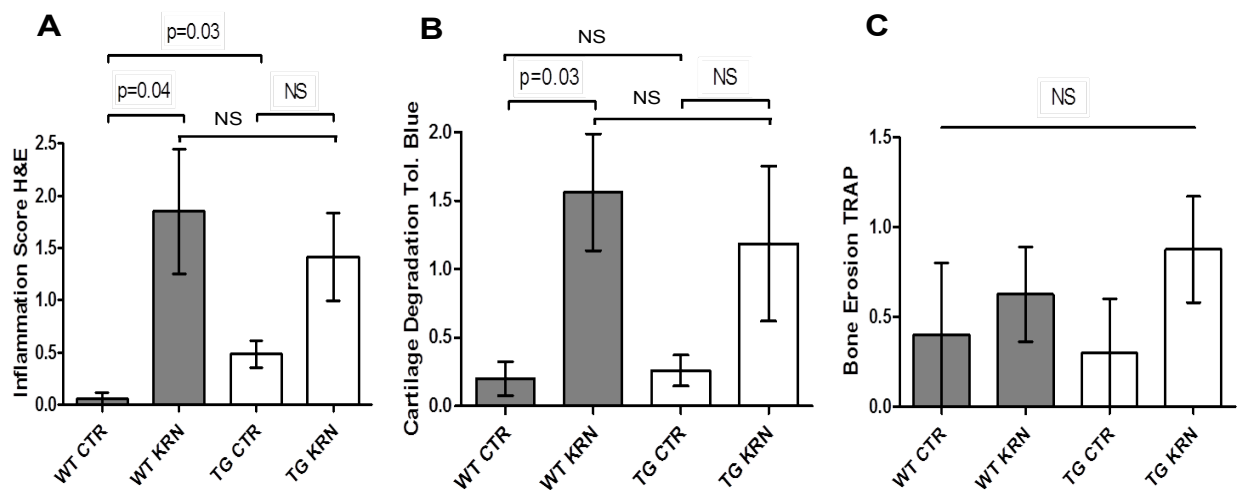
Figure 3.1.4.1: Histological assessment of ankle joints of arthritic WT KRN and tg KRN mice after 42 days of K/BxN arthritis after injection of K/BxN serum and of non-arthritic WT CTR and tg CTR mice after PBS injection. Histopathological scores for inflammation (A), cartilage degradation (B) and bone erosion (C).
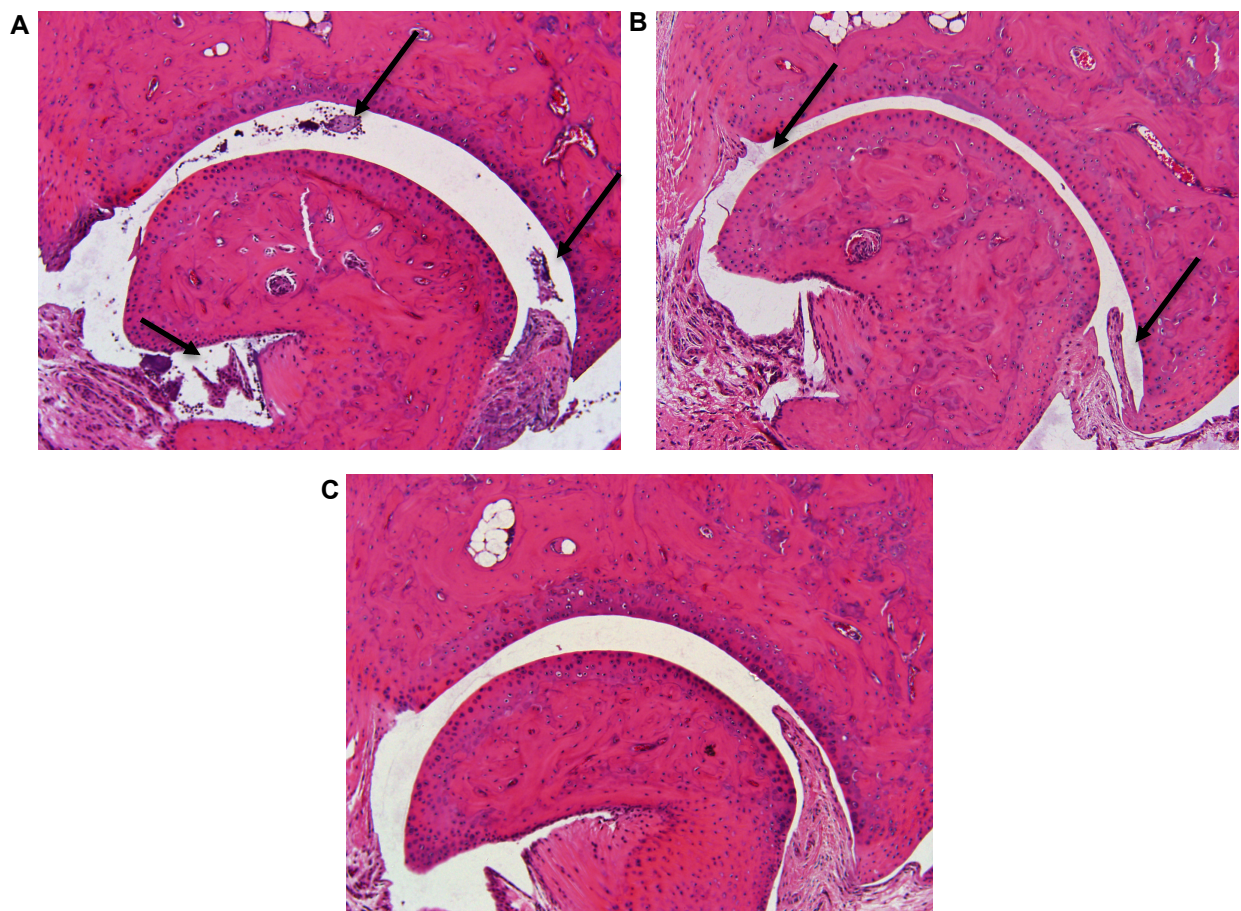
Figure 3.1.4.2: 10x magnification of 3 representative H&E stained microscope slides showing inflammation of the ankle of a WT KRN mouse which was rated 4 with marked infiltration and marked edema (A), versus the ankle of a tg KRN animal which was rated 2 with mild infiltration (B), and the ankle of a non-arthritic WT CTR mouse which was rated 0 with no changes (C).
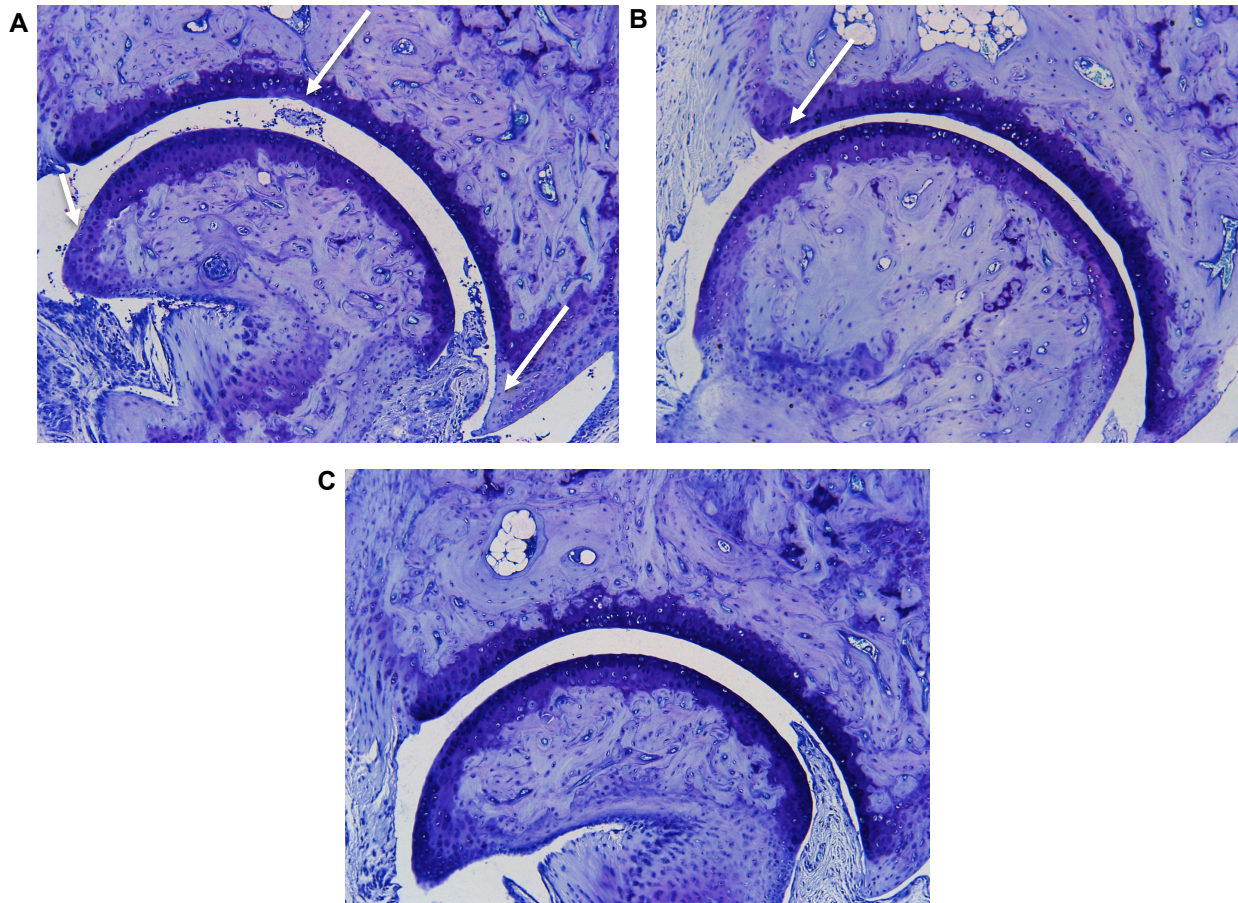

Figure 3.1.4.3: 10x magnification of 3 representative toluidine blue-stained microscope slides showing cartilage damage of the ankle of a WT KRN animal which was rated 3 with moderate loss of cartilage (A), versus the ankle of a tg KRN mouse which was rated 1 with minimal cartilage damage (B), and the ankle of a non-arthritic WT CTR mouse which was rated 0 with no changes (C).
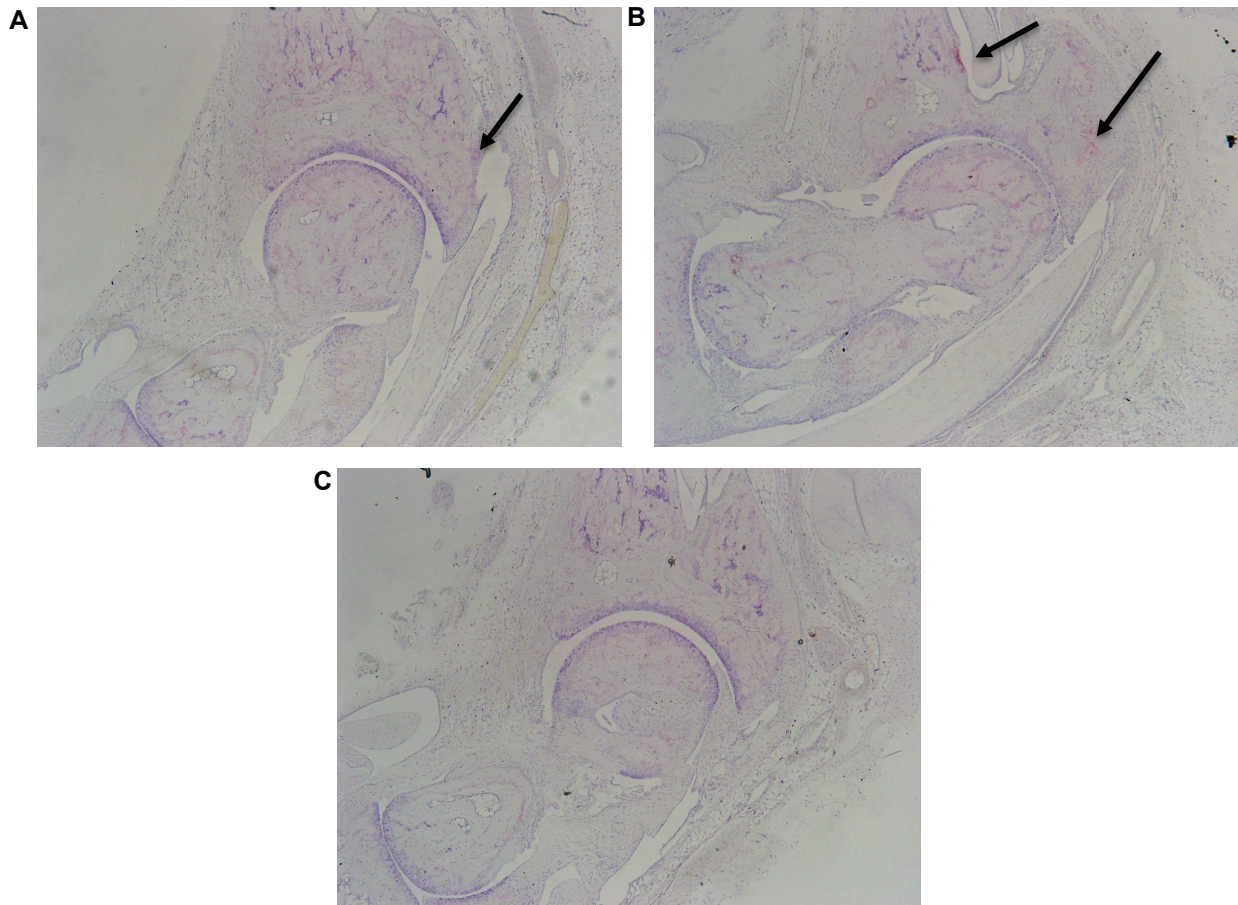
Figure 3.1.4.4: 4x magnification of 3 representative TRAP-stained microscope slides showing bone erosions of the ankle of a WT KRN mouse which was rated 2 with numerous areas of resorption (A), versus the ankle of a tg KRN animal which was rated 1 with small areas of resorption (B), and the ankle of a non-arthritic WT CTR mouse which was rated 0 with no changes (C).

3.1.5 Micro-CT

With the exception of a difference in trabecular separation (Tb.Sp) between both CTR groups (WT CTR and tg CTR) for the tibia, no significant group difference was revealed in micro-CT analyses.
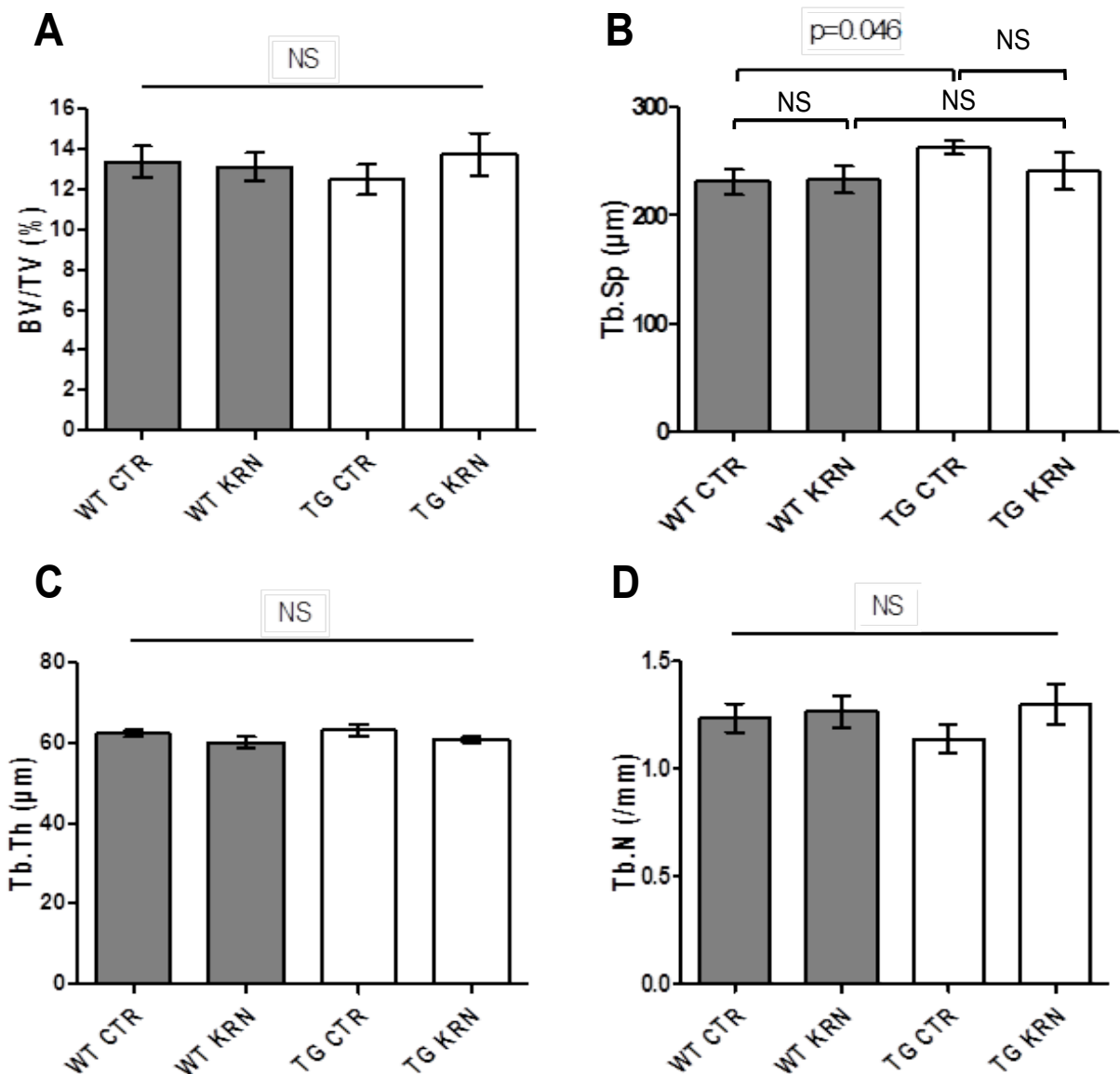
Figure 3.1.5.1: Micro-CT analysis of tibial samples of WT KRN and tg KRN mice after 42 days of K/BxN-arthritis after injection of K/BxN serum and of non-arthritic WT CTR and tg CTR mice after PBS injection. BV/TV in % (A), Tb.Sp in μm (B), Tb.Th in μm (C) and Tb.N in /mm (D).

Bone turnover was quantified through micro-CT analysis of the cortical bone of the tibia at site of the ankle joint. The semi-quantitative evaluation of cross sections of tibia and fibula did not show any significant differences in structural bone changes between tg KRN and WT KRN mice.
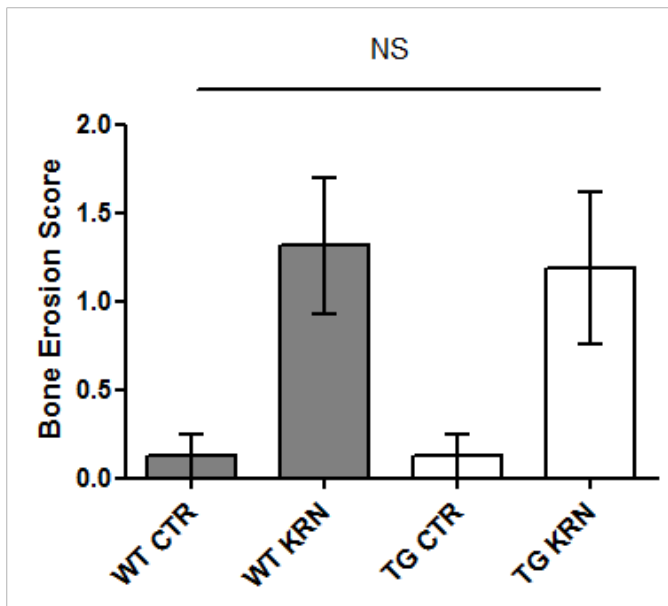
Figure 3.1.5.2: Micro-CT based semi-quantitative score of bone turnover of ankle joint cortical bone of WT KRN and tg KRN mice after 42 days of K/BxN arthritis after injection of K/BxN serum and non-arthritic WT CTR and tg CTR mice after PBS injection.
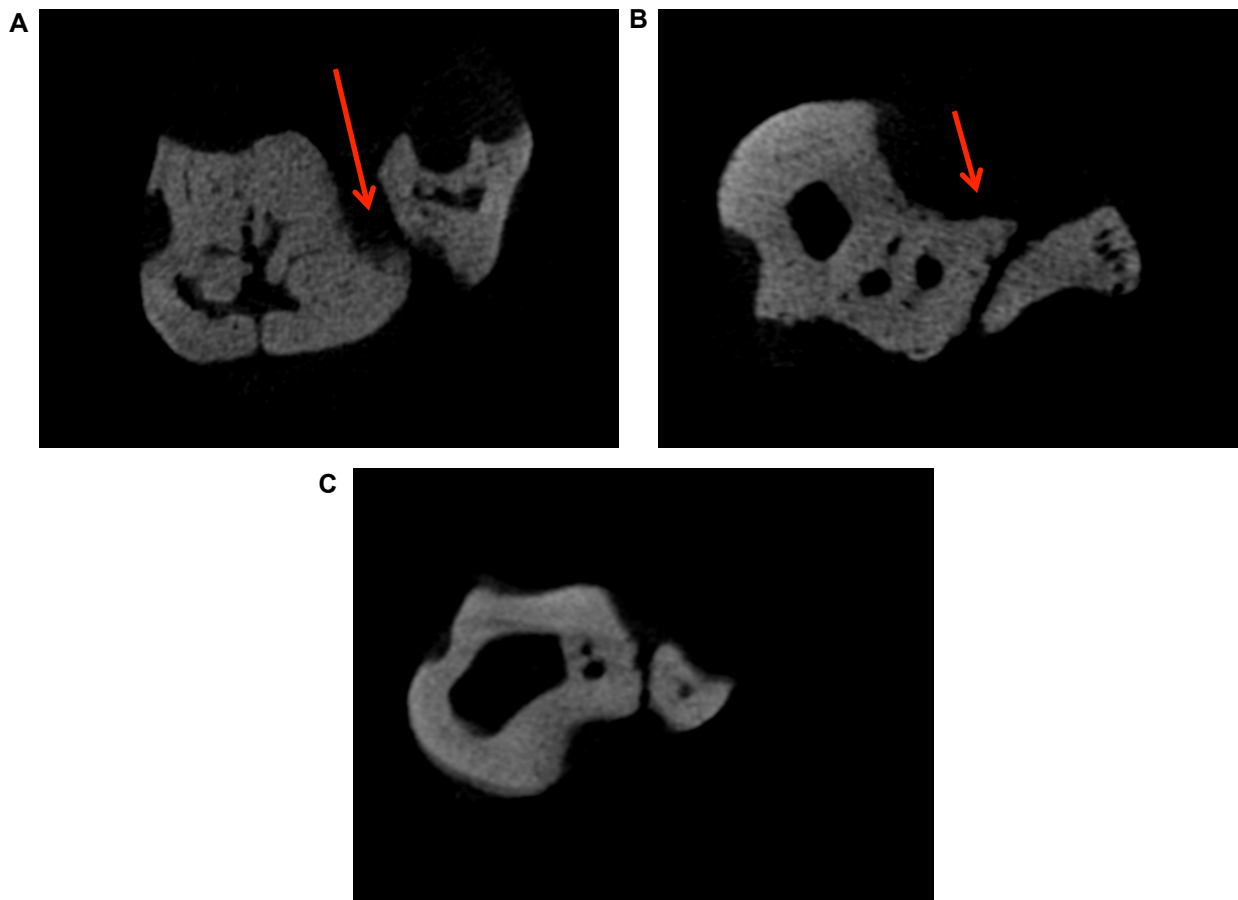
Figure 3.1.5.3: ROIs of 3 representative 2-D micro-CT slides of the lower limb of a WT KRN mouse which was rated 2 with moderate changes with erosions and vacuoles (A), versus the lower limb of a tg KRN animal which was rated 1 with mild bone transformation (B), and the lower limb of a non-arthritic WT CTR which was rated 0 with no changes (C).

3.1.6   Histomorphometry

The histomorphological analysis of the tibia showed no significant difference after 42 days of K/BxN serum-induced arthritis in bone formation (Ob.S/BS), however there was a significantly greater N.Oc/BS in WT KRN mice compared to the WT CTR group (p = 0.045), which can be attributed to bone resorption. Further, we found that tg CTR mice had a significantly higher number and greater surface of osteoclasts (N.Oc/BS and Oc.S/BS) compared to WT CTR mice (p = 0.008). The surface of osteoclasts was significantly smaller in arthritic tg KRN mice compared to the non-arthritic tg CTR mice (p = 0.02).
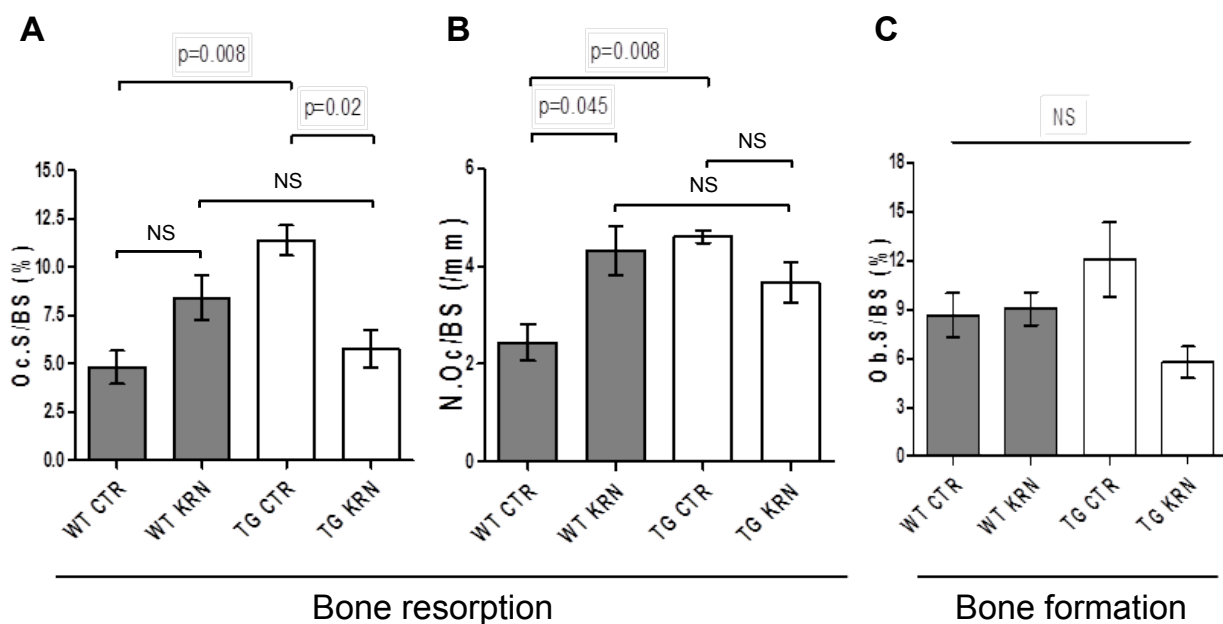

Figure 3.1.6.1: Histomorphological analysis of tibial samples of WT KRN and tg KRN mice after 42 days of K/BxN arthritis and non-arthritic WT CTR and tg CTR mice after PBS injection. Oc.S/BS in % (A) and N.Oc/BS in /mm (B), both representing bone resorption, and Ob.S/BS in % (C), representing bone formation.

3.1.7   Spleen weight

Mean spleen weight showed a significant difference between tg KRN mice and tg CTR group (p = 0.004). No significant difference was observed between tg KRN and WT KRN after 42 days of K/BxN arthritis.

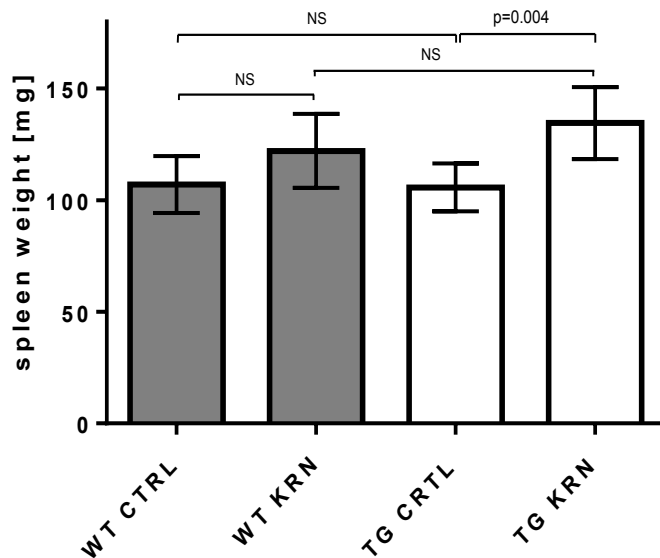Figure 3.1.7.1: Mean spleen weight on day 42 of WT KRN and tg KRN mice after injection of K/BxN serum and non-arthritic WT CTR and tg CTR mice after PBS injection.

3.2   8-week-old arthritic Col2.3-11β-HSD2 tg mice versus arthritic WT mice

In order to further minimize the possible altering effects of arthritis and growth processes, we repeated the experiments on 8-week-old Col2.3-11β-HSD2 tg and WT mice opposed to those 5 weeks of age on day 0. K/BxN serum or PBS was injected in the same fashion on days 0 and 2. With this approach, there was no significant difference between WT KRN and tg KRN in body weight and ankle size on day 0. As there was no influence of the body weight on day 0 on the increase of body weight over the course of time, no correction for growth rate was necessary in the RMA used. Although we were able to implement arthritis in all animals of the WT KRN and tg KRN groups, no significant differences in ankle size or clinical score were observed at any timepoint in the 2 groups. As we obtained the results from ankle size and clinical scores for the 8-week-old mice (on day 0), we decided not to analyze the animals further, as no changes to the previous findings were expected.

3.2.1 Body weight
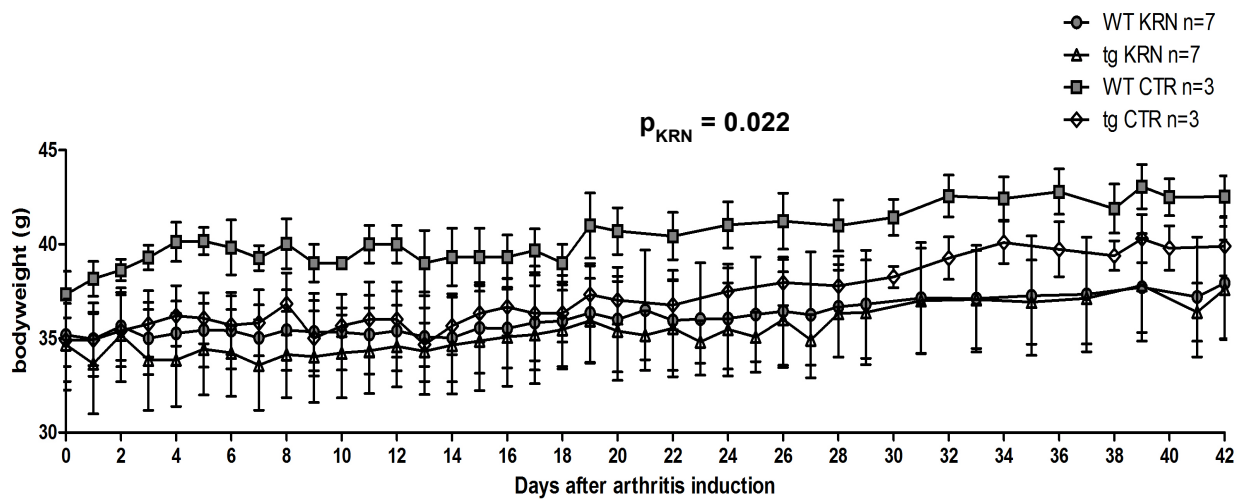
Figure 3.2.1.1: Development in body weight over 42 days of WT KRN and tg KRN mice after injection of K/BxN serum and non-arthritic CTR mice after PBS injection. Through RMA, the p_{KRN} value represents the defined significance of difference in all 4 experimental groups.

3.2.2 Average ankle size

Figure 3.2.1.1: Course of average ankle size over 42 days of WT KRN and tg KRN mice after injection of K/BxN serum and non-arthritic WT CTR und tg CTR mice after PBS injection. Through RMA, the p_{KRN} value represents the defined significance of difference in tg KRN and WT KRN mice.

3.2.3 Clinical score
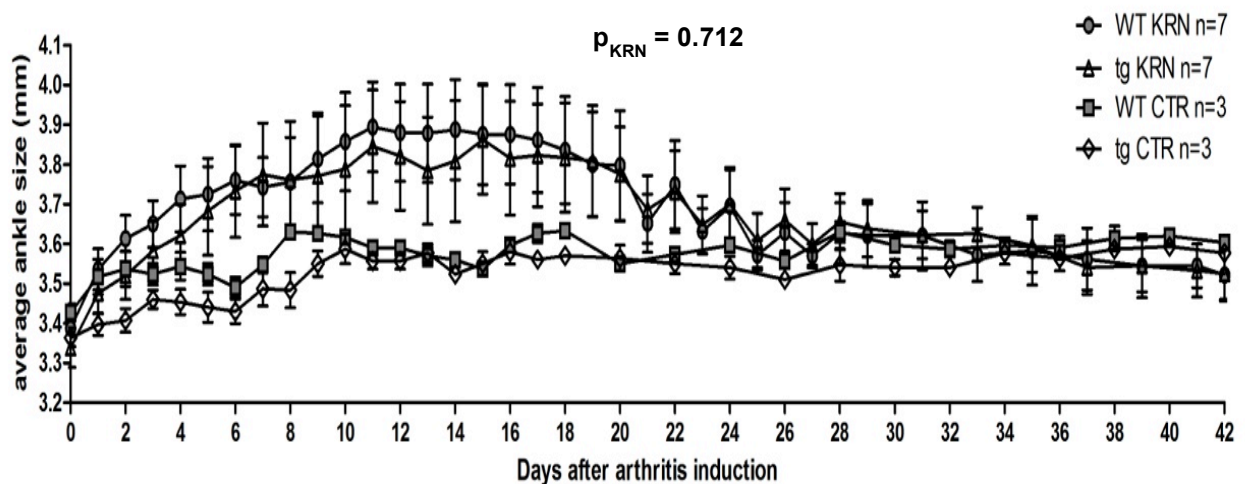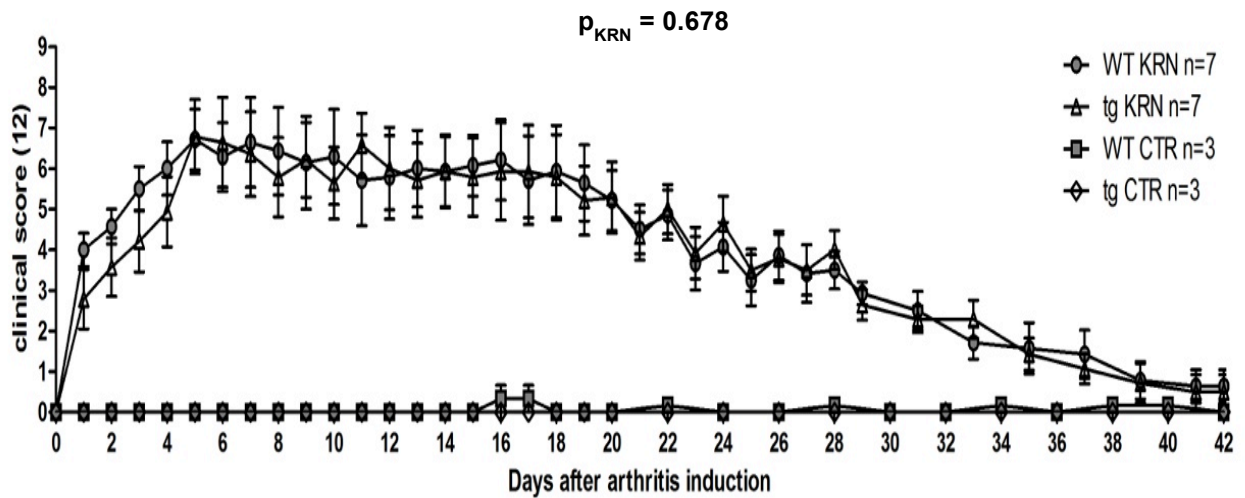

Figure 3.2.3: Course of clinical score over 42 days of WT KRN and tg KRN mice after injection of K/BxN serum and non-arthritic WT CTR and tg CTR mice after PBS injection. Through RMA the p_{KRN} value represents the defined significance of difference in tg KRN and WT KRN mice.

4 DISCUSSION

4.1 Discussion of the K/BxN serum transfer arthritis model and Col2.3-11β-HSD2 mice

In the present study, we were able to successfully display the clinical course of K/BxN arthritis *in vivo* in a long-term experiment over 42 days. All experimental mice that received K/BxN serum showed pronounced signs of arthritis. After peaking around day 10, the clinical signs of arthritis declined for the remaining duration of the experiment. We were not able to show significant differences between WT KRN mice and tg KRN mice with disrupted GC signalling in mature osteoblasts and osteocytes. Yet, the tendencies we saw in our experimental results are in line with the results of Buttgereit et al.'s study from 2009 which investigated the acute state of arthritis over 14 days in the same murine model (146). Our results revealed a tendency towards a more pronounced inflammation and cartilage degradation in WT KRN mice compared to their tg KRN littermates. The same was the case for bone erosions, yet again, none of the findings reached statistical significance. It is plausible that this is due to changes in the genomic status of the experimental animals used in this study compared to the mice used in the experiments from 2009.

Previously, the K/BxN serum transfer mouse model has been successfully used to study causes and effects of inflammatory arthritic diseases. The model mainly mimics aspects of human RA but may also be valuable for other less reported arthritides in man. It is a highly effective model to induce severe arthritis within several days, and it is a valuable model to uncover the effector mechanisms and clinical course of the disease (157). Well-documented clinical and histological outcome measures of arthritis and established animal methods allowed us to use this model as a reliable tool to study various aspects of RA.

In our study, we used the K/BxN serum transfer mouse model in Col2.3-11β-HSD2 tg mice and their WT littermates. Our aim was to observe the disease in tg animals which - through pre-receptor overexpression of the GC-inactivating enzyme 11β-HSD type 2 in mature osteoblasts and osteocytes - provided a suitable genetic background to study the effects of endogenous GCs on bone in the effector and resolution phase of K/BxN arthritis. The effector phase relies on antibody-dependent components, such as ICs, complement, and Fc receptors, which are responsible for activating effector cells such as neutrophils and macrophages. One point of critique of the K/BxN model is that it only mimics the effector phase but not the priming phase of the immune response (157). The priming phase is defined by the first contact of a B or T cell

with an antigen and the following differentiation into effector B or T cells. The priming phase is, however, present in for example the CIA (collagen-induced arthritis) model (see below). It is therefore only possible to study one particular phase of RA pathogenesis in the K/BxN model (158). Christensen et al. suggested connecting the different animal models to a RA "pathogenesis map". This helpful tool could assist researchers when trying to choose the appropriate type of animal model for their study and further help in designing future studies to create a more complete picture of RA pathogenesis (157).

Mice as experimental organisms have proven to be immensely valuable for studying and mimicing human pathophysiology. The advances in genomic manipulation have made possible the creation of mouse models of human diseases and the discovery of numerous therapeutic regimens. Altering genomics, however, also has its limitations and critical parameters. Unwanted gene mutations can occur as a result of the integration of transgenes into mouse genomes. Due to the random nature of transgene integration, there is a chance of inactivating normal gene sequences which may only appear in homozygotes as a result of haploinsufficiency. Transgene silencing, which is the insertion of the transgene into a transcriptionally inactive region, may lead to a lack of transcript through the positional effect. This silencing effect appears when mice with a high reproduction number age. If the transgene is unexpectedly inserted near a promoter, it may lead to a "leaky" expression, meaning that the gene expression will decrease and eventually stop after several generations. Finally, mosaic mice and accidentally mixed mice are another sporadically reported issue when using tg mouse models (159). To reduce the incidence of these unwanted effects, thorough genotyping was performed on DNA from 9-to-12-day-old pups. Repeated PCR analysis was performed at a later time point to confirm genotypes. However as mentioned before, it cannot be ruled out that a change in the genomic status has occurred which could explain the lack of significance in our study compared to results from previous experiments.

Furthermore, it is worth noting that there is a body weight difference between genders in experimental mice. This difference is also apparent in the size of the skeleton. In order to rule out this confounder, we used only male mice in the present study. As reported previously, we also observed that Col2.3-11β-HSD2 mice were smaller than their WT littermates (100).

4.2 Discussion of 11β-HSD type 2

In 1988, Funder proposed that the connection between 11β-HSD type 2 and aldosterone-specific tissues lies in the enzyme and not the receptor (66), yet he also questioned the overall relevance of the 11β-HSD type 2 in terms of GC inactivation in a review from 2005 (160). Funder points out that a natural ratio of plasma-free cortisol to aldosterone of 100:1 is unlikely to be altered to a much lower intracellular concentration of cortisol by 11β-HSD type 2 (160). Experiments have shown that in classical epithelial aldosterone target tissues like kidney or colon, normal working 11β-HSD type 2 will not exclude GCs from MRs but actually leave MRs occupied in a great number by GCs, however these MRs will not be activated by GCs. The mechanism behind this phenomenon remains unknown. If 11β-HSD type 2 is blocked, GCs activate MRs as seen in the syndrome of AME. GCs therefore seem to "block" MRs and deprive MCs of the chance to bind and activate their receptor if 11β-HSD type 2 is active (160). So, although experiments have shown that the Col2.3-11β-HSD2 mouse model shows GC disruption (100, 146, 161, 162), Funder's remarks are worth noting and could initiate a discussion of whether mechanisms, which need yet to be determined, could fully explain the role of 11β-HSD type 2 in altering the actual ratio between active cortisol and inactive cortisone.

Another important point concerning 11β-HSD type 2 is its tg instability over time. The mice used in this experiment did not have a tg overexpression of 11β-HSD type 2 in 100% of the targeted cells. It has been reported that the transgene can undergo a loss of expression over time and in the course of breeding (163).

4.3 Discussion of statistical analysis, study design and other mouse models

Statistical analyses for body weight, ankle size and clinical score were performed using RMA. RMA were conducted unadjusted, corrected for growth rate and with testing for potential confounders i.e. ankle size on day 0 and body weight on day 0 as an adjusting covariate to eliminate overlaying effects of growth and arthritis.

The initial weight of WT KRN animals in the study performed by Buttgereit et al. was also significantly higher than that of tg KRN mice on day 0 of this experiment (29.7 ± 0.3 g vs. 26.5 ± 0.4 g, p = 0.001). The same applied to ankle size (3.4 ± 0.02 mm vs. 3.3 ± 0.02 mm, p = 0.001) on day 0. It is, however, of note that the tg animals in the present study were slightly and in part markedly smaller than the mice in the study of 2009 (146).

The model of K/BxN serum transfer arthritis has been described extensively in the past, and although it is reported to be a very stable model in terms of prevalence after injection, different time points of arthritis onset were observed (109) and inter-individual variability in the severity of clinical appearance within one mouse strain was reported (164). A 100% consistent severity could therefore not be provided, and this is in line with our own findings. We discovered that at the peak of disease manifestation, animals within the WT KRN and the tg KRN group showed variations in the severity of arthritis and were therefore given different clinical scores. This problem could be overcome by increasing the number of animals which would have softened the single animal's impact in regard to inter-individual differences in our results. The number of animals in the study conducted by Buttgereit et al. in 2009 (146) was higher, as the study involved 28 tg and 27 WT animals receiving K/BxN serum. The mice were subdivided into 11 tg KRN animals sacrificed on day 7, 17 tg KRN animals sacrificed on day 14, 11 WT KRN animals sacrificed on day 7 and 16 WT KRN animals sacrificed on day 14. In our study, we used 8 tg KRN and 8 WT KRN animals receiving K/BxN serum which were all sacrificed on day 42. When we repeated the study with 8-week-old mice, the study consisted of 7 WT KRN and 7 tg KRN animals receiving K/BxN serum. It is also important to note that the histological inflammation scores given in the 2009 study were almost 2 times higher for WT KRN animals than the ones for WT KRN animals in our present study. It might therefore be that the extent of arthritis manifestation or the number of experimental animals in our study was not high enough to reach significant results.

Other arthritis models such as the CIA model, which is based on active immunization rather than a passive antibody serum transfer, have also been widely used in arthritis research. In the CIA model, stimulation of collagen-specific T cells leads to antibody production by B cells which in consequence leads to the development of arthritis. It is of note that fewer strains are susceptible to CIA than to K/BxN serum transfer arthritis. Although there is a certain variability in the onset and severity of arthritis in the K/BxN mouse model overall, the CIA model shows a lower disease incidence and a less pronounced severity of the disease (157).

The AIA model, another murine arthritis model, relies primarily on T cells. It follows the principle of a T cell-dependent antibody-mediated inflammatory response based on an antigen. The AIA model has been used before to investigate the role of endogenous GCs in inflammatory arthritis. A study conducted by our group showed that the GC-dependent pathway and its immune modulating response is in fact independent of T cells, and it could be concluded that AIA is not affected by disruption of osteoblastic GC signalling (162). Taking these models into

consideration, the K/BxN serum transfer arthritis model proved to be the best suited and was therefore used in our experiments.

Handling of animals and intraperitoneal injections of K/BxN serum on days 0 and 2 were well tolerated by the animals. Wellbeing of mice was monitored daily by weighing and assessment of general appearance. None of the experimental animals suffered adverse events or premature death. As the clinical appearance of the animals changed in direct correlation to the injections, arthritis development could be attributed to the K/BxN serum transfer.

4.4 Discussion of results

The results of this study suggest that GC signalling does have an effect on arthritis development. In a long-term study, these findings support previous findings suggesting that GC signalling attenuates K/BxN arthritis over the course of 14 days.

A recent study employing the CAIA (collagen antibody-induced arthritis) model, another arthritis model rather similar to the K/BxN model, as it also depends on antibodies and immune complex formation, showed the involvement of endogenous GC signalling in attenuating arthritis development (157). Administration of monoclonal antibodies to type II collagen and LPS led to severe arthritis in 8-week-old male mice. The clinical score showed that tg CAIA mice plateaued at day 6, whereas WT CAIA mice worsened up until day 10 and had significantly more severe arthritis from days 9 to 11. Consistent with these findings, the histopathology of the front paws showed a significantly higher inflammatory activity and bone erosion in WT CAIA mice compared to tg CAIA animals. The CAIA model of arthritis is reported to be clinically more pronounced in the front paws than in the hindlimbs. Interestingly, for micro-CT parameters (BV/TV, Tb.N, Tb.Sp and Tb.Th), there was no significant difference between WT CAIA and tg CAIA mice (161). As described in the foregoing, AIA is not affected by the disruption of GC signalling in mature osteoblasts and osteocytes (162). Looking at the immunological background of these models, the present K/BxN model as well as the CAIA model relies on antibodies and therefore the innate immune system. Animals devoid of lymphocytes still developed arthritis in both models (115, 165). For AIA, on the other hand, the adaptive immune system seems to play the main role, with specific T cells targeting the administered antigen. It has been proposed by Buttgereit et al. and Tu et al. that osteoblasts therefore modulate the innate immune response rather than the adaptive immune system through GC signalling (146, 161). In our study, we were able in part to reproduce these former findings.

We successfully showed the pronounced effects of arthritis such as inflammation and cartilage degradation in tg KRN and WT KRN mice. Compared to CTR animals, arthritic WT KRN mice received significantly higher inflammation scores and showed greater cartilage degradation. Further, tg KRN animals tended to have less inflammation and cartilage degradation than WT KRN mice which all is in line with the findings of Buttgereit et al. (146). We also found that tg KRN mice tended to show more severe bone erosions than their WT KRN littermates. This might be explained by the fact that WNT signalling is disrupted in Col2.3-11β-HSD2 tg mice (166) and therefore osteoblastogenesis is also markedly impaired, which leads to a more pronounced osteoclastogenesis in Col2.3-11β-HSD2 tg animals and subsequently to more bone erosions.

Micro-CT analysis showed no difference between any groups for BV/TV, for Tb.S, Tb.Th and Tb.N. A possible explanation is that although there might be more severe bone erosions in tg KRN animals, there might also be additional bone formation in these animals which eventually leaves tg KRN animals with similar values as WT KRN animals as erosion and formation even each other out.

The histomorphometry results show that tg CTR animals tend to exhibit higher overall N.Oc/BS as well as a bigger Oc.S/BS, or, in short, a more pronounced osteoclastogenesis compared to WT CTR mice. This could point to a generally higher bone turnover in tg animals. Thus it appears that if osteoblasts are deprived of GCs, as is the case in Col2.3-11β-HSD2 tg animals, numbers and surface of osteoclasts increase. It can therefore be speculated that GCs in osteoblasts are needed in order to control osteoclasts.

In WT KRN animals with no attenuation of GC signalling, arthritis leads to a high N.Oc/BS and bigger Oc.S/BS compared to the WT CTR animals. This bone resorption process could be explained by the arthritic process itself. Yet, in tg KRN animals, where GC signalling is attenuated, arthritis leads to less Oc.S/BS and N.Oc/BS compared to tg CTR. It can be speculated that a functioning GC signalling in osteoblasts is needed for the arthritic processes to increase osteoclastogenesis. In Col2.3-11β-HSD2 tg mice without functioning GC signalling in osteoblasts, arthritis seems to decrease osteoclastogenesis in contrast to in non-arthritic tg CTR mice. Looking at bone formation, it appears that the arthritic process in tg KRN mice exhibits a tendency towards a decreased Ob.S/BS compared to arthritic WT KRN animals. This might indicate that GC signalling in osteoblasts is not only needed to increase osteoclastogenisis in arthritis, but also to increase bone formation in arthritic animals.

Bearing these findings in mind, it is of note that arthritis is known to increase the amount of endogenous GCs with disease activity (167). From our results it can be speculated that inhibiting

osteoblast-GC signalling in experimental arthritic animals might actually be beneficial to the bone structure, as there is a tendency towards less bone resorption but also less bone formation - overall less bone turnover. This is consistent with findings that diseases altering bone turnover do in fact lead to reduction in bone strength (168).

The originally described K/BxN mouse strain presented with systemic signs of arthritis with hypergammaglobulinemia and splenomegaly (108). B cell clones with anti-GPI specificities were found in high numbers in arthritic K/BxN spleens. The spleen was understood to be the main site of production of anti-GPI antibodies in the K/BxN model (115). These antibodies are the key component in the K/BxN serum transfer model to implement arthritis in serum-receiving hosts. Spleen weight has been shown to increase with experimental arthritis in rats (169), and RA in man can be associated with splenomegaly and neutropenia referred to as Felty's Syndrome (170). We were able to show a greater spleen weight in arthritic tg KRN mice than in their tg CTR group. Yet, our study was not able to show a difference in spleen weight between tg KRN and WT KRN mice, indicating that GC signalling in mature osteoblasts and osteocytes has no or only a limited effect on the systemic manifestation of arthritis.

4.5   Prospect

The findings of this study are a promising addition to the understanding of long-term effects of endogenous GCs on bone remodelling processes in arthritic diseases such as RA. The intertwined roles of endogenous GCs and osteoblasts are pivotal in the process of immune modulation occurring in autoantibody-mediated K/BxN arthritis. The effect of endogenous GCs on the acute state of inflammation in arthritis, as well as on the resolution phase was shown to have a lasting impact especially on bone structure and cartilage composition.

Rheumatologists and physicians alike have started taking the important role of endogenous GCs into consideration when treating RA (171), and 11β-HSD metabolism has become a target for novel treatment strategies. Selective 11β-HSD type 1 inhibitors have shown to improve insulin sensitivity in type 2 diabetes (172). Yet the role of the 11β-HSD enzymes remains controversial. It has yet not been determined if the abundance of local endogenous GCs through 11β-HSD type 1 activity solely supports the state of inflammation or if its anti-inflammatory features prevail. A study from 2016 showed that high levels of endogenous GCs also occur as a response to inflammation in muscle tissue similar to high levels of endogenous GCs in inflamed rheumatoid synovium. The authors found that endogenous GCs in fact protect muscle tissues from wasting, accompanied by a clear anti-inflammatory effect (173).

Although animal studies can always only be models trying to imitate a clinical reality, new insights and theories often start with animal experiments before they potentially evolve into clinical practice. Studies conducted in 2010 and 2012 assessing pain in the K/BxN serum transfer arthritis mouse model and the CAIA mouse model discovered that gabapentin relieves allodynia and hypersensitivity following the state of acute inflammation. The data suggested that the inflammatory state and acute state of pain progressed to a neuropathic pain condition which was successfully treated with the anticonvulsive drug (174, 175). Although data on neuromodulators for pain management in RA patients is still being collected, a widespread clinical acceptance of neuromodulator as an adjuvant has been established (176). Through animal models we gain more and more insights on the pathogenesis of complex diseases such as RA and their potential treatment options. Through further experimental research and clinical trials we hope to obtain answers for unsolved questions in the future.

More data will need to be acquired in regard to whether endogenous GCs' effects on immune modulation through osteoblasts are primarily dose-dependent as originally presumed and recently supported by Tu et al. (161, 177). It will also be exciting to follow the progress of potential promising agents altering 11β-HSD enzymes and to see if they will actually lead to clinical improvement in RA in the years to come (171, 178).

5 REFERENCES

1.   Hench PS, Kendall EC, Slocumb CH, Polley HF. The effect of a hormone of the adrenal cortex (17-hydroxy-11-dehydrocorticosterone; compound E) and of pituitary adrenocorticotropic hormone on rheumatoid arthritis. Proc Staff Meet Mayo Clin. 1949;24(8):181-97.

2.   Pura M, Kreze A, Jr. [From the history of endocrinology: reminiscence of the discovery of adrenocortical hormones]. Cas Lek Cesk. 2005;144(9):648-50; discussion 50-1.

3.   West KM. Response of the blood glucose to glucocorticoids in man; determination of the hyperglycemic potencies of glucocorticoids. Diabetes. 1959;8(1):22-8.

4.   Wong S, Tan K, Carey KT, Fukushima A, Tiganis T, Cole TJ. Glucocorticoids stimulate hepatic and renal catecholamine inactivation by direct rapid induction of the dopamine sulfotransferase Sult1d1. Endocrinology. 2010;151(1):185-94.

5.   Schacke H, Docke WD, Asadullah K. Mechanisms involved in the side effects of glucocorticoids. Pharmacol Ther. 2002;96(1):23-43.

6.   Del Prato S, Nosadini R, Tiengo A, Tessari P, Avogaro A, Trevisan R, Valerio A, Muggeo M, Cobelli C, Toffolo G. Insulin-mediated glucose disposal in type I diabetes: evidence for insulin resistance. J Clin Endocrinol Metab. 1983;57(5):904-10.

7.   Baron AD, Wallace P, Brechtel G. In vivo regulation of non-insulin-mediated and insulin-mediated glucose uptake by cortisol. Diabetes. 1987;36(11):1230-7.

8.   Di Dalmazi G, Pagotto U, Pasquali R, Vicennati V. Glucocorticoids and type 2 diabetes: from physiology to pathology. Journal of nutrition and metabolism. 2012;2012:525093.

9.   Dimitriadis G, Leighton B, Parry-Billings M, Sasson S, Young M, Krause U, Bevan S, Piva T, Wegener G, Newsholme EA. Effects of glucocorticoid excess on the sensitivity of glucose transport and metabolism to insulin in rat skeletal muscle. Biochem J. 1997;321 (Pt 3):707-12.

10.   Rodman HM, Bleicher SJ. Plasma cortisol during normal glucose tolerance. Metabolism. 1973;22(5):745-8.

11.   Stancakova A, Vajo J. The effect of glucose on the metabolism and excretion of cortisol in man. Horm Metab Res. 1985;17(2):93-8.

12.   Son GH, Chung S, Kim K. The adrenal peripheral clock: glucocorticoid and the circadian timing system. Front Neuroendocrinol. 2011;32(4):451-65.

13.   Belda X, Fuentes S, Daviu N, Nadal R, Armario A. Stress-induced sensitization: the hypothalamic-pituitary-adrenal axis and beyond. Stress. 2015;18(3):269-79.

14.   Schmit JP, Rousseau GG. Structure and conformation of glucocorticoids. Monogr Endocrinol. 1979;12:79-95.

15.   McMahon M, Gerich J, Rizza R. Effects of glucocorticoids on carbohydrate metabolism. Diabetes Metab Rev. 1988;4(1):17-30.

16.   Christiansen JJ, Djurhuus CB, Gravholt CH, Iversen P, Christiansen JS, Schmitz O, Weeke J, Jorgensen JO, Moller N. Effects of cortisol on carbohydrate, lipid, and protein metabolism: studies of acute cortisol withdrawal in adrenocortical failure. J Clin Endocrinol Metab. 2007;92(9):3553-9.

17.   Cogan MG, Sargent JA, Yarbrough SG, Vincenti F, Amend WJ, Jr. Prevention of prednisone-induced negative nitrogen balance. Effect of dietary modification on urea generation rate in patients on hemodialysis receiving high-dose glucocorticoids. Ann Intern Med. 1981;95(2):158-61.

18.   Kaji DM, Thakkar U, Kahn T. Glucocorticoid-induced alterations in the sodium potassium pump of the human erythrocyte. J Clin Invest. 1981;68(2):422-30.

19.   Barnes PJ. Anti-inflammatory actions of glucocorticoids: molecular mechanisms. Clin Sci (Lond). 1998;94(6):557-72.

20.   Coutinho AE, Chapman KE. The anti-inflammatory and immunosuppressive effects of glucocorticoids, recent developments and mechanistic insights. Mol Cell Endocrinol. 2011;335(1):2-13.

21.   Diederich S, Scholz T, Eigendorff E, Bumke-Vogt C, Quinkler M, Exner P, Pfeiffer AF, Oelkers W, Bahr V. Pharmacodynamics and pharmacokinetics of synthetic mineralocorticoids and glucocorticoids: receptor transactivation and prereceptor metabolism by 11beta-hydroxysteroid-dehydrogenases. Horm Metab Res. 2004;36(6):423-9.

22.   Liu D, Ahmet A, Ward L, Krishnamoorthy P, Mandelcorn ED, Leigh R, Brown JP, Cohen A, Kim H. A practical guide to the monitoring and management of the complications of systemic corticosteroid therapy. Allergy Asthma Clin Immunol. 2013;9(1):30.

23.   Albrecht K, Huscher D, Eidner T, Kleinert S, Spathling-Mestekemper S, Bischoff S, Zink A. [Medical treatment of rheumatoid arthritis in 2014 : Current data from the German Collaborative Arthritis Centers]. Z Rheumatol. 2016.

24.   Thiele K, Buttgereit F, Huscher D, Zink A, Arbeitsgemeinschaft Regionaler Kooperativer R. [Prescription of glucocorticoids by rheumatologists in patients with rheumatoid arthritis in Germany]. Z Rheumatol. 2005;64(3):149-54.

25.   Kirschke E, Goswami D, Southworth D, Griffin PR, Agard DA. Glucocorticoid receptor function regulated by coordinated action of the Hsp90 and Hsp70 chaperone cycles. Cell. 2014;157(7):1685-97.

26.   Oakley RH, Cidlowski JA. Cellular processing of the glucocorticoid receptor gene and protein: new mechanisms for generating tissue-specific actions of glucocorticoids. J Biol Chem. 2011;286(5):3177-84.

27.   Anbalagan M, Huderson B, Murphy L, Rowan BG. Post-translational modifications of nuclear receptors and human disease. Nuclear receptor signaling. 2012;10:e001.

28.   Abbinante-Nissen JM, Simpson LG, Leikauf GD. Corticosteroids increase secretory leukocyte protease inhibitor transcript levels in airway epithelial cells. Am J Physiol. 1995;268(4 Pt 1):L601-6.

29.   Lasa M, Abraham SM, Boucheron C, Saklatvala J, Clark AR. Dexamethasone causes sustained expression of mitogen-activated protein kinase (MAPK) phosphatase 1 and phosphatase-mediated inhibition of MAPK p38. Mol Cell Biol. 2002;22(22):7802-11.

30.   Roviezzo F, Getting SJ, Paul-Clark MJ, Yona S, Gavins FN, Perretti M, Hannon R, Croxtall JD, Buckingham JC, Flower RJ. The annexin-1 knockout mouse: what it tells us about the inflammatory response. J Physiol Pharmacol. 2002;53(4 Pt 1):541-53.

31.   Ehrchen J, Steinmuller L, Barczyk K, Tenbrock K, Nacken W, Eisenacher M, Nordhues U, Sorg C, Sunderkotter C, Roth J. Glucocorticoids induce differentiation of a specifically activated, anti-inflammatory subtype of human monocytes. Blood. 2007;109(3):1265-74.

32.   Santos GM, Fairall L, Schwabe JW. Negative regulation by nuclear receptors: a plethora of mechanisms. Trends Endocrinol Metab. 2011;22(3):87-93.

33.   Siebenlist U, Franzoso G, Brown K. Structure, regulation and function of NF-kappa B. Annu Rev Cell Biol. 1994;10:405-55.

34.   De Bosscher K, Vanden Berghe W, Haegeman G. The interplay between the glucocorticoid receptor and nuclear factor-kappaB or activator protein-1: molecular mechanisms for gene repression. Endocr Rev. 2003;24(4):488-522.

35.   Didonato JA, Saatcioglu F, Karin M. Molecular mechanisms of immunosuppression and anti-inflammatory activities by glucocorticoids. Am J Respir Crit Care Med. 1996;154(2 Pt 2):S11-5.

36.   Bougarne N, Paumelle R, Caron S, Hennuyer N, Mansouri R, Gervois P, Staels B, Haegeman G, De Bosscher K. PPARalpha blocks glucocorticoid receptor alpha-mediated transactivation but cooperates with the activated glucocorticoid receptor alpha for transrepression on NF-kappaB. Proc Natl Acad Sci U S A. 2009;106(18):7397-402.

37.   Cooper MS, Zhou H, Seibel MJ. Selective glucocorticoid receptor agonists: glucocorticoid therapy with no regrets? J Bone Miner Res. 2012;27(11):2238-41.

38.   Cazzola M, Coppola A, Rogliani P, Matera MG. Novel glucocorticoid receptor agonists in the treatment of asthma. Expert Opin Investig Drugs. 2015;24(11):1473-82.

39.   Lesovaya E, Yemelyanov A, Swart AC, Swart P, Haegeman G, Budunova I. Discovery of Compound A--a selective activator of the glucocorticoid receptor with anti-inflammatory and anti-cancer activity. Oncotarget. 2015;6(31):30730-44.

40.   Falkenstein E, Norman AW, Wehling M. Mannheim classification of nongenomically initiated (rapid) steroid action(s). J Clin Endocrinol Metab. 2000;85(5):2072-5.

41.   Haller J, Mikics E, Makara GB. The effects of non-genomic glucocorticoid mechanisms on bodily functions and the central neural system. A critical evaluation of findings. Front Neuroendocrinol. 2008;29(2):273-91.

42.   Buttgereit F, Scheffold A. Rapid glucocorticoid effects on immune cells. Steroids. 2002;67(6):529-34.

43.   Stahn C, Buttgereit F. Genomic and nongenomic effects of glucocorticoids. Nat Clin Pract Rheumatol. 2008;4(10):525-33.

44.   Buttgereit F, Burmester GR, Brand MD. Bioenergetics of immune functions: fundamental and therapeutic aspects. Immunol Today. 2000;21(4):192-9.

45.   Malcher-Lopes R, Franco A, Tasker JG. Glucocorticoids shift arachidonic acid metabolism toward endocannabinoid synthesis: a non-genomic anti-inflammatory switch. Eur J Pharmacol. 2008;583(2-3):322-39.

46.   Bartholome B, Spies CM, Gaber T, Schuchmann S, Berki T, Kunkel D, Bienert M, Radbruch A, Burmester GR, Lauster R, Scheffold A, Buttgereit F. Membrane glucocorticoid receptors (mGCR) are expressed in normal human peripheral blood mononuclear cells and up-regulated after in vitro stimulation and in patients with rheumatoid arthritis. FASEB J. 2004;18(1):70-80.

47.   Spies CM, Schaumann DH, Berki T, Mayer K, Jakstadt M, Huscher D, Wunder C, Burmester GR, Radbruch A, Lauster R, Scheffold A, Buttgereit F. Membrane glucocorticoid receptors are down regulated by glucocorticoids in patients with systemic lupus erythematosus and use a caveolin-1-independent expression pathway. Ann Rheum Dis. 2006;65(9):1139-46.

48.   Siiteri PK, Murai JT, Hammond GL, Nisker JA, Raymoure WJ, Kuhn RW. The serum transport of steroid hormones. Recent Prog Horm Res. 1982;38:457-510.

49.   Hammond GL, Smith CL, Goping IS, Underhill DA, Harley MJ, Reventos J, Musto NA, Gunsalus GL, Bardin CW. Primary structure of human corticosteroid binding globulin, deduced

from hepatic and pulmonary cDNAs, exhibits homology with serine protease inhibitors. Proc Natl Acad Sci U S A. 1987;84(15):5153-7.

50. Pemberton PA, Stein PE, Pepys MB, Potter JM, Carrell RW. Hormone binding globulins undergo serpin conformational change in inflammation. Nature. 1988;336(6196):257-8.

51. Zhou A, Wei Z, Stanley PL, Read RJ, Stein PE, Carrell RW. The S-to-R transition of corticosteroid-binding globulin and the mechanism of hormone release. J Mol Biol. 2008;380(1):244-51.

52. Pugeat M, Bonneton A, Perrot D, Rocle-Nicolas B, Lejeune H, Grenot C, Dechaud H, Brebant C, Motin J, Cuilleron CY. Decreased immunoreactivity and binding activity of corticosteroid-binding globulin in serum in septic shock. Clin Chem. 1989;35(8):1675-9.

53. Garrel DR. Corticosteroid-binding globulin during inflammation and burn injury: nutritional modulation and clinical implications. Horm Res. 1996;45(3-5):245-51.

54. Balkovec JM, Thieringer R, Mundt SS, Hermanowski-Vosatka A, Graham DW, Patel GF, Aster SD, Waddell ST, Olson SH, Maletic M. 11-beta-hydroxysteroid dehydrogenase 1 inhibitors useful for the treatment of diabetes, obesity and dyslipidemia. Google Patents; 2007.

55. Stewart PM, Krozowski ZS. 11 beta-Hydroxysteroid dehydrogenase. Vitam Horm. 1999;57:249-324.

56. Hewitt KN, Walker EA, Stewart PM. Minireview: hexose-6-phosphate dehydrogenase and redox control of 11{beta}-hydroxysteroid dehydrogenase type 1 activity. Endocrinology. 2005;146(6):2539-43.

57. Bujalska IJ, Kumar S, Hewison M, Stewart PM. Differentiation of adipose stromal cells: the roles of glucocorticoids and 11beta-hydroxysteroid dehydrogenase. Endocrinology. 1999;140(7):3188-96.

58. Jamieson PM, Chapman KE, Edwards CR, Seckl JR. 11 beta-hydroxysteroid dehydrogenase is an exclusive 11 beta- reductase in primary cultures of rat hepatocytes: effect of physicochemical and hormonal manipulations. Endocrinology. 1995;136(11):4754-61.

59. Kannisto K, Pietilainen KH, Ehrenborg E, Rissanen A, Kaprio J, Hamsten A, Yki-Jarvinen H. Overexpression of 11beta-hydroxysteroid dehydrogenase-1 in adipose tissue is associated with acquired obesity and features of insulin resistance: studies in young adult monozygotic twins. J Clin Endocrinol Metab. 2004;89(9):4414-21.

60. Winnick JJ, Ramnanan CJ, Saraswathi V, Roop J, Scott M, Jacobson P, Jung P, Basu R, Cherrington AD, Edgerton DS. Effects of 11beta-hydroxysteroid dehydrogenase-1 inhibition on hepatic glycogenolysis and gluconeogenesis. Am J Physiol Endocrinol Metab. 2013;304(7):E747-56.

61. Alberts P, Nilsson C, Selen G, Engblom LO, Edling NH, Norling S, Klingstrom G, Larsson C, Forsgren M, Ashkzari M, Nilsson CE, Fiedler M, Bergqvist E, Ohman B, Bjorkstrand E, Abrahmsen LB. Selective inhibition of 11 beta-hydroxysteroid dehydrogenase type 1 improves hepatic insulin sensitivity in hyperglycemic mice strains. Endocrinology. 2003;144(11):4755-62.

62. Sandeep TC, Yau JL, MacLullich AM, Noble J, Deary IJ, Walker BR, Seckl JR. 11Beta-hydroxysteroid dehydrogenase inhibition improves cognitive function in healthy elderly men and type 2 diabetics. Proceedings of the National Academy of Sciences of the United States of America. 2004;101(17):6734-9.

63. Dhingra D, Parle M, Kulkarni SK. Memory enhancing activity of Glycyrrhiza glabra in mice. Journal of ethnopharmacology. 2004;91(2-3):361-5.

64. Edwards CR, Stewart PM, Burt D, Brett L, McIntyre MA, Sutanto WS, de Kloet ER, Monder C. Localisation of 11 beta-hydroxysteroid dehydrogenase--tissue specific protector of the mineralocorticoid receptor. Lancet. 1988;2(8618):986-9.

65. Walker BR, Campbell JC, Williams BC, Edwards CR. Tissue-specific distribution of the NAD(+)-dependent isoform of 11 beta-hydroxysteroid dehydrogenase. Endocrinology. 1992;131(2):970-2.

66. Funder JW, Pearce PT, Smith R, Smith AI. Mineralocorticoid action: target tissue specificity is enzyme, not receptor, mediated. Science. 1988;242(4878):583-5.

67. Whorwood CB, Ricketts ML, Stewart PM. Epithelial cell localization of type 2 11 beta-hydroxysteroid dehydrogenase in rat and human colon. Endocrinology. 1994;135(6):2533-41.

68. Edwards CR, Benediktsson R, Lindsay RS, Seckl JR. Dysfunction of placental glucocorticoid barrier: link between fetal environment and adult hypertension? Lancet. 1993;341(8841):355-7.

69. Brown RW, Chapman KE, Murad P, Edwards CR, Seckl JR. Purification of 11 beta-hydroxysteroid dehydrogenase type 2 from human placenta utilizing a novel affinity labelling technique. Biochem J. 1996;313 (Pt 3):997-1005.

70. Condon J, Gosden C, Gardener D, Nickson P, Hewison M, Howie AJ, Stewart PM. Expression of type 2 11beta-hydroxysteroid dehydrogenase and corticosteroid hormone receptors in early human fetal life. J Clin Endocrinol Metab. 1998;83(12):4490-7.

71. Al-Harbi T, Al-Shaikh A. Apparent mineralocorticoid excess syndrome: report of one family with three affected children. J Pediatr Endocrinol Metab. 2012;25(11-12):1083-8.

72. Palermo M, Quinkler M, Stewart PM. Apparent mineralocorticoid excess syndrome: an overview. Arq Bras Endocrinol Metabol. 2004;48(5):687-96.

73.   Omar HR, Komarova I, El-Ghonemi M, Fathy A, Rashad R, Abdelmalak HD, Yerramadha MR, Ali Y, Helal E, Camporesi EM. Licorice abuse: time to send a warning message. Therapeutic advances in endocrinology and metabolism. 2012;3(4):125-38.

74.   Bland R, Worker CA, Noble BS, Eyre LJ, Bujalska IJ, Sheppard MC, Stewart PM, Hewison M. Characterization of 11beta-hydroxysteroid dehydrogenase activity and corticosteroid receptor expression in human osteosarcoma cell lines. J Endocrinol. 1999;161(3):455-64.

75.   Cooper MS, Walker EA, Bland R, Fraser WD, Hewison M, Stewart PM. Expression and functional consequences of 11beta-hydroxysteroid dehydrogenase activity in human bone. Bone. 2000;27(3):375-81.

76.   Eyre LJ, Rabbitt EH, Bland R, Hughes SV, Cooper MS, Sheppard MC, Stewart PM, Hewison M. Expression of 11 beta-hydroxysteroid dehydrogenase in rat osteoblastic cells: pre-receptor regulation of glucocorticoid responses in bone. J Cell Biochem. 2001;81(3):453-62.

77.   Liesegang P, Romalo G, Sudmann M, Wolf L, Schweikert HU. Human osteoblast-like cells contain specific, saturable, high-affinity glucocorticoid, androgen, estrogen, and 1 alpha,25-dihydroxycholecalciferol receptors. J Androl. 1994;15(3):194-9.

78.   Cushing H. The basophil adenomas of the pituitary body. Ann R Coll Surg Engl. 1969;44(4):180-1.

79.   Weinstein RS, Jilka RL, Parfitt AM, Manolagas SC. Inhibition of osteoblastogenesis and promotion of apoptosis of osteoblasts and osteocytes by glucocorticoids. Potential mechanisms of their deleterious effects on bone. J Clin Invest. 1998;102(2):274-82.

80.   Weinstein RS, Chen JR, Powers CC, Stewart SA, Landes RD, Bellido T, Jilka RL, Parfitt AM, Manolagas SC. Promotion of osteoclast survival and antagonism of bisphosphonate-induced osteoclast apoptosis by glucocorticoids. J Clin Invest. 2002;109(8):1041-8.

81.   MacAdams MR, White RH, Chipps BE. Reduction of serum testosterone levels during chronic glucocorticoid therapy. Ann Intern Med. 1986;104(5):648-51.

82.   Montecucco C, Caporali R, Caprotti P, Caprotti M, Notario A. Sex hormones and bone metabolism in postmenopausal rheumatoid arthritis treated with two different glucocorticoids. J Rheumatol. 1992;19(12):1895-900.

83.   Zhou H, Cooper MS, Seibel MJ. Endogenous Glucocorticoids and Bone. Bone research. 2013;1(2):107-19.

84.   Yeh S, Tsai MY, Xu Q, Mu XM, Lardy H, Huang KE, Lin H, Yeh SD, Altuwaijri S, Zhou X, Xing L, Boyce BF, Hung MC, Zhang S, Gan L, Chang C. Generation and

characterization of androgen receptor knockout (ARKO) mice: an in vivo model for the study of androgen functions in selective tissues. Proc Natl Acad Sci U S A. 2002;99(21):13498-503.

85.   Oz OK, Hirasawa G, Lawson J, Nanu L, Constantinescu A, Antich PP, Mason RP, Tsyganov E, Parkey RW, Zerwekh JE, Simpson ER. Bone phenotype of the aromatase deficient mouse. J Steroid Biochem Mol Biol. 2001;79(1-5):49-59.

86.   Weinstein RS, Jia D, Powers CC, Stewart SA, Jilka RL, Parfitt AM, Manolagas SC. The skeletal effects of glucocorticoid excess override those of orchidectomy in mice. Endocrinology. 2004;145(4):1980-7.

87.   Weinstein RS. Clinical practice. Glucocorticoid-induced bone disease. N Engl J Med. 2011;365(1):62-70.

88.   Saag KG, Shane E, Boonen S, Marin F, Donley DW, Taylor KA, Dalsky GP, Marcus R. Teriparatide or alendronate in glucocorticoid-induced osteoporosis. N Engl J Med. 2007;357(20):2028-39.

89.   Saag KG, Agnusdei D, Hans D, Kohlmeier LA, Krohn KD, Leib ES, MacLaughlin EJ, Alam J, Simonelli C, Taylor KA, Marcus R. Trabecular Bone Score in Patients With Chronic Glucocorticoid Therapy-Induced Osteoporosis Treated With Alendronate or Teriparatide. Arthritis Rheumatol. 2016;68(9):2122-8.

90.   Sher LB, Woitge HW, Adams DJ, Gronowicz GA, Krozowski Z, Harrison JR, Kream BE. Transgenic expression of 11beta-hydroxysteroid dehydrogenase type 2 in osteoblasts reveals an anabolic role for endogenous glucocorticoids in bone. Endocrinology. 2004;145(2):922-9.

91.   Sher LB, Harrison JR, Adams DJ, Kream BE. Impaired cortical bone acquisition and osteoblast differentiation in mice with osteoblast-targeted disruption of glucocorticoid signaling. Calcif Tissue Int. 2006;79(2):118-25.

92.   O'Brien CA, Jia D, Plotkin LI, Bellido T, Powers CC, Stewart SA, Manolagas SC, Weinstein RS. Glucocorticoids act directly on osteoblasts and osteocytes to induce their apoptosis and reduce bone formation and strength. Endocrinology. 2004;145(4):1835-41.

93.   Cooper MS, Bujalska I, Rabbitt E, Walker EA, Bland R, Sheppard MC, Hewison M, Stewart PM. Modulation of 11beta-hydroxysteroid dehydrogenase isozymes by proinflammatory cytokines in osteoblasts: an autocrine switch from glucocorticoid inactivation to activation. J Bone Miner Res. 2001;16(6):1037-44.

94.   Cooper MS, Rabbitt EH, Goddard PE, Bartlett WA, Hewison M, Stewart PM. Osteoblastic 11beta-hydroxysteroid dehydrogenase type 1 activity increases with age and glucocorticoid exposure. J Bone Miner Res. 2002;17(6):979-86.

95.   Kaur K, Hardy R, Ahasan MM, Eijken M, van Leeuwen JP, Filer A, Thomas AM, Raza K, Buckley CD, Stewart PM, Rabbitt EH, Hewison M, Cooper MS. Synergistic induction of local glucocorticoid generation by inflammatory cytokines and glucocorticoids: implications for inflammation associated bone loss. Ann Rheum Dis. 2010;69(6):1185-90.

96.   Roldan JF, Del Rincon I, Escalante A. Loss of cortical bone from the metacarpal diaphysis in patients with rheumatoid arthritis: independent effects of systemic inflammation and glucocorticoids. J Rheumatol. 2006;33(3):508-16.

97.   Cooper MS, Blumsohn A, Goddard PE, Bartlett WA, Shackleton CH, Eastell R, Hewison M, Stewart PM. 11beta-hydroxysteroid dehydrogenase type 1 activity predicts the effects of glucocorticoids on bone. J Clin Endocrinol Metab. 2003;88(8):3874-7.

98.   Eijken M, Koedam M, van Driel M, Buurman CJ, Pols HA, van Leeuwen JP. The essential role of glucocorticoids for proper human osteoblast differentiation and matrix mineralization. Mol Cell Endocrinol. 2006;248(1-2):87-93.

99.   Eijken M, Hewison M, Cooper MS, de Jong FH, Chiba H, Stewart PM, Uitterlinden AG, Pols HA, van Leeuwen JP. 11beta-Hydroxysteroid dehydrogenase expression and glucocorticoid synthesis are directed by a molecular switch during osteoblast differentiation. Mol Endocrinol. 2005;19(3):621-31.

100.   Kalak R, Zhou H, Street J, Day RE, Modzelewski JR, Spies CM, Liu PY, Li G, Dunstan CR, Seibel MJ. Endogenous glucocorticoid signalling in osteoblasts is necessary to maintain normal bone structure in mice. Bone. 2009;45(1):61-7.

101.   Zhou H, Mak W, Zheng Y, Dunstan CR, Seibel MJ. Osteoblasts directly control lineage commitment of mesenchymal progenitor cells through Wnt signaling. The Journal of biological chemistry. 2008;283(4):1936-45.

102.   Sher LB, Harrison JR, Adams DJ, Kream BE. Impaired cortical bone acquisition and osteoblast differentiation in mice with osteoblast-targeted disruption of glucocorticoid signaling. Calcif Tissue Int. 2006;79(2):118-25.

103.   Justesen J, Mosekilde L, Holmes M, Stenderup K, Gasser J, Mullins JJ, Seckl JR, Kassem M. Mice deficient in 11beta-hydroxysteroid dehydrogenase type 1 lack bone marrow adipocytes, but maintain normal bone formation. Endocrinology. 2004;145(4):1916-25.

104.   Scott DL, Wolfe F, Huizinga TW. Rheumatoid arthritis. Lancet. 2010;376(9746):1094-108.

105.   Cohen SB, Dore RK, Lane NE, Ory PA, Peterfy CG, Sharp JT, van der Heijde D, Zhou L, Tsuji W, Newmark R, Denosumab Rheumatoid Arthritis Study G. Denosumab treatment effects on structural damage, bone mineral density, and bone turnover in rheumatoid arthritis: a

twelve-month, multicenter, randomized, double-blind, placebo-controlled, phase II clinical trial. Arthritis Rheum. 2008;58(5):1299-309.

106. van den Berg WB. Lessons from animal models of arthritis over the past decade. Arthritis Res Ther. 2009;11(5):250.

107. McDevitt H, Singer S, Tisch R. The role of MHC class II genes in susceptibility and resistance to type I diabetes mellitus in the NOD mouse. Horm Metab Res. 1996;28(6):287-8.

108. Kouskoff V, Korganow AS, Duchatelle V, Degott C, Benoist C, Mathis D. Organ-specific disease provoked by systemic autoimmunity. Cell. 1996;87(5):811-22.

109. Ditzel HJ. The K/BxN mouse: a model of human inflammatory arthritis. Trends Mol Med. 2004;10(1):40-5.

110. Korganow AS, Ji H, Mangialaio S, Duchatelle V, Pelanda R, Martin T, Degott C, Kikutani H, Rajewsky K, Pasquali JL, Benoist C, Mathis D. From systemic T cell self-reactivity to organ-specific autoimmune disease via immunoglobulins. Immunity. 1999;10(4):451-61.

111. Kyburz D, Carson DA, Corr M. The role of CD40 ligand and tumor necrosis factor alpha signaling in the transgenic K/BxN mouse model of rheumatoid arthritis. Arthritis Rheum. 2000;43(11):2571-7.

112. Martin P, Talabot-Ayer D, Seemayer CA, Vigne S, Lamacchia C, Rodriguez E, Finckh A, Smith DE, Gabay C, Palmer G. Disease severity in K/BxN serum transfer-induced arthritis is not affected by IL-33 deficiency. Arthritis Res Ther. 2013;15(1):R13.

113. Kyburz D, Corr M. The KRN mouse model of inflammatory arthritis. Springer Semin Immunopathol. 2003;25(1):79-90.

114. Kay J, Upchurch KS. ACR/EULAR 2010 rheumatoid arthritis classification criteria. Rheumatology (Oxford). 2012;51 Suppl 6:vi5-9.

115. Maccioni M, Zeder-Lutz G, Huang H, Ebel C, Gerber P, Hergueux J, Marchal P, Duchatelle V, Degott C, van Regenmortel M, Benoist C, Mathis D. Arthritogenic monoclonal antibodies from K/BxN mice. J Exp Med. 2002;195(8):1071-7.

116. Mancardi DA, Jonsson F, Iannascoli B, Khun H, Van Rooijen N, Huerre M, Daeron M, Bruhns P. Cutting Edge: The murine high-affinity IgG receptor FcgammaRIV is sufficient for autoantibody-induced arthritis. J Immunol. 2011;186(4):1899-903.

117. Nimmerjahn F, Ravetch JV. Fc-receptors as regulators of immunity. Adv Immunol. 2007;96:179-204.

118. Ji H, Ohmura K, Mahmood U, Lee DM, Hofhuis FM, Boackle SA, Takahashi K, Holers VM, Walport M, Gerard C, Ezekowitz A, Carroll MC, Brenner M, Weissleder R, Verbeek JS,

Duchatelle V, Degott C, Benoist C, Mathis D. Arthritis critically dependent on innate immune system players. Immunity. 2002;16(2):157-68.

119.   Boross P, van Lent PL, Martin-Ramirez J, van der Kaa J, Mulder MH, Claassens JW, van den Berg WB, Arandhara VL, Verbeek JS. Destructive arthritis in the absence of both FcgammaRI and FcgammaRIII. J Immunol. 2008;180(7):5083-91.

120.   Corr M, Crain B. The role of FcgammaR signaling in the K/B x N serum transfer model of arthritis. J Immunol. 2002;169(11):6604-9.

121.   Benoist C, Mathis D. Mast cells in autoimmune disease. Nature. 2002;420(6917):875-8.

122.   Lee DM, Friend DS, Gurish MF, Benoist C, Mathis D, Brenner MB. Mast cells: a cellular link between autoantibodies and inflammatory arthritis. Science. 2002;297(5587):1689-92.

123.   Feyerabend TB, Weiser A, Tietz A, Stassen M, Harris N, Kopf M, Radermacher P, Moller P, Benoist C, Mathis D, Fehling HJ, Rodewald HR. Cre-mediated cell ablation contests mast cell contribution in models of antibody- and T cell-mediated autoimmunity. Immunity. 2011;35(5):832-44.

124.   Monach PA, Nigrovic PA, Chen M, Hock H, Lee DM, Benoist C, Mathis D. Neutrophils in a mouse model of autoantibody-mediated arthritis: critical producers of Fc receptor gamma, the receptor for C5a, and lymphocyte function-associated antigen 1. Arthritis Rheum. 2010;62(3):753-64.

125.   Chen M, Lam BK, Kanaoka Y, Nigrovic PA, Audoly LP, Austen KF, Lee DM. Neutrophil-derived leukotriene B4 is required for inflammatory arthritis. J Exp Med. 2006;203(4):837-42.

126.   Kim ND, Chou RC, Seung E, Tager AM, Luster AD. A unique requirement for the leukotriene B4 receptor BLT1 for neutrophil recruitment in inflammatory arthritis. J Exp Med. 2006;203(4):829-35.

127.   Tager AM, Dufour JH, Goodarzi K, Bercury SD, von Andrian UH, Luster AD. BLTR mediates leukotriene B(4)-induced chemotaxis and adhesion and plays a dominant role in eosinophil accumulation in a murine model of peritonitis. J Exp Med. 2000;192(3):439-46.

128.   Chou RC, Kim ND, Sadik CD, Seung E, Lan Y, Byrne MH, Haribabu B, Iwakura Y, Luster AD. Lipid-cytokine-chemokine cascade drives neutrophil recruitment in a murine model of inflammatory arthritis. Immunity. 2010;33(2):266-78.

129.   Solomon S, Rajasekaran N, Jeisy-Walder E, Snapper SB, Illges H. A crucial role for macrophages in the pathology of K/B x N serum-induced arthritis. Eur J Immunol. 2005;35(10):3064-73.

130.   Italiani P, Boraschi D. From Monocytes to M1/M2 Macrophages: Phenotypical vs. Functional Differentiation. Front Immunol. 2014;5:514.

131.   Misharin AV, Cuda CM, Saber R, Turner JD, Gierut AK, Haines GK, 3rd, Berdnikovs S, Filer A, Clark AR, Buckley CD, Mutlu GM, Budinger GR, Perlman H. Nonclassical Ly6C(-) monocytes drive the development of inflammatory arthritis in mice. Cell reports. 2014;9(2):591-604.

132.   Kim HY, Kim S, Chung DH. FcgammaRIII engagement provides activating signals to NKT cells in antibody-induced joint inflammation. J Clin Invest. 2006;116(9):2484-92.

133.   Ji H, Pettit A, Ohmura K, Ortiz-Lopez A, Duchatelle V, Degott C, Gravallese E, Mathis D, Benoist C. Critical roles for interleukin 1 and tumor necrosis factor alpha in antibody-induced arthritis. J Exp Med. 2002;196(1):77-85.

134.   Maini R, St Clair EW, Breedveld F, Furst D, Kalden J, Weisman M, Smolen J, Emery P, Harriman G, Feldmann M, Lipsky P. Infliximab (chimeric anti-tumour necrosis factor alpha monoclonal antibody) versus placebo in rheumatoid arthritis patients receiving concomitant methotrexate: a randomised phase III trial. ATTRACT Study Group. Lancet. 1999;354(9194):1932-9.

135.   Alten R, Maleitzke T. Tocilizumab: a novel humanized anti-interleukin 6 (IL-6) receptor antibody for the treatment of patients with non-RA systemic, inflammatory rheumatic diseases. Ann Med. 2013;45(4):357-63.

136.   Katayama M, Ohmura K, Yukawa N, Terao C, Hashimoto M, Yoshifuji H, Kawabata D, Fujii T, Iwakura Y, Mimori T. Neutrophils are essential as a source of IL-17 in the effector phase of arthritis. PLoS One. 2013;8(5):e62231.

137.   Jacobs JP, Wu HJ, Benoist C, Mathis D. IL-17-producing T cells can augment autoantibody-induced arthritis. Proc Natl Acad Sci U S A. 2009;106(51):21789-94.

138.   Block KE, Zheng Z, Dent AL, Kee BL, Huang H. Gut Microbiota Regulates K/BxN Autoimmune Arthritis through Follicular Helper T but Not Th17 Cells. J Immunol. 2016;196(4):1550-7.

139.   Kugyelka R, Kohl Z, Olasz K, Mikecz K, Rauch TA, Glant TT, Boldizsar F. Enigma of IL-17 and Th17 Cells in Rheumatoid Arthritis and in Autoimmune Animal Models of Arthritis. Mediators Inflamm. 2016;2016:6145810.

140.   Ohmura K, Nguyen LT, Locksley RM, Mathis D, Benoist C. Interleukin-4 can be a key positive regulator of inflammatory arthritis. Arthritis Rheum. 2005;52(6):1866-75.

141.   Ehrnthaller C, Ignatius A, Gebhard F, Huber-Lang M. New insights of an old defense system: structure, function, and clinical relevance of the complement system. Mol Med. 2011;17(3-4):317-29.

142.   Tu Z, Bu H, Dennis JE, Lin F. Efficient osteoclast differentiation requires local complement activation. Blood. 2010;116(22):4456-63.

143.   Monach PA, Verschoor A, Jacobs JP, Carroll MC, Wagers AJ, Benoist C, Mathis D. Circulating C3 is necessary and sufficient for induction of autoantibody-mediated arthritis in a mouse model. Arthritis Rheum. 2007;56(9):2968-74.

144.   Vetto AA, Mannik M, Zatarain-Rios E, Wener MH. Immune deposits in articular cartilage of patients with rheumatoid arthritis have a granular pattern not seen in osteoarthritis. Rheumatol Int. 1990;10(1):13-9.

145.   Klaus GG, Pepys MB, Kitajima K, Askonas BA. Activation of mouse complement by different classes of mouse antibody. Immunology. 1979;38(4):687-95.

146.   Buttgereit F, Zhou H, Kalak R, Gaber T, Spies CM, Huscher D, Straub RH, Modzelewski J, Dunstan CR, Seibel MJ. Transgenic disruption of glucocorticoid signaling in mature osteoblasts and osteocytes attenuates K/BxN mouse serum-induced arthritis in vivo. Arthritis Rheum. 2009;60(7):1998-2007.

147.   Matzelle MM, Gallant MA, Condon KW, Walsh NC, Manning CA, Stein GS, Lian JB, Burr DB, Gravallese EM. Resolution of inflammation induces osteoblast function and regulates the Wnt signaling pathway. Arthritis Rheum. 2012;64(5):1540-50.

148.   Zhou H, Mak W, Kalak R, Street J, Fong-Yee C, Zheng Y, Dunstan CR, Seibel MJ. Glucocorticoid-dependent Wnt signaling by mature osteoblasts is a key regulator of cranial skeletal development in mice. Development. 2009;136(3):427-36.

149.   Feldman AT, Wolfe D. Tissue processing and hematoxylin and eosin staining. Methods Mol Biol. 2014;1180:31-43.

150.   Bendele A, McAbee T, Sennello G, Frazier J, Chlipala E, McCabe D. Efficacy of sustained blood levels of interleukin-1 receptor antagonist in animal models of arthritis: comparison of efficacy in animal models with human clinical data. Arthritis Rheum. 1999;42(3):498-506.

151.   Geyer G, Linss W. Toluidine blue staining of cartilage proteoglycan subunits. Acta Histochem. 1978;61(1):127-34.

152.   Poole AR. The relationship between toluidine blue staining and hexuronic acid content of cartilage matrix. Histochem J. 1970;2(5):425-30.

153.   Rico H, Villa LF. Serum tartrate-resistant acid phosphatase (TRAP) as a biochemical marker of bone remodeling. Calcif Tissue Int. 1993;52(2):149-50.

154.   Guldberg RE, Lin AS, Coleman R, Robertson G, Duvall C. Microcomputed tomography imaging of skeletal development and growth. Birth defects research Part C, Embryo today : reviews. 2004;72(3):250-9.

155.   Bentley MD, Ortiz MC, Ritman EL, Romero JC. The use of microcomputed tomography to study microvasculature in small rodents. Am J Physiol Regul Integr Comp Physiol. 2002;282(5):R1267-79.

156.   Ritman EL, Jorgensen SM, Beighley PE, Thomas PJ, Dunsmuir JH, Romero JC, Turner RT, Bolander ME. Synchrotron-based micro-CT of in-situ biological basic functional units and their integration. Developments in X-Ray Tomography. 1997;3149 :13--24.

157.   Christensen AD, Haase C, Cook AD, Hamilton JA. K/BxN Serum-Transfer Arthritis as a Model for Human Inflammatory Arthritis. Front Immunol. 2016;7:213.

158.   Yamazaki H, Takeoka M, Kitazawa M, Ehara T, Itano N, Kato H, Taniguchi S. ASC plays a role in the priming phase of the immune response to type II collagen in collagen-induced arthritis. Rheumatol Int. 2012;32(6):1625-32.

159.   Haruyama N, Cho A, Kulkarni AB. Overview: engineering transgenic constructs and mice. Current protocols in cell biology. 2009;Chapter 19:Unit 19 0.

160.   Funder JW. Mineralocorticoid receptors: distribution and activation. Heart failure reviews. 2005;10(1):15-22.

161.   Tu J, Zhang Y, Kim S, Wiebe E, Spies CM, Buttgereit F, Cooper MS, Seibel MJ, Zhou H. Transgenic Disruption of Glucocorticoid Signaling in Osteoblasts Attenuates Joint Inflammation in Collagen Antibody-Induced Arthritis. Am J Pathol. 2016;186(5):1293-301.

162.   Spies CM, Wiebe E, Tu J, Li A, Gaber T, Huscher D, Seibel MJ, Zhou H, Buttgereit F. Acute murine antigen-induced arthritis is not affected by disruption of osteoblastic glucocorticoid signalling. BMC Musculoskelet Disord. 2014;15:31.

163.   Davis J, Maillet M, Miano JM, Molkentin JD. Lost in transgenesis: a user's guide for genetically manipulating the mouse in cardiac research. Circ Res. 2012;111(6):761-77.

164.   Monach P, Hattori K, Huang H, Hyatt E, Morse J, Nguyen L, Ortiz-Lopez A, Wu HJ, Mathis D, Benoist C. The K/BxN mouse model of inflammatory arthritis: theory and practice. Methods Mol Med. 2007;136:269-82.

165.   Nandakumar KS, Backlund J, Vestberg M, Holmdahl R. Collagen type II (CII)-specific antibodies induce arthritis in the absence of T or B cells but the arthritis progression is enhanced by CII-reactive T cells. Arthritis Res Ther. 2004;6(6):R544-50.

166.   Zhou H, Mak W, Zheng Y, Dunstan CR, Seibel MJ. Osteoblasts directly control lineage commitment of mesenchymal progenitor cells through Wnt signaling. J Biol Chem. 2008;283(4):1936-45.

167.   Buttgereit F, Zhou H, Seibel MJ. Arthritis and endogenous glucocorticoids: the emerging role of the 11beta-HSD enzymes. Ann Rheum Dis. 2008;67(9):1201-3.

168.   Unnanuntana A, Rebolledo BJ, Khair MM, DiCarlo EF, Lane JM. Diseases affecting bone quality: beyond osteoporosis. Clin Orthop Relat Res. 2011;469(8):2194-206.

169.   Milanino R, Moretti U, Concari E, Marrella M, Velo GP. Copper and zinc status in adjuvant-arthritic rat: studies on blood, liver, kidneys, spleen and inflamed paws. Agents Actions. 1988;24(3-4):365-76.

170.   Owlia MB, Newman K, Akhtari M. Felty's Syndrome, Insights and Updates. Open Rheumatol J. 2014;8:129-36.

171.   Spies CM, Bijlsma JW, Burmester GR, Buttgereit F. Pharmacology of glucocorticoids in rheumatoid arthritis. Curr Opin Pharmacol. 2010;10(3):302-7.

172.   Morgan SA, Tomlinson JW. 11beta-hydroxysteroid dehydrogenase type 1 inhibitors for the treatment of type 2 diabetes. Expert Opin Investig Drugs. 2010;19(9):1067-76.

173.   R.S. Hardy ZH, M. Pearson, A. Filer, C. Buckley, G. Lavery, M. Coope, K. Raza. SAT0039 Endogenous Glucocorticoid Production by The Enzyme 11beta-Hydroxysteroid Dehydrogenase Type 1 Is Increased with Inflammation In Muscle, Where It Suppresses Inflammatory Cytokine Output and Protects against Muscle Wasting In Vivo. Ann Rheum Dis. 2016;75(Suppl 2):677-8.

174.   Christianson CA, Corr M, Firestein GS, Mobargha A, Yaksh TL, Svensson CI. Characterization of the acute and persistent pain state present in K/BxN serum transfer arthritis. Pain. 2010;151(2):394-403.

175.   Bas DB, Su J, Sandor K, Agalave NM, Lundberg J, Codeluppi S, Baharpoor A, Nandakumar KS, Holmdahl R, Svensson CI. Collagen antibody-induced arthritis evokes persistent pain with spinal glial involvement and transient prostaglandin dependency. Arthritis Rheum. 2012;64(12):3886-96.

176.   Richards BL, Whittle SL, Buchbinder R. Neuromodulators for pain management in rheumatoid arthritis. Cochrane Database Syst Rev. 2012;1:CD008921.

177. Straub RH, Dhabhar FS, Bijlsma JW, Cutolo M. How psychological stress via hormones and nerve fibers may exacerbate rheumatoid arthritis. Arthritis Rheum. 2005;52(1):16-26.

178. Chapman K, Holmes M, Seckl J. 11beta-hydroxysteroid dehydrogenases: intracellular gate-keepers of tissue glucocorticoid action. Physiol Rev. 2013;93(3):1139-206.

6 APPENDIX

6.1 Eidesstattliche Versicherung

Ich, Tazio David Maleitzke, versichere an Eides statt durch meine eigenhändige Unterschrift, dass ich die vorgelegte Dissertation mit dem Thema: "**Long-term effects of transgenic disruption of glucocorticoid signalling in mature osteoblasts and osteocytes in K/BxN mouse serum-induced arthritis"** selbstständig und ohne nicht offengelegte Hilfe Dritter verfasst und keine anderen als die angegebenen Quellen und Hilfsmittel genutzt habe.

Alle Stellen, die wörtlich oder dem Sinne nach auf Publikationen oder Vorträgen anderer Autoren beruhen, sind als solche in korrekter Zitierung (siehe „Uniform Requirements for Manuscripts (URM)" des ICMJE -*www.icmje.org*) kenntlich gemacht. Die Abschnitte zu Methodik (insbesondere praktische Arbeiten, Laborbestimmungen, statistische Aufarbeitung) und Resultaten (insbesondere Abbildungen, Graphiken und Tabellen) entsprechen den URM (s.o) und werden von mir verantwortet.

Meine Anteile an etwaigen Publikationen zu dieser Dissertation entsprechen denen, die in der untenstehenden gemeinsamen Erklärung mit dem/der Betreuer/in, angegeben sind. Sämtliche Publikationen, die aus dieser Dissertation hervorgegangen sind und bei denen ich Autor bin, entsprechen den URM (s.o) und werden von mir verantwortet.

Die Bedeutung dieser eidesstattlichen Versicherung und die strafrechtlichen Folgen einer unwahren eidesstattlichen Versicherung (§156,161 des Strafgesetzbuches) sind mir bekannt und bewusst.

03.04.2017   Tazio David Maleitzke

6.2   CV

Mein Lebenslauf wird aus datenschutzrechtlichen Gründen in der elektronischen Version meiner Arbeit nicht veröffentlicht.

6.3 Publications

Alten R, <u>Maleitzke T.</u> Tocilizumab: a novel humanized anti-interleukin 6 (IL-6) receptor antibody for the treatment of patients with non-RA systemic, inflammatory rheumatic diseases. Ann Med. 2013;45(4):357-63.

6.4   Acknowledgements